The Expression of Hsf1 in the Rat Myometrium During Pregnancy and Labour

By

Sarah Ellen Dinn

A thesis submitted to the School of Graduate Studies in fulfillment of the requirements for the degree of Master of Science in Medicine.

Biomedical Sciences

Faculty of Medicine

Memorial University of Newfoundland

St. John's, Newfoundland, Canada

May 2016

Abstract

Heat shock factor 1 (Hsf1) is a protein known to be involved in both stress and developmental processes through the regulation of heat shock proteins. However, to date, no studies have been performed on examining its expression in the myometrium during pregnancy. During pregnancy, the uterus undergoes many structural and functional changes, and it also endures both mechanical and hormonal stresses. Therefore, the purpose of this thesis was to characterize the expression of Hsf1, and its associated factors in the uterus during pregnancy.

Immunoblot analysis determined that Hsf1 protein expression was high early in gestation (day (d) 6) and then decreased significantly from mid gestation onwards (specifically when compared to d15, d17 and d22, $p<0.05$, $n=5$). Immunofluorescence analysis, demonstrated that Hsf1 was readily detectable in the myometrium but did not markedly change over gestation. Hsf1 was also localized mainly in the cytoplasm of myometrial cells, with some granular staining in the nucleus. Many related proteins of Hsf1 were also detectable in the myometrium, during pregnancy, such as PARP-1 and Hsf2. These results indicate that Hsf1 could play an important role early in gestation either to aid in myometrial cell proliferation or to upregulate expression of key genes necessary for subsequent myometrial differentiation.

Acknowledgements

The past few years in the MacPhee lab have been such an amazing experience. I have learned so much about not only uterine biology but about myself as a person. I would like to first and foremost thank Dr. MacPhee. He has been the most patient person with me and the other students. His door has always been open and he has happily answered any question I may have. He has definitely gone above and beyond the role of a master's supervisor and has helped me achieve my goals both during this program and my other goals outside of research. I will miss Dr. MacPhee's sense of humour and his strong opinions on car brands. I truly owe him for not only my success as a graduate student, but for many of my successes in the future. There are not enough "thank yous" that could show my appreciation enough.

I would also like to thank my labmates Joanne Delaney, Noelle Marsh, Gina Hamilton, Trina Kirby, Ewa Miskiewicz, Justin Pater and Mandy Peach. To Joanne Delaney, thanks for making our lab, and team uterus, number one for the summer! You definitely helped keep things interesting with all your stories of New Brunswick and your adventures here! To Noelle, thank you for being the best friend around. We have been through every other aspect of school together it only made sense that we would work in the same lab for our Master's! I seriously don't know anyone else who could keep me on track, and work as well with me as you did. We are like two peas in a pod and I'm so happy we went through one more adventure together!! To Gina, although you may be team placenta I still had the best time with you! I am so happy we met in the lab and started our journey through school together right here! So many memories started in the MacPhee lab and I can't wait to see what else is in store for us as we go through medical

school together! Loves ya! Trina, although our time was short in the lab together, you were always there whenever I needed help or an answer to a question. Thank you for your guidance! To Ewa; you have seriously saved my behind so many times with your lab knowledge and advice. I actually don't know if I would have graduated without you! You were always there for guidance, helping with an experiment or just for a chat. I will miss our time in the lab together for sure! To Justin, another member of team placenta! I love that you love T Swift as much as the rest of us and you definitely shared a lot of laughs with us in the lab! Thanks for making the lab an enjoyable place to be. And finally, thank you to Mandy. Mandy, you were like my lab mother. You showed me all the ropes and held my hand through all of my first experiments and helped me learn. I also learned a lot about online shopping and discovered many new places like Charlotte Russe…for that my wallet does NOT thank you haha!

I would also like to thank my supervisory committee, Drs. Reza Tabrizchi and Karen Mearow for all their insight and excellent suggestions. Finally, I would like to thank my family and friends for all of their love and support throughout the years. This degree would not have been possible without your help.

This research was supported by an operating grant from NSERC (National Sciences and Engineering Research Council) and an Alexander Graham Bell Canada Graduate Scholarship from NSERC.

Table of Contents

List of Figures

List Of Tables

Abbreviations

ACTH	adrenocorticotropic hormone
AD1/2	activation domains
Akt	protein kinase B
ANOVA	analysis of variance
ATP	adenosine triphosphate
BSA	bovine serum albumin
CaM	calmodulin
cAMP	cyclic adenosine monphosphate
CAP	contraction associated protein
CASP3	caspase 3
ChIP	chromatin immunoprecipitation
Cont	Contractile
CRH	corticotrophin-releasing hormone
d	day
DAPI	4',6-Diamidino-2-Phenylindole
DBD	DNA-binding domain
ddH_2O	double deionized water
DHEA	dehyroepiandrosterone
DHEA-S	sulfated dehydroepiandrosterone
DMEM/F12	Dulbecco's modified Eagle's medium nutrient mixture F-12
DNA	deoxynucleic acid
DSIF	DRB sensitivity-inducing factor
ECL	electrochemiluminescence
ECM	extracellular matrix protein
EDTA	ethylenediaminetetraacetic acid
ER	estrogen receptor
FAK	focal adhesion kinase
FBS	fetal bovine serum
FitC	fluorescein isothiocyanate
FN	fibronectin
G	gravid
HBSS	Hank's Balanced Salt Solution
HPA	hypothalamic-pituitary-adrenal axis
h	hour
HRP	horseradish peroxidase
HR-A/B/C	heptad repeats
HSE	heat shock element
Hsf	heat shock factor
Hsp	heat shock protein

HSR	heat shock response
hTERT-HM	Human Telomerase Reverse Transcriptase- Human Myometrial cells
IGF	insulin-like growth factor
IgG	immunoglobulin G
IRS	insulin receptor substrate
kDa	kilodalton
L	Litre
Min	minute
MLCK	myosin light chain kinase
MLC	myosin light chain
mRNA	messenger ribonucleic acid
mTOR	mammalian target of rapamycin
MTS	3-(4,5-dimethylthiazol-2-yl)-5-(3-carboxymethoxyphenyl)-2-(4-sulfophenyl)-2H-tetrazolium
NELF	negative elongation factor
NG	non-gravid
NP	non-pregnant
nPR	nuclear progesterone receptors
PARP-1	poly(ADP)-ribose polymerase 1
PBS	phosphate buffered saline
PCR	polymerase chain reaction
PDSM	phosphorylation-dependent sumoylation motif
PFA	paraformaldehyde
pI	isoelectric point
PI3K	phosphoinisitide-3-kinase
PMS	phenazine methosulfate
PP	post-partum
PR	progesterone receptor
PR- A/B/C	progesterone receptor A/B/C
pSer230 HSF1	phosphorylated HSF1
pSer303 HSF1	phosphorylated HSF1

P-TEFb	positive transcription elongation factor b
RD	regulatory domains
RIPA	radioimmunoprecipitation assay
RNAP II	RNA Polymerase II
S6K1	S6-kinase-1
SDS	sodium dodecyl sulfate
SDS-PAGE	sodium dodecyl sulfate polyacrylamide gel electrophoresis
Ser	serine
sHsp	small heat shock protein
SMC	smooth muscle cell
SSC	saline sodium citrate buffer
SUMO	small ubiquitin like modifier
TBST	tris-buffered saline-tween
TSS	transcription start site
TUNEL	terminal deoxynucleotidyl transferase dUTP nick end labeling
V	volts
VP	vasopressin
XChIP	cross-linked ChIP

Chapter One

Introduction

1.1 Preterm Birth

Preterm birth is the most common cause of perinatal mortality and morbidity in the developed world and is characterized as any infant born before the full 37 weeks of human gestation (Lumley 1993). In Canada, approximately 75-85% of all infant deaths, excluding babies with congenital defects, are a direct result of preterm birth (Shynlova et al., 2009). In 2005, it was estimated that 9.6% of births worldwide (or 12.9 million births) were preterm, with the majority of these births (11.9 million or 92.3%) occurring in Africa, Asia, Latin America, and the Caribbean (Beck et al., 2010). Preterm babies with weights lower than 2500 g occur in 10% of the total babies born every year. As these babies have a higher risk of long-term health defects, preterm birth has become a problem of huge clinical importance (Garfield & Maner, 2007). Furthermore, in the past 20 to 30 years the incidence of preterm birth has not decreased, and is actually higher in certain population groups including within Canada (Challis 2001). This increase is most prominently observed in more high-income countries as the rate of medically indicated preterm babies in singleton births increases along with the number of pregnancies that are conceived with assisted reproductive technologies (Goldenberg et al., 2008).

Preterm birth is often associated with a variety of long-term health defects such as cerebral palsy, blindness, deafness, respiratory illness and complications resulting from their stay in intensive care (Hack & Fanaroff, 1999; Ward & Beachy, 2003). Approximately 30% of preterm births occur as a result of an underlying infectious

process, while 50% are of unknown origin (Challis, 2001). There are also several established risk factors for preterm labour such as previous low birth weight or preterm delivery, placental anomalies, cervical and uterine anomalies, gestational bleeding, in vitro fertilization pregnancy, infection, and cigarette smoking (Creasy et al., 1980; Goldenberg et al., 1996). There is also a substantial cost in simply caring for preterm babies. In Canada, the direct medical costs of the initial hospital stay for preterm births is approximately $20 million per year (Lasiuk et al., 2013).

As of now, there is no treatment to prevent preterm labour, which is one of the underlying reasons for the high mortality rate associated with the condition (Garfield & Maner, 2007). Therefore, the main goal of research in this field is to gain a better understanding of the normal process of myometrial differentiation during pregnancy, including how the uterus becomes a highly contractile tissue. This information is critical if better methods to detect, diagnose, and prevent preterm labour are going to be developed.

1.2 The Myometrium: An Overview

The uterus is a hollow organ, found only in females, and is located within the pelvis. It is composed of three distinct layers: a well-differentiated lining (endometrium), a thick muscular wall (myometrium) and a serosal outer layer (Aguilar & Mitchell, 2010). Throughout the course of pregnancy, the uterus undergoes major physiological adaptations to accommodate the developing fetus, placenta and amniotic fluid (Shynlova et al., 2007). As a result, the non-pregnant uterus has a volume of

approximately 10 mL, whereas, at term, the uterus has a volume of approximately 5L (Monga & Sanborn, 1995). The uterus as a whole serves two major functions during pregnancy: 1) to harbour the fetus and placenta in a safe and calm environment and 2) to coordinate the smooth muscle contractions at both the appropriate time and strength necessary to expel the fetus into the extra-uterine environment (Hertelendy & Zakar, 2004). In the latter case, the contractions are mediated by the smooth muscle component of the uterus termed the myometrium.

Smooth muscle is incredibly adaptable to changes in its environment and can accommodate the large amount of stimuli that act upon it (Taggart & Morgan, 2007). Therefore the myometrium, composed solely of smooth muscle, is vital in aiding several processes involved in reproduction, such as sperm and embryo transport, implantation and most notably, parturition (Aguilar & Mitchell, 2010).

The rat myometrium has two very distinct muscle layers, the longitudinal muscle layer and the circular muscle layer, neither of which are distinctly recognizable in the human uterus (Huszar & Naftolin,1984). The longitudinal muscle layer in cross section appears as muscle bundles that run the length of the uterine tube, whereas the inner circular muscle layer, located next to the endometrium, runs circumferentially around the uterine horn. Both myometrial layers are fed by an extensive layer of blood vessels, known as the vascular plexus, which runs between the two layers (Shynlova et al., 2005; Williams et al., 2010; Figure 1.1).

Figure 1.1 Diagrammatic representation of the rat uterus. On the left is a diagram representing a pregnant rat uterus. On the right is a non-pregnant rat uterus. On the bottom is a representation of a cross section of a rat uterine horn showing all the muscle layers. The smooth muscle is composed of two layers, an outer longitudinal layer and an inner circular layer. Under a light microscope, the longitudinal layer in cross section appears as muscle bundles while the circular layer encircles the length of the tube next to the endometrium. Both layers work in unison to expel the fetus by producing strong contractions during parturition. Figure from Peach, 2010.

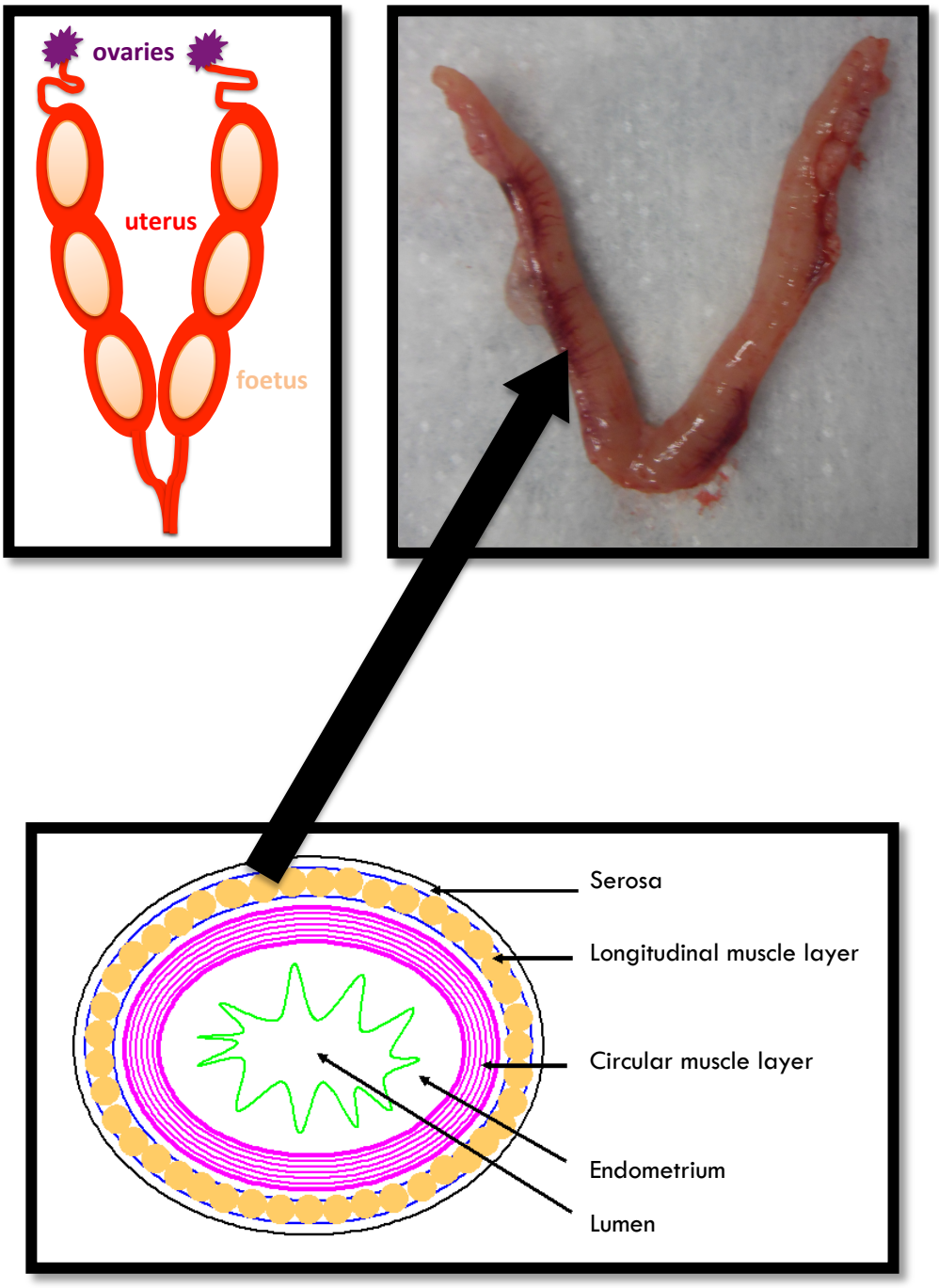
ovaries
uterus
foetus
Serosa
Longitudinal muscle layer
Circular muscle layer
Endometrium
Lumen

1.3 Regulation of Smooth Muscle Contraction

The smooth muscle cells (SMCs) of the uterus are composed of actin-containing thin filaments and myosin-containing thick filaments arranged in long bundles that extend around the periphery of the cell. Hence, they are not arranged in sarcomeres like other muscle types (Guilford & Warshaw, 1998). A third filament, the intermediate filament, has also been found in the cytoplasmic space of smooth muscle and is thought to act as anchorage sites for these thick and thin filaments (Bond & Somylo, 1982). It is this arrangement that allows for the sliding-filament crossbridge theory to be applied to uterine smooth muscle. This means that uterine contraction depends upon the interplay between these muscle fibres arranged approximately between successive myocytes (Kelly & Rice, 1969; Mounier & Arrigo, 2002).

In SMCs there are two predominant forms of actin, α- and γ-actin (Aguilar & Mitchell, 2010). Smooth muscle also has a different type of myosin, where the ATPase activity is much slower, which decreases the rate of crossbridge cycling and lengthens the contraction phase. This type of myosin contains regulatory protein chains, called myosin light chains (MLC), located in the neck region of the myosin filament. These elements of the cytoskeleton have several functions in terms of structure and flexibility that help to generate force from the muscle fibres (Herrera et al., 2005; Silverthorn, 2010).

The contractile cycle of activation, involving these actin and myosin filaments for smooth muscle depends heavily on the movement of several ions; Na^{+}, Ca^{2+} and Cl^{-} ions moving into the cytosolic compartment from the extracellular space, and movement

of K^+ ions into the extracellular space from the cytosolic compartment (Taggart & Morgan, 2007). When the cytosol experiences an increased concentration of calcium, depolarization occurs, and thus the contraction cycle is initiated (Wray, 1993). The sarcoplasmic reticulum releases the calcium, which then enters the cytoplasmic fluid (Garfield & Maner, 2007). The next step involves a cytosolic calcium binding protein, calmodulin, which is activated upon the binding of four calcium ions. This is an additional difference from skeletal muscle in which calcium binds to troponin, which is lacking in smooth muscle (Silverthorn, 2010). The calcium-calmodulin complex activates the enzyme myosin light chain kinase (MLCK) by inducing a conformational change. In the presence of ATP, MLCK can then phosphorylate the MLCs, located in myosin heads (Aguilar & Mitchell, 2010). Specifically, MLCK will phosphorylate Serine 19 on MLC and it causes another conformational change. The conformational change occurs in the neck region of the heavy chains of the myosin motor. This is change in shape is what allows for the formation of the crossbridges between actin and myosin filaments (Aguilar and Mitchell, 2010). The myosin motor chains also undergo a conformational change from their folded state to an extended state. This allows for the myosin crossbridges to be able to slide along the actin filaments and thereby create muscle tension, or what is known as a power stroke (Taggart & Morgan, 2007). Once the calcium levels decrease, the smooth muscle relaxes until the next stimulus causes the cycle to start again (Silverthorn, 2010; Figure 1.2).

Figure 1.2 Smooth muscle components involved in contraction. Myosin thick filaments and actin thin filaments are anchored to dense bodies and comprise the contractile elements of smooth muscle. The movement of the actin thin filaments is caused by phosphorylation of myosin light chains followed by ATP hydrolysis by the myosin II ATPase. Myosin II, composed of two heavy chains, two light chains and two regulatory light chains, gets phosphorylated forming a cross bridge between the actin and myosin filaments. This cross bridge formation also changes the angle of the neck region of myosin, causing motion of the actin thin filaments, which ultimately results in shortening of the cell. Thus, the ATP hydrolysis by myosin II ATPase causes the distance between the anchor points to decrease, resulting in contraction. Figure from Aguilar and Mitchell, 2010 (Appendix B).

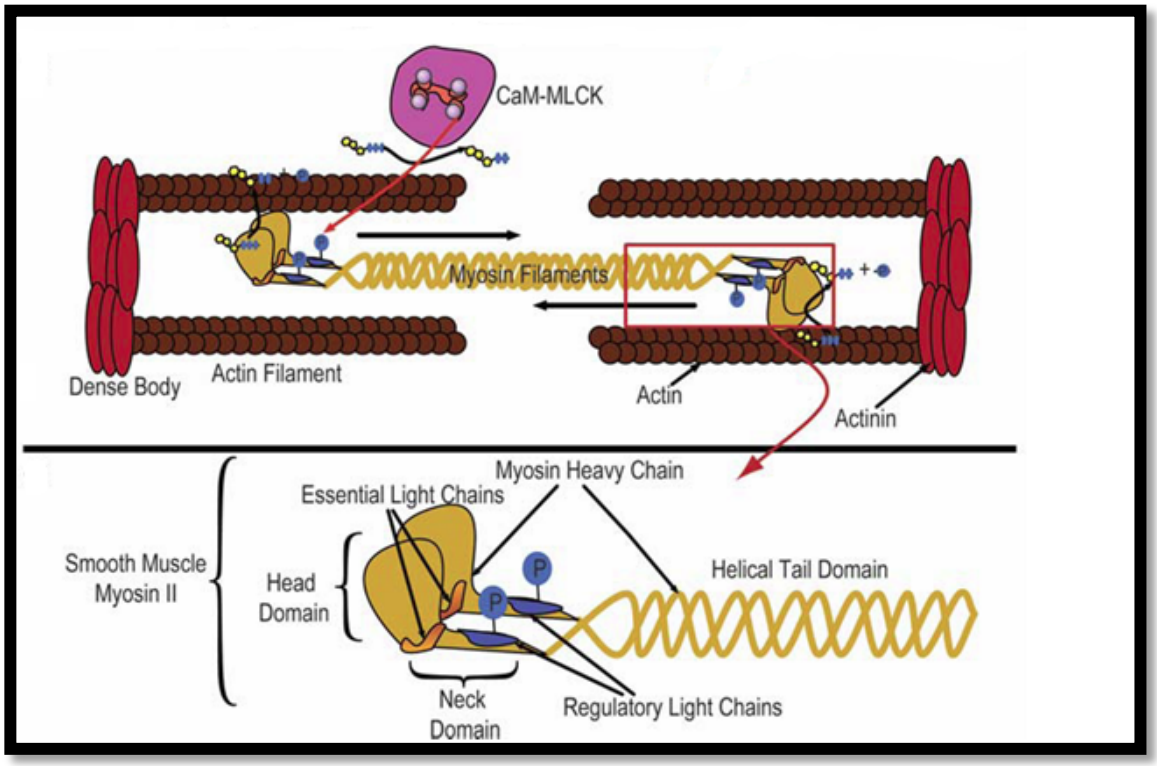
CaM-MLCK
Myosin Filaments
Dense Body
Actin Filament
Actin
Actinin
Myosin Heavy Chain
Essential Light Chains
Smooth Muscle
Myosin II
Head
Domain
P
P
Helical Tail Domain
Neck
Domain
Regulatory Light Chains

1.4 Parturition

While the mechanism of smooth muscle contraction, and how it is used to expel the fetus, is understood, the exact mechanism(s) of what initiates human parturition is not fully understood; however, the general sequence of events in parturition are known. Once contractions begin, a positive feedback loop involving hormonal and mechanical factors is initiated. It is thought that these mechanical factors, namely the initial uterine contractions, are what causes the first release of oxytocin from neurons in the hypothalamus, which are upregulated during late pregnancy (Carson et al., 2013). The fetus, usually head down, moves to the lower abdomen and is pushed on the already softened cervix promoting a neuroendocrine reflex that stimulates oxytocin secretion from the pituitary, which drives uterine contraction. Thus, the pushing on the cervix instigates a positive feedback loop to release more oxytocin, causing stronger and more frequent contractions to occur (Neumann et al., 1996). The wave of contraction starts from the top of the uterus and moves downwards towards the cervix to push the fetus further down towards the pelvis. There is also evidence that this increase in oxytocin secretion may stimulate production of prostaglandins in the uterus that cause even further contractions to help expel the fetus (Blanks & Thorton, 2003).

The contractions intensify even more, and push the fetus through the vagina and out of the maternal body. The placenta, then unattached from the fetus, is expelled a little later (Silverthorn, 2010). Despite a sound understanding of the events involved in parturition, the exact molecular mechanisms regulating the transition of the normally quiescent myometrium into a powerful, contractile tissue remain poorly understood. It is

this limited knowledge that restricts the treatments for preterm labor (López Bernal, 2007).

1.5 Phases of Myometrial Differentiation

Throughout pregnancy, the uterus, especially the myometrium, undergoes several changes and remodels to accommodate the growing fetus (reviewed by Challis et al., 2000). As a result of mechanical stretch and hormonal influence, the SMCs of the myometrium differentiate through four separate phases during gestation: an early proliferative phase, an intermediate synthetic phase, a phase where cells assume a contractile phenotype, and the final phase where the cells become highly active and committed to labour (Shynlova et al., 2009). Since this thesis is focused around the rat model of the uterus, this section will concentrate on the phases of rat myometrial development (Figure 1.3).

1.5.1 Proliferative Phase

The proliferative phase of myometrial development occurs from d1 of pregnancy until approximately d14. Proliferation is described as a period of rapid uterine myocyte proliferation; also termed hyperplasia. This increase in cell number occurs predominantly in the longitudinal layer of both gravid and non-gravid horns of unilaterally pregnant rats, which suggests the stimulant of this phase may be primarily endocrine related and not induced by mechanical signals (Shynlova et al., 2006). The uterine muscle proliferation was confirmed by Shynlova and colleagues (2006) when

Figure 1.3 The phases of myometrial differentiation over gestation. From NP- d14 the uterus is in the proliferative phase which is characterized by an increase in cell number, also known as hyperplasia. During this phase, the myometrial smooth muscle cells (SMCs) proliferate. From approximately d14-d21 the uterus enters the synthetic phase, where the cells no longer increase in number, but rather in size. In particular, cells associated with the extracellular matrix are associated with this increase in size, or hypertrophy. d21 marks the transition into the contractile phase, where the myocytes begin to develop into a contractile phenotype. This stage lasts until d23 when the rat is in labour. When in labour, the myometrium is highly active and responsive to uterine agonists. This active uterus is then able to form coordinated contractions which eventually lead to the expelling of the fetus. Figure adapted from Peach, 2010.

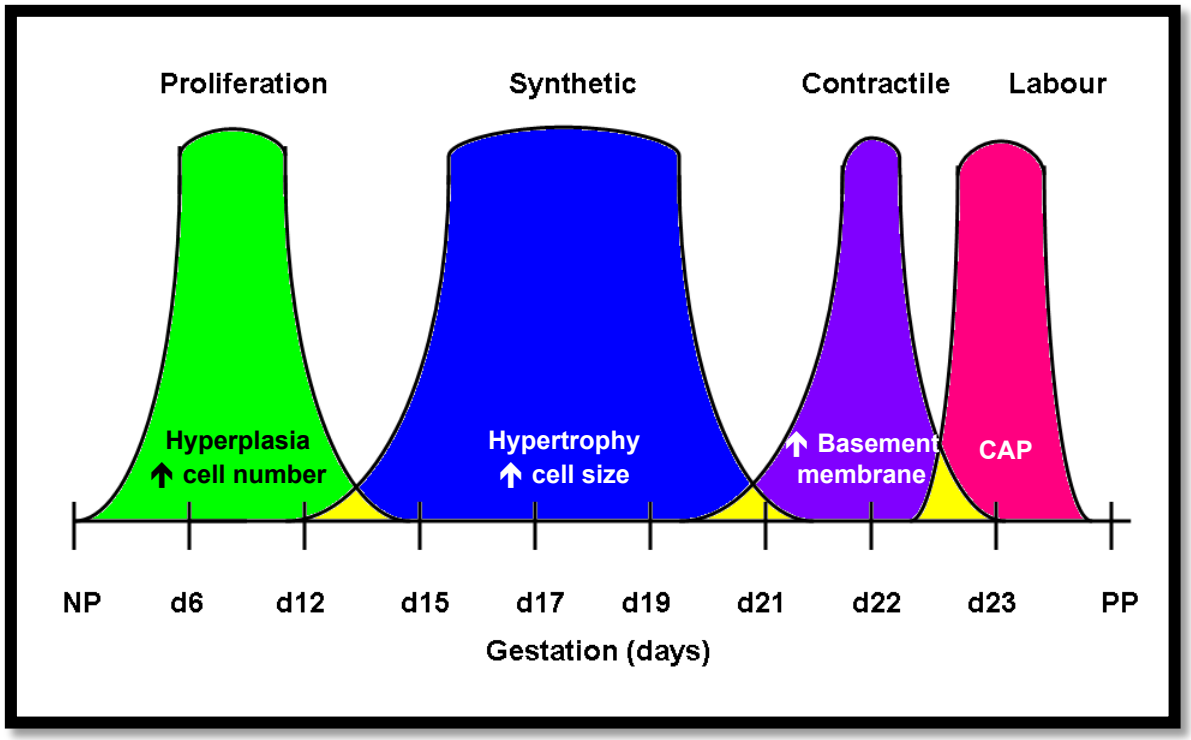
Proliferation
Synthetic
Contractile
Labour
Hyperplasia
↑ cell number
Hypertrophy
↑ cell size
↑ Basement
membrane
CAP
NP
d6
d12
d15
d17
d19
d21
d22
d23
PP
Gestation (days)

they detected an increased incorporation of 5-bromo-2'-deoxyuridine incorporation, a well-known indicator of hyperplasia, in uterine myocytes during the early phase of pregnancy.

Endocrine signals, such as 17β- Estradiol and the insulin-like growth factor (IGF) system play an important role in regulating the cell proliferation cycle in various tissues (Le Roith, 2003; Yin et al., 2007). In fact, both the 17β- Estradiol and IGF-I signalling pathways have been shown to be interconnected in human endometrial cancer models whereby IGF signalling was blocked and resulted in a reduced proliferative effect of 17β- Estradiol in the human endometrium cells (Gielen et al., 2005). Also, Lye and colleagues (2001) showed in non-pregnant models that myometrial proliferation is induced by estrogen-regulated growth factors like IGF-1 and EGF. Both factors are able to induce cell proliferation in reproductive tissues by a cascade of reactions initially through phosphorylation of insulin receptor substrate (IRS) and recruitment of phosphoinositide-3-kinase (PI3K; Jaffer et al., 2009). Protein kinase B (Akt) is subsequently phosphorylated and positively regulates the mammalian target of rapamycin (mTOR). mTOR is a serine/threonine kinase that is critical in the growth and development of cells (reviewed by Cornu et al., 2013). mTOR forms two multiprotein complexes which have slightly different functions in cellular development; mTORC1 results in activation of transcription, ribosome biosynthesis and protein synthesis, whereas mTORC2 regulates the actin cytoskeleton and cell polarity (Wullschleger et al., 2006).

Once mTORC is activated, it too will activate several downstream targets that are known to initiate and promote processes such as translation, which would result in an increase in cell number. One such target of mTOR is S6-kinase-1 (S6K1), a kinase that phosphorylates S6, a protein component of the 40S ribosomal subunit (Ruvinsky et al., 2005). Once S6 is phosphorylated, it becomes activated and results in an increase in both ribosomal biogenesis as well as cellular capacity for protein synthesis (Lee et al., 2007).

Jaffer et al (2009) analysed the protein levels of PI3K, mTOR and S6K1 throughout gestation in the rat myometrium. They found that the phosphorylated forms of these three proteins were highly upregulated during the proliferative phase of gestation, which strongly suggested that activation of the PI3K/mTOR pathway was responsible for the induction of myometrial hyperplasia during early gestation. It was further demonstrated that inhibition of mTOR signalling in the myometrium through the administration of rapamycin to pregnant rats, reduced the number of proliferating cells in the pregnant rat myometrium which confirmed the vital role of mTOR in proliferation of the tissue (Jaffer et al., 2009).

The total increase in cell number during proliferation depends on the balance between total cell production and total cell loss. Specifically during the proliferative phase, one would expect to see an increase in mitotic activity accompanied by a decrease in programmed cell death, i.e. apoptosis (Shynlova et al., 2006). Since the proliferative phase is concerned mainly with the increase in cell number, the amount of cell death, or apoptosis, must be regulated. Apoptosis is defined as a physiological process by which excess or dysfunctional cells are removed during development or normal tissue

homeostasis (Vandaele & Van Soom, 2011). This process becomes particularly important in dynamic systems, such as reproduction and in many tissues like the placenta, the endometrium, mammary glands, and the myometrium (Leppert, 1998; Mu et al., 2002). In fact, some anti-apoptotic factors have been shown to be highly expressed during the proliferative phase, such as Bcl-2. It is thought that it has a role in contributing to the overall increase in cell number by decreasing the level of apoptosis and therefore allowing cell proliferation to occur (Shynlova et al., 2009).

1.5.2 Synthetic Phase

While the proliferative phase is a period of uterine growth caused by an increase in cell number, the subsequent synthetic phase is due to an increase in cell size known as hypertrophy (Shynlova et al., 2009). In the rat, it occurs from approximately day 15 to approximately day 21 and is marked by an increase in the protein:DNA ratio of the myometrium as well as a marked increase in the thickness of the uterine muscle (Shynlova et al., 2006). It is a period of time where there is significant synthesis and deposition of the interstitial matrix through expression of interstitial matrix proteins such as collagen I (Harkness & Harkness, 1954). In fact, Shynlova and colleagues (2004) showed a peak in the expression of fibrillar collagens (type I and III) at d19 during rat gestation which then decreased until labour. This extra-cellular matrix (ECM) is required to form the ground substance of the myometrium, which plays a crucial role during labour (White et al., 2011). Furthermore, this hypertrophic phase is characterized by: an increase in cellular protein synthesis such as thick, thin and intermediate filaments, increases in cellular organelles such as mitochondria, and finally a transition

into a more contractile phenotype which varies in protein content and organization (Shynlova et al., 2006).

The synthetic phase has also been found to coincide with the activation of apoptotic cascade machinery (Shynlova et al., 2006). Several apoptosis-promoting caspases such as 3, 6 and 7 are upregulated near the beginning of the synthetic phase; however, Shynlova et al (2006) showed, through terminal deoxynucleotidyl transferase dUTP nick end labeling (TUNEL), that labels terminal ends of fragmented deoxynucleic acid (DNA), that there was no evidence of apoptosis occurring in the rat myometrium. Thus, these caspases may have additional unknown roles in the myometrium at this time.

During this phase there is enhanced expression of focal adhesions, which aid in critical cell-ECM communication as the cells get bigger. Focal adhesions are clusters of integrin receptors that are the sites where extracellular ligands are coupled to cytoplasmic F-actin, (a major component of muscle fibre thin filaments) allowing for critical cell-matrix interactions to occur, which will become crucial for proper regulation of the subsequent contractile and labour phases (Williams et al., 2005; Shynlova et al., 2009). This adhesion formation also involves the interaction of several signaling proteins such as FAK, paxillin and adapter proteins like vinculin (MacPhee & Lye, 2000). It is also associated with an increased expression of ECM proteins, which are crucial to anchor other growing cells to the surrounding matrix proteins. During this phase, several different types of ECM molecules can be found in uterine muscle like collagen type IV, laminin and fibronectin (Shynlova et. al, 2009).

The major regulators of myometrial growth during the synthetic phase were recently determined by Shynlova et al (2010). They were able to directly correlate the extensive rat myometrial growth during this stage of pregnancy with a threefold increase in myocyte size. Through stretch studies using the unilaterally pregnant rat model, they were able to determine that the major cause of this growth was uterine distension caused by the fetus in normal gestation. The stretched (pregnant) horn of the uterus had a myocyte volume approximately 3-fold larger than the non-gravid (non stretched) horn.

Although the synthetic phase is clearly dependent on physical influences, hormones, such as progesterone are also important in regulating the synthetic phase of myometrial development in the rat (Shynlova et al., 2004). Progesterone has several crucial roles in the myometrium during gestation such as support of uterine growth, matrix synthesis and the inhibition of contractile associated protein (CAP) expression. Lye and colleagues (2001) showed for example that when mifepristone (RU486), a competitive progesterone receptor antagonist, was administered during this period, hypertrophy was significantly reduced. Shynlova and collegues (2004) also demonstrated that administering RU486 to pregnant rats during the synthetic phase at d17 resulted in an interruption of hypertrophy and poor uterine development. Essentially, progesterone is important for the cessation of labour, as removal of the source of progesterone earlier than day 23 in the rat results in termination of pregnancy (Ou et al., 1998). Progesterone also appears to be a crucial regulator of several genes encoding ECM proteins required to form the aforementioned interstitial matrix such as collagen I, collagen III and elastin as inhibition of progesterone action resulted in decreased expression of these proteins (Shynlova et al., 2007).

1.5.3 Contractile Phase

At approximately day 21 of pregnancy the myometrium transitions into the contractile phase, a phase dedicated to preparing the uterus for labour. Here, hypertrophy has stabilized and there are marked changes around the myocyte, but also in the interaction between the myocyte and the underlying matrix (Shynlova et al., 2009). Another change is that proteins that were expressed earlier in gestation are now expressed as different isoforms. For example, more γ-actin is expressed in this phase compared to the α-smooth muscle actin expressed in non-pregnant situations (Shynlova et al., 2005).

Although the exact mechanism by which this phase arises is unknown, Shynlova et al. (2010) have previously shown that this phase may be regulated by mechanical stretch in the uterus caused by the growing fetus. In a unilateral stretch study, it was reported that the gravid, or stretched, horn produced increased levels of caspase 3 (CASP3), an effector protein that cleaves cellular substrates and promotes morphological changes and/or cell death in the myometrium. The upregulation of this protein in the gravid horn suggests that stretch is important in cellular differentiation in the uterus (Shynlova et al., 2010).

The transition into this phase is also marked by a distinct change in the synthesis of matrix proteins, specifically those that form the basement membrane to which the myocytes will anchor themselves in order to ensure cohesive contractions throughout the myometrium (Robinson et al., 2004; Williams et al., 2005). Shynlova and colleagues (2009) demonstrated a significant upregulation of fibronectin (FN), laminin β2 and

collagen IV expression that coincided with the initation of the contractile phase and the expression of these proteins remained high until term. They showed using immunofluorescent detection procedures that during the synthetic phase, these proteins were only detectable sporadically around myocytes, however, during the contractile phase they were detected as continuous and organized structures.

Like other phases in myometrial development, this phase is regulated by both hormonal and mechanical influences. This was shown in an earlier study by Shynlova and colleagues (2004). Through unilateral stretch studies, the increased expression of the aforementioned proteins was found to occur as a result of a drop in progesterone levels. In fact, when RU486 was administered before d21 in pregnant rats it induced the switch from interstitial matrix protein synthesis to basement membrane protein synthesis. The authours observed an increase in mRNA levels of collagen IV, fibronectin and laminin,. They also found that this increase in basement membrane protein expression only occurred in the gravid horn, which strongly implied that uterine stretch regulated expression of these proteins.

1.5.4 Labour

At approximately d23 of gestation, the myometrium switches into the final phase of development, the labour phase. This stage is marked by a decrease in the levels of progesterone and is the stage where the myometrium becomes fully committed to the development and execution of intense coordinated contractions, which will result in the expulsion of the fetus (Lye et al., 2001). In order to evoke these coordinated contractions, the phenotype of the SMCs must change in order for these cells to interact

in a more synchronized manner. This is elicited, at least in part, through the FAK signalling pathway. During labour, a notable decrease in FAK activity has been reported in the rat myometrium, which may suggest that myocytes are anchoring to the basement membrane (MacPhee and Lye, 2000). It has been shown that decreased FAK activity is associated with the formation of stable SMC-ECM interactions which form focal adhesions and thus connect the ECM matrix to the actin cytoskeleton through clusters of integrin molecules (Ilić et al., 1995). This anchorage reinforces the ligand-integrin interaction, which through cell-ECM communication will allow for smooth muscle cohesive contractions during labour (Shynlova et al., 2009). Essentially, these now formed focal adhesions act as the primary points for force transduction, and thereby allow the myocytes to work as a mechanical syncytium (Williams et al., 2005).

During the contractile phase, uterine growth has ceased but fetal growth continues, which places an enormous tension on the myometrium. This stress will signal the expression of a cassette of genes to form contractile associated proteins (CAPs) such as the sodium channel, oxytocin receptor, prostaglandin F receptor, and Cx43 which is a gap junction protein needed to increase the electrical excitability of myocytes (reviewed by Shynlova et al., 2009, Mitchell & Lye, 2002; Ou et al., 1997; Ou et al., 1998). CAPs are thought to be substances that modulate myometrial tone and contractility within the myometrium throughout labour. For example, Lye et al (1993) found that Cx-43 transcripts in the rat myometrium were low or undetectable throughout most of pregnancy, but increased dramatically immediately before the onset of labor. It is thought that Cx-43 like other CAPs mediate the increased electrical coupling between cells within the myometrium during labor. Ou et al (1998) showed however that increased uterine

stretch and a decrease in progesterone levels are not adequate to induce expression of these labour dependent genes. Insertion of a polyvinyl tube at d17 in the rat myometrium, while progesterone levels were still high, did not induce labour. Similarly, administration of exogenous progesterone on d20, when uterine stretch was high, blocked labour or expression of CAPs as progesterone promotes relaxation, not contraction. Therefore, it has become widely understood that the labour phase is dependent on both mechanical and endocrine influences.

1.6 Small Heat Shock Proteins

In almost all organisms, from bacteria to humans, small heat shock proteins (sHsps) are ubiquitously distributed and their expression is induced by a multitude of stresses (Laskowska et al., 2010). To date, 10 sHsps (HspB1- HspB10) have been identified in mammals, with different but highly important roles (Golenhofen et al., 2004; Orejuela et al., 2007; Table 1.1). For example, HspB8 and HspB1 have been shown to have opposing functions with respect to apoptosis; HspB8 shows a pro-apoptotic activity in a cell-specific manner while HspB1 has an anti-apoptotic action both upstream and downstream of the apoptosome (Gober et al., 2003). In addition to heat, sHsps functionally respond to oxidative stress, osmotic stress, cold shock and heavy metals (Gusev et al., 2005; Laskowska et al., 2010).

Typically these small stress proteins are 15-40 kDa in size and are able to form large oligomeric complexes (Orejuela et al., 2007). The basic monomeric structure of all sHsps contains a conserved ~90 amino acid α-crystallin domain, which is found in the

Table 1.1 Characteristics and tissue distribution of mammalian small heat shock proteins (sHSPs). Adapted from Hu et al., 2007.

Protein name (old nomenclature in parenthesis)	pI	Mass (kDa)	Length (aa)	Tissue distribution
HspB1 (Hsp27)	6.4	22.8	205	Ubiquitous
HspB2 (MKBP)	4.8	20.2	182	Heart and muscle
HspB3	5.9	17.0	150	Heart and muscle
HspB4 (αA/CRY AA)	6.2	19.9	173	Eye lens
HspB5 (αB)	7.4	20.2	175	Ubiquitous
HspB6 (Hsp20)	6.4	16.8	157	Ubiquitous
HspB7 (cvHsp)	6.5	18.6	170	Heart and muscle
HspB8 (H11/Hsp22)	4.7	21.6	196	Ubiquitous
HspB9	9.0	17.5	159	Testis
HspB10 (ODF1/ODF27)		30	262	Testis

Defined abbreviations: pI= Isoelectric point, kDa= kilodaltons, aa= Amino Acids.

form of a β-sheet sandwich that dimerizes to form the basic functional unit of all sHsps. These β-sheets are composed of two layers of three and five antiparallel strands that are connected but an interdomain loop (van Montfort et al., 2001). Oligomerization then becomes possible because of the amino- and carboxy- terminal end of the monomers (Leroux et al., 1997). These oligomers have many different structures and are essential in the chaperone functions of sHsps (Laskowska et al., 2010). In fact, many sHsps must undergo phosphorylation and then subsequent oligomerization into multimeric complexes in order to evoke any function, but especially as molecular chaperones (Bruey et al., 2000; Arrigo et al., 2007). For example, Bruey et al, (2000) showed that when a mutated form of Hsp B1 was unable to form large oligomers, its protein expression and function was greatly reduced in colorectal cancer REG cells compared to cells that did not possess a mutated Hsp B1 protein.

Furthermore, most Hsps undergo some form of post-translational modifications, which influence the function of Hsps, such as deamidation, acylation, and most commonly, phosphorylation (Groenen et al., 1994; Gaestel 2002). For example, HspB1 has been shown to undergo crucial phosphorylation on three different serines, S15, S78 and S82. Phosphorylation on these sites can influence both the structure and function of HspB1, such as oligomerization, which is dependent on this post-translational modification (Landry et al., 1992). For example, phosphorylation of these sites has been shown to increase the molecular chaperone activity and thermotolerance of HspB1 (Thériault et al., 2004)

As ATP-independent chaperones, most sHsps bind misfolded proteins and prevent the formation of aggregates. They maintain protein solubility in times of stress

until other chaperones can refold them to their native state (Ehrnsperger et al., 1997). For example, HspB5 is one of the most abundant proteins in the mammalian eye lens to prevent protein aggregation, which may lead to the formation of cataract (Horwitz, 2009). Furthermore, these chaperones may have an important function in smooth muscle, such as the myometrium. An investigation by White et al., (2005) demonstrated that in the rat myometrium HspB1 has a potential role as a CAP as its mRNA expression has a distinct pattern of expression; peaking at d19 of rat gestation and then decreases until labour. Immunoblot analysis also showed that HspB1 has high protein expression late in pregnancy between day 21 and 1 day post-partum (PP) inclusive. Another study by Cross et al (2007) showed HspB6 was also present in the myometrium. Both HspB6 mRNA and protein expression decreased near the end of gestation, during labour and PP. This could indicate that HspB6 has a role in smooth muscle relaxation. While both HspB1 and HspB6 proteins have distinct patterns of expression throughout gestation, it remains unknown as to what is regulating their expression. Salinthorne et. al (2008) suggested that under normal conditions sHsps help maintain smooth muscle function such as maintaining cytoskeletal structure, normal redox conditions and regulating translation, whereas under times of stress, such as disease, they are responsible for helping the smooth muscle adapt to stress.

1.7 Heat Shock Transcription Factors

In order to maintain homeostasis in times of stress, a first line of cellular defense for an organism is a heat shock response (HSR), which results in the induced expression

of several Hsps (Akerfelt et al., 2007). This response is carefully regulated by a family of transcriptional activators, called heat shock transcription factors (Hsfs) which were discovered in the 1980s (Wu, 1984). In mammals, three active Hsf homologues are found: Hsf1, Hsf2, and Hsf4 (reviewed by Akerfelt et al., 2010). Each Hsf plays a different role in the HSR, but combined, form the required machinery for the specific transcription and translation of stress-related genes (Anckar & Sistonen, 2007).

Hsfs all have the same general structure, which is composed of several different functional domains (Akerfelt et al., 2010). The first domain is the DNA-binding domain (DBD) which is the best preserved domain in all Hsfs and is considered to be the signature domain for the family. It forms a compact globular structure and has a flexible loop that is located between β-strands 3 and 4. This loop is what allows for critical protein-protein interactions between other subunits of the Hsf trimer (Damberger et al., 1994). Trimer formation in turn results in high-affinity DNA binding. Hydrophobic heptad repeats (HR-A and HR-B) also assist in Hsf trimerization. They form a coiled coil structure, similar to that in a leucine zipper (Sorger & Nelson, 1989). This trimerization is inhibited by another hydrophobic repeat, HR-C (Rabindran et al., 1993). At the carboxyl terminus of all Hsfs, with the exception of yeast, is the transactivation domain (AD). The transactivation domain is composed of two modules, AD1 and AD2, which are rich in hydrophobic and acidic residues. Together these residues ensure a rapid and prolonged response to stress (Newton et al., 1996; Figure 1.4).

The HSR is a well understood process in all mammals. First the Hsfs all undergo some form of posttranslational modification, such as phosphorylation and sumoylation. Phosphorylation occurs in the regulatory domain of Hsfs, and has only been shown to

Figure 1.4 A modular representation of the heat shock factor 1 (Hsf1) protein. Hsf1 contains a DNA-binding domain (DBD), three heptad repeats (HR-A, HR-B and HR-C), a phosphorylation-dependent sumoylation motif (PDSM), a Regulatory domain (RD), and two activation domains (AD1 and AD2). The figure shows the DBD and several of the post-translational modification sites. The effect of acetylation on Lys-80 is still unknown however it is thought that this modification may prevent the DBD from binding to the HSE on target genes. Phosphorylation on Ser-230 causes an increase in the trans-activation capacity of Hsf1 whereas phosphorylation on Ser-303 and Ser-307 causes a loss of the transactivation capacity of Hsf1. Sumoylation is the addition of small ubiquitin like modifier (SUMO) protein which also results in a loss in the transactivation capacity of Hsf1. This modification is often mediated by phosphorylation on site Ser-303. From Akerfelt et al., 2010.

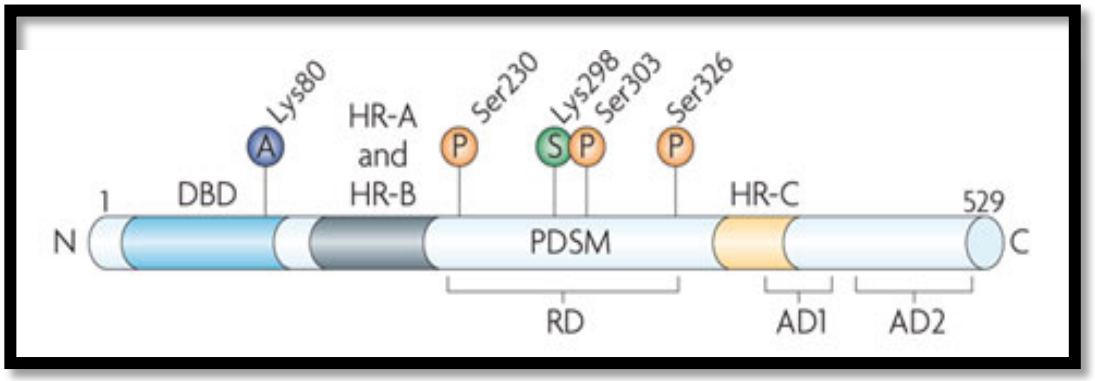
Lys80
A
HR-A
and
HR-B
Ser230
P
Lys298
Ser303
S
P
Ser326
P
1
DBD
HR-C
529
N
PDSM
C
RD
AD1
AD2

occur on serine (Ser) residues. Some examples of known phosphorylation sites are Ser 230, 303, and 307 (Knauf et al., 1996). Sumoylation occurs in a special motif, located in the regulatory domain, known as the phosphorylation-dependent sumoylation motif. It consists of an amino acid consensus sequence of I/L/ V-K-X-E-X-X-S-P and is located around amino acid position 297−304. It is implicated in repressing the transactivating capacity of Hsf1 (Hietakangas et al., 2006). The type of post-translational modification that does occur depends on what Hsf members are being activated. Once activated, the Hsfs often transition from their monomeric form to either a dimer or a trimer in an Hsf-specific manner (Akerfelt et al., 2007). Once fully activated, the Hsf binds to one of the multiple copies of a heat shock element (HSE) found in the promoter region of several Hsps and stress-inducible genes (Trinklein et al., 2004). HSEs all possess multiple inverted repeats of the same conserved sequence nGAAn. The DBD on the Hsf recognizes this HSE in the major groove of the double helix and binds to it (Akerfelt et al., 2007). Since the target gene contains more than one HSE, it allows Hsfs to bind cooperatively– when one Hsf binds, it facilitates the binding of the next transcription factor (Anckar & Sistonen, 2007; Figure 1.5).

1.8 Hsf1

Of the three mammalian Hsfs, Hsf1 is the recognized stress-responsive prototype. Its role cannot be replaced by any other Hsf, since mice that lacked Hsf1 had no HSR whatsoever (McMillian et al., 1998; Xiao et al., 1999; Akerfelt et al., 2007).

Figure 1.5 The mechanism of Hsf action. First Hsfs undergo some form of post-translational modification, such as phosphorylation and sumoylation. Once activated, the Hsfs often transition from their monomeric form to either a dimer or a trimer. Once fully activated, the Hsf binds to one of the multiple copies of heat shock elements (HSE) found in the promoter region of several heat shock proteins (Hsps) and stress/developmentally-inducable genes. Since the target DNA contains more than one HSE, it allows Hsfs to bind cooperatively– when one Hsf binds, it facilitates the binding of the next transcription factor. This all leads to the up-regulation of Hsps or other developmental genes, thus initiating the heat shock response (HSR). Adapted from Trepel et al., 2010.

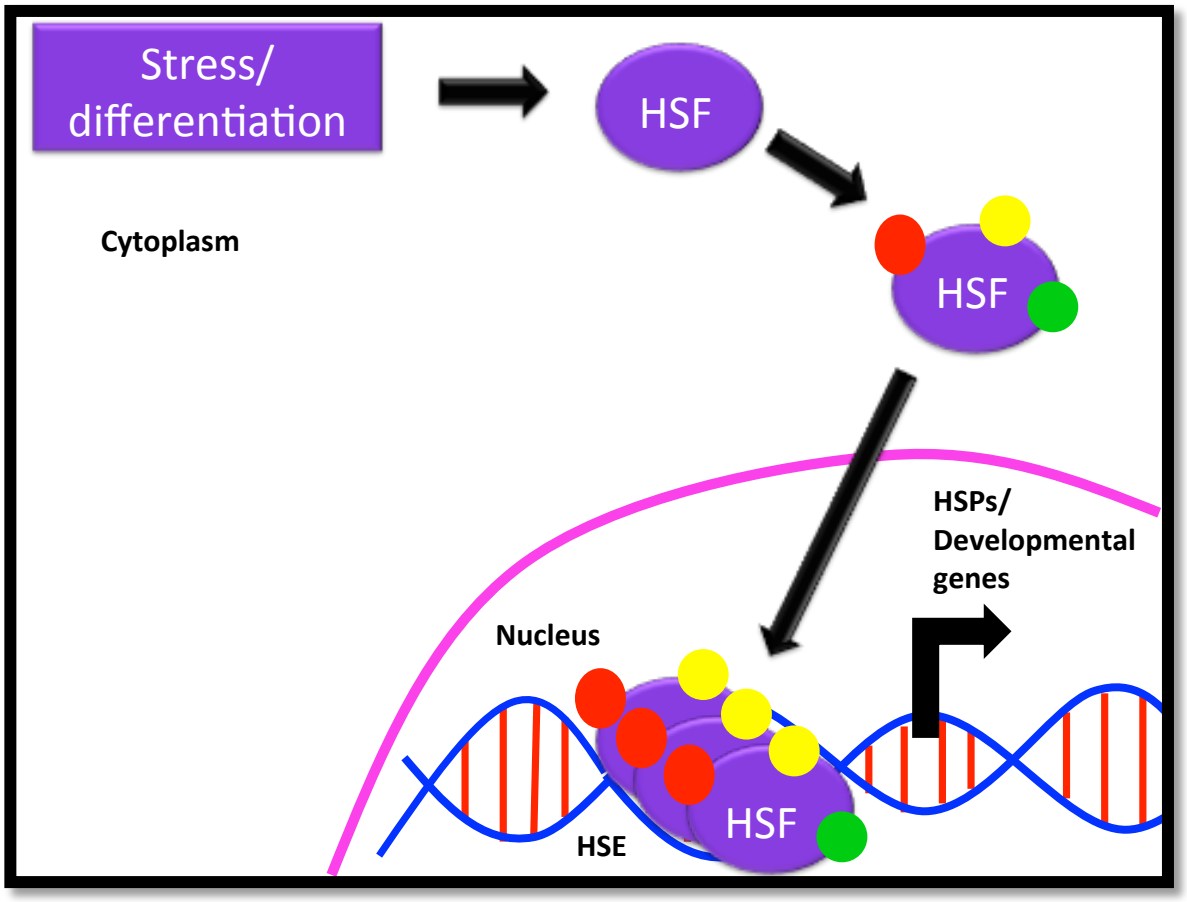
Stress/
differentiation
HSF
Cytoplasm
HSF
HSPs/
Developmental
genes
Nucleus
HSF
HSE

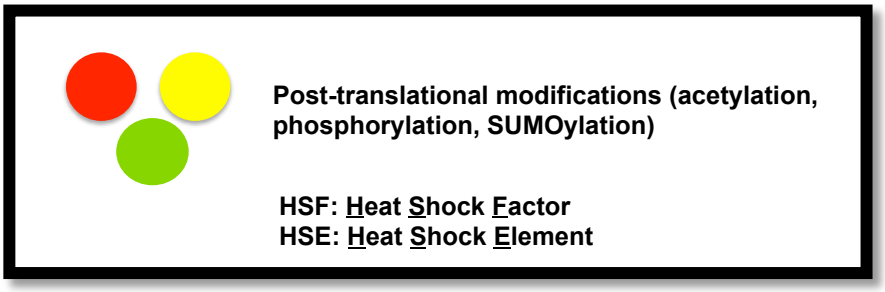
Post-translational modifications (acetylation, phosphorylation, SUMOylation)
HSF: Heat Shock Factor
HSE: Heat Shock Element

Under non-stressed conditions, Hsf1 remains in an inactive monomeric form in the nucleoplasm and to a much smaller extent in the cytosol (Anckar & Sistonen, 2007). Intramolecular interactions between the many leucine zippers present on Hsf1 are able to help stabilize and keep the protein in this inactive state (Cotto, 1996). Any number of developmental cues can cause Hsf1 to be activated, as long as they generate an increased number of non-native proteins (Anckar & Sistonen, 2007). Hsf1 is activated in the same way as all other Hsfs, including trimerization, movement to the nucleus and then binding to DNA (Akerfelt et al., 2007). Hsf1 can bind to any gene that contains a HSE in their promoter region and the HSE must also allow Hsf1 to bind in either its dimeric or trimeric form (Pirkkala et al., 2001). Hsf1 initiates the transcription of several Hsps, which act as molecular chaperones, such Hsp70, Hsp90 and HspB1 (Nadeau et al., 1993; Rasmussen & Lis, 1993; Holbrook & Udelsman, 1994). These Hsps start a negative-feedback loop and are able to inhibit any further activation of Hsf1 until another HSR is required (Westerheide et al., 2009). However, simply binding of Hsf1 to the target gene is not enough to activate transcription, but the exact mechanism of transcriptional activation by Hsf1 is still poorly understood. The best studied is the activation of Hsp 70; however Fossati et al (2006) has indicated that the mechanism of action is likely species and tissue specific. When a cell is exposed to heat shock, Hsf1 binds to HSEs in the promoter region of Hsp 70 and this binding then causes recruitment of positive transcription elongation factor b (P-TEFb) (Marshall et al., 1996). P-TEFb phosphorylates the C-terminal domain of RNAP II as well as the DRB sensitivity-inducing factor (DSIF) and the negative elongation factor (NELF) (Brès et al., 2008). This, in turn, causes the removal of NELF from the RNAP II, thereby facilitating

transcriptional elongation. Furthermore, the binding of Hsf1 to the HSE also results in an initial round of nucleosome displacement, which is regulated by the enzymatic activity of poly(ADP)-ribose polymerase 1 (PARP-1; Petesch et al., 2008). RNAP II moves across the *hsp70* gene as transcription-dependent chromatin arrangement occurs, which is likely facilitated by the actions of several histone assembly/reassembly factors such as suppressor of Tyrosine 6 and Facilitates Chromatin Transcription complex (Saunders et al., 2003; Ardehali et al., 2009; Figure 1.6).

In its trimeric form, Hsf1 was found to be heavily phosphorylated on at least 12 different serine residues located in its regulatory region (Guettouche et al., 2005). This phosphorylation of Hsf1 is most often a direct result of HSR activation (Jurivich et al., 1995). Currently, there are only two known phosphorylation sites on Hsf1 which lead to transactivation, Ser-230 and Ser-236 (Holmberg et al., 2001; Boellmann et al., 2004). These phosphorylation sites are thought to act as a switch that can overcome the inhibitory effect of the regulatory domain on the Hsf1 transactivation capacity (Anckar & Sistonen, 2007); however, it should be noted that although phosphorylation is the main form of Hsf1 activation, phosphorylation is not solely responsible for the initiation of transcriptional activity. In fact, phosphorylation of several sites, including Ser-303 and Ser-307, in the regulatory domain actually inhibit the transcriptional activity of Hsf1 (Knauf et al., 1996; Kline & Morimoto, 1997). These phosphorylated sites maintain Hsf1 in its inactive state, only to be overridden by heat shock (Anckar & Sistonen, 2007).

Although present in both higher invertebrates and vertebrates, Hsf1 is not required for survival; however it is required to maintain a normal body size, sufficient

Figure 1.6 Mechanism of Hsp70 gene activation with and without heat shock. A) In the absence of stress, the Hsp70 gene is not transcribed. RNA Polymerase II (RNAP II) is bound to a region 20-40 base pairs down stream of the transcription start site (TSS). In this position, it is kept inactive by the DRB sensitivity-inducing factor (DSIF) and the negative elongation factor (NELF). B) However in the presence of heat shock or stress, the transcription of the Hsp70 gene is allowed to occur. Hsf1 binds to the HSEs located in the promoter region, and this causes a recruitment of the positive elongation factor b (P-TEFb). P-TEFb promotes transcriptional elongation through its ability to phosphorylate RNAP II, DSIF and NELF, which results in the dissociation of NELF from RNAP II. Concurrently, Hsf1 also regulates the enzymatic activity of PARP-1 which once activated causes rapid nucleosome displacement. Adapted from Anckar & Sistonen, 2011.

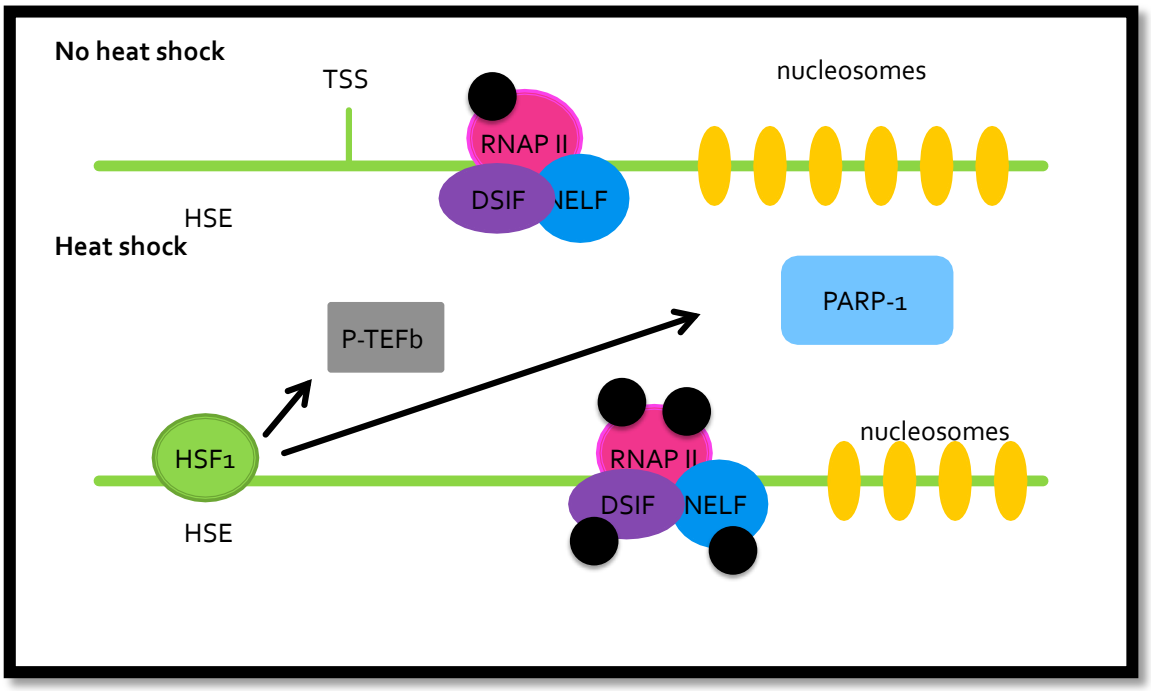
No heat shock
TSS
nucleosomes
RNAP II
DSIF
NELF
HSE
Heat shock
PARP-1
P-TEFb
HSF1
nucleosomes
RNAP II
DSIF
NELF
HSE

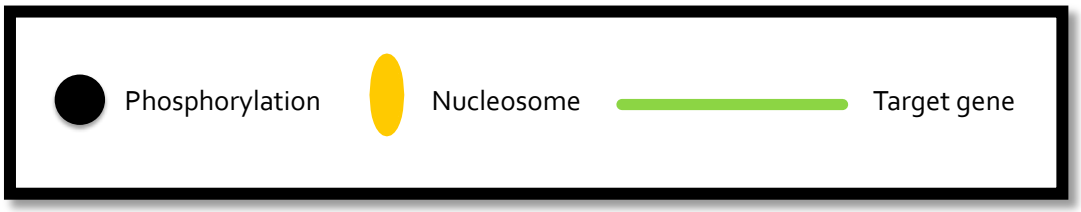
Phosphorylation
Nucleosome
Target gene

embryonic development and to prevent many reproductive disturbances (reviewed by Anckar & Sistonen, 2007). Specifically, Hsf1 null mouse embryos showed no extensive defects; however, the placenta was found to have abnormal architecture, suggesting a problem with the extra-embryonic tissue. Upon mating Hsf1-/- female with wild type male mice, no fertilized oocytes developed past the zygotic stage with two pronuclei and a second polar body. These two results show that Hsf1 is a maternal factor, necessary for early postfertilization development (Christians et al., 2000). Therefore, it was concluded that a disturbance in maternal Hsf1 could be one cause of infertility and high prenatal lethality in mammals (Anckar & Sistonen, 2007).

Several cancer studies have shown that in certain carcinomas, Hsf1 may in fact induce increased proliferation of tumour cells (Dai et al., 2007; Santagata et al., 2011). The exact mechanism for this is still poorly understood; however, it is thought that in the malignant state, the tumour cells endure a variety of stressors like hypoxia, acidosis, nutrient depletion, as well as immune attacks from the host, that lead to drastic changes in core cellular physiology that are hallmarks of cancer. Hsf1, being a stress-responsive protein, may permit cancer cells to cope with the stressors, allowing tumour cells to reconfigure their metabolism and protein homeostasis. Once homeostasis is maintained through Hsf1, only then can tumour cell proliferation occur. Calderwood and Gong (2011) have recently proposed a more causative effect; that Hsf1 protein expression increases as a result of pre-existing proliferation in order to initiate the HSR as a result of stress caused by the increased proliferation.

1.9 Objectives; Hypothesis

Very little information exists on the expression or the roles of Hsf1 in the rat myometrium during pregnancy. Previous work in the lab by Bryan White and Brandon Cross has shown expression of Hsf1 target genes HspB1 and HspB6, in the rat myometrium during pregnancy. Both proteins have robust expression in mid-gestation, however what regulates their expression remains unknown. Therefore, since HspB1 and HspB6 are Hsf1 target genes, the goal of this thesis was to characterize Hsf1 expression in the rat myometrium throughout pregnancy and to investigate a possible correlation between Hsf1 expression and the production of various Hsps throughout rat gestation. It was hypothesized that Hsf1 would be highly expressed in the myometrium during pregnancy and that it could be important during the proliferative phase of myometrium differentiation to activate expression of key genes necessary for this phase.

Significance: The expression of Hsf1 has never been examined in the myometrium, so the work described in this thesis will add novel data to the Hsf1 research field in defining the expression of Hsf1 in smooth muscle containing tissues. Hsf1 patterns of expression may also provide some clue as to what Hsps are upregulated as a result of Hsf1 expression.

General Research Plan:

I. To investigate if total Hsf1 protein expression changes temporally and/or spatially throughout gestation in the rat myometrium.

II. To determine the regulation of Hsf1 expression in the myometrium.

III. To perform *in vitro* experiments in human myometrial cell lines to see the effects of overexpression of Hsf1 on factors such as cell proliferation and expression of target genes.

Experiments utilized a pre-existing bank of frozen uterine tissue samples, tissue embedded in paraffin wax and tissue lysates collected by previous graduate students; Bryan White, Brandon Cross, Joy Williams and Mandy Peach. Additional samples were collected for this thesis when necessary to re-stock the bank, but all experimental work described in this thesis was performed by myself.

Chapter Two

Materials and Methods

2.1 Animals

Sprague Dawley rats were acquired from the Mount Scio Vivarium (Memorial University of Newfoundland, St. John's, NL, Canada). Rats were housed under standard environment conditions of 12 hour light and 12 hour darkness at the Animal Care Unit at the Health Sciences Centre, Memorial University of Newfoundland. Animals were provided water *ad libitum* and were fed LabDiet Prolab RMH 3000 (PMI Nutrition International, Brentwood, MO, USA). For all uterine studies, virgin female rats (approximately 220-250 g) were mated with stud male rats to induce pregnancy. Observation of a vaginal plug the morning following mating would mark day 1 of pregnancy, thus delivery was on day 23 under these standard conditions. All experiments were approved by the institutional animal care committee under protocols 08-02-DM to 10-02-DM.

2.2 Uterine Tissue Collection During Normal Pregnancy

Individual non-pregnant or pregnant female rats were placed in a euthanasia chamber and exposed to an increasing concentration of carbon dioxide gas resulting in asphyxiation causing death within 5 minutes. For immunoblot analysis, the uterine horns were removed from the rat and opened longitudinally, exposing the fetuses and placentae, which were removed and discarded. The tissue was then placed on a chilled petri dish filled with phosphate-buffered saline (PBS) (pH = 7.4) where the endometrial layer was

scraped off with a scalpel blade (White et al., 2005). To store these samples, and to aid in their preservation, they were flash-frozen in liquid nitrogen and stored at -80 ^{o}C .

For immunofluorescence detection, cross sectional portions of rat uterine horn were fixed in 4% paraformaldehyde (PFA) in PBS (pH 7.4) with shaking overnight at room temperature. Tissues were processed, paraffin embedded, sectioned and mounted on microscope slides by the Histology Unit of Memorial University of Newfoundland School of Medicine. All tissue sections utilized for experiments contained visible longitudinal and circular muscle layers of the myometrium.

Each tissue set for both immunoblot and immunofluorescence studies were composed of samples from ten time points throughout gestation including: non-pregnant (NP), day 6, 12, 15, 17, 19, 21, 22, 23 (labour) and 1 day PP. Labour samples were collected after delivery of 2-3 pups when labour was still active.

2.3 Experimental Design

2.3.1 *Unilateral Pregnancy Model*

Tissue samples from a unilateral pregnancy model were provided by Dr. Bryan White and specific details on the production of these samples can be found elsewhere (White & MacPhee, 2011). Briefly, virgin female rats were anaesthesized using a 1:1 ratio of ketamine hydrochloride (ketaset) (Wyeth Animal Health, Guelph, Ontario) and xylazine (rompun) (Bayer HealthCare, Toronto, Ontario) per 100 grams weight. Once under general anaesthesia, a unilateral tubal ligation was performed through a flank incision. In doing so, this allowed pregnancy to occur in only one horn (Shynlova et al.,

2007). Rats were given a 7-day recovery period, after which they were mated. Myometrial samples of the pregnant rat were collected on days 15 (n = 4), 19 (n = 4) and 23 (labour; n = 8) of gestation from both non-gravid (empty) and gravid (stretched) uterine horns. Labour samples were collected after delivery of 2-3 pups when labour was still active.

2.4 Immunoblot Analysis

Immunoblot analysis was performed on samples obtained from normal pregnancy, a unilateral pregnancy model, or Human Telomerase Reverse Transcriptase- Human Myometrial cells (hTERT-HM) cell lysates (see section 2.6). Four independent sets of protein samples (n = 4 rats per gestational time point, n=4 different cell lysates) were used for all studies. Previously frozen rat myometrial samples were pulverized under liquid nitrogen and homogenized in radioimmunoprecipitation assay (RIPA) buffer (50 mM Tris-HCL (pH 7.5), 150 mM NaCl, 1% (wt/vol) sodium deoxycholate, 1% (vol/vol) Triton X-100, and 0.1% (wt/vol) sodium dodecyl sulfate (SDS) containing phosphatase inhibitor cocktail and Complete^{TM} mini ethylenediaminetetraacetic acid (EDTA)-free protease inhibitors (Roche Molecular Biochemicals, Laval, Quebec, Canada) using a PreCellys Bead Mill. All samples were centrifuged at 15 000 x g at 4 ^{o}C for 15 minutes, after which the supernatants were collected. A Bradford Assay (Bradford, 1976) using Bio-rad protein assay dye reagent (Bio-Rad Laboratories, Mississauga, Ontario, Canada) was used to determine the protein concentration of all protein lysates. The Bradford Method can determine the concentration of a protein sample by comparing the

spectrophotometric absorbance (A595 nm) of the sample to the absorbance of known standards (0, 2.5, 5, 10, 15, 20, 25 mg/ml bovine serum albumin (BSA) plotted on a standard curve. Protein standards were prepared in duplicate, diluted in double deionized water (ddH_2O) and the absorbance of the standards (A_{595}) measured following addition of 1mL 1X Bio-Rad protein assay dye reagent (Bio-Rad Laboratories, Mississauga, Ontario, Canada) using a Shimadzu BioMini spectrophotometer. A standard curve of A595 versus protein standard concentration was created using Microsoft Excel and used to determine the protein concentrations for each protein sample. To prepare each sample for the assay, 1μL of each protein lysate was combined with 24μL of ddH_2O and then 1mL of 1X Bio-Rad protein assay dye reagent was added to each sample.

40 µg of each sample were separated by SDS-polyacrylamide gel electrophoresis (SDS-PAGE) in 12% resolving gels according to Laemmli (1970) and proteins were electroblotted to 0.2 µm nitrocellulose membranes (Thermo Scientific, Rockford, Illinois, USA). All subsequent antisera incubations and washes were performed with constant agitation on a shaker at room temperature. Membranes were washed for 5 minutes with Tris-buffered saline-Tween-20 (TBST; 20 mM Tris base, 137 mM NaCl, and 0.1% Tween-20; pH 7.6) followed by a 1 hour (h) block in 5% milk powder/TBST. Membranes were all probed with a primary antisera (Table 2.1) at the corresponding dilution for 2 hours. Membranes then underwent 1 x 20min and 4 x 5min washes with TBST. Blots were then probed with the appropriate secondary antisera (Table 2.1) at the corresponding dilutions followed by 1 x 20min and 4 x 5min washes with TBST. A Pierce SuperSignal West Pico chemiluminescent substrate detection system (MJS

Table 2.1 Primary antisera utilized for experiments. Information provided includes the specificity of the antisera, the catalogue information and dilution with blocking solution.

Antisera	**Method**	**Dilution**	**Company**	**Catalogue #**
Heat Shock Factor 1 (Hsf1)	IB	1:4000	Sigma MO, USA	H 4163
Heat Shock Factor 1 (Hsf1)	IF	1:200	Sigma MO, USA	H 4163
p-Hsf1 (Ser 230)-R	IB	1:500	Santa Cruz CA, USA	Sc-30443-R
Heat Shock Factor 1 Ab-4 (Cones 4B4+ 10H4+ 10H8)	IB	1:4000	Thermo Scientific CA, USA	#RT-629-P0, P1 or -P
Hsf1, pAB	IB	1:4000	Enzo Life Sciences PA, USA	ADI-SPA-901-D
Mouse monoclonal (AC88) to HSP 90	IB	1:2000	Abcam MA, USA	Ab13492
Mouse monoclonal (AC88) to HSP 90	IB	1:4000	Abcam MA, USA	Ab53497
Hsp90	IB	1:2000	StressMarq BC. Canada	SMC-107 A/B
Hsf1 Antibody	IB	1:1000	Cell Signalling ON, Canada	#4356
Heat Shock Factor 2	IB	1: 4000	Sigma MO, USA	H 6788

Heat Shock Factor 2	IF	1: 500	Sigma MO, USA	H 6788
Calponin	IB	1:100 000	Sigma MO, USA	C2687
Anti-Mouse IgG (H+L) HRP Conjugate	IB	1:10 000	Promega WI, USA	W402B
Anti-Rabbit IgG (H+L) Conjugate	IB	1:10 000	Promega WI, USA	W401B
Anti-Rabbit IgG (whole molecule)-FITC antibody	IF	1:250	Sigma MO, USA	F7512
FITC-conjugated Affinipure Donkey Anti-Rabbit IgG (H+L)	IF	1:1000	Jackson ImmunoResearch PA, USA	711-095-152
TO-PRO®-3 Iodide (642/661)	IF	1:100	Invitrogen NY, USA	T3605
PARP-1	IB	1:2000	Invitrogen NY, USA	436400
Monoclonal ANTI-FLAG M2	IB	1:2000	Sigma MO, USA	F1804
HspB8	IB	1:1000	Lifespan Biosciences, WA, USA	LS-C81990
HspB8	IB	1:1000	Cell Signalling, ON, CA	3059

Hsp70	IB	1:1000	Enzo Life Sciences, NY, USA	ADI-SPA-810
Hsp B1	IB	1:1000	EMD Millipore, ON, CA	06-517

IB= Immunoblot
IF= Immunofluorescence

Biolynx, Inc., Brockville, Ontario, Canada) was used to detect protein expression. Several different blot exposure on Amersham enhanced chemiluminescence (ECL) film (GE Healthcare Limited, Little Chalfont, BKM, UK) were taken to ensure the exposure level of films were comparable between the sets and to ensure that the film response was in the linear range of detection.

After probing the blots for the appropriate protein of interest, blots were then stripped for 45 minutes in Restore™ Western Blot Stripping Buffer (Thermo Scientific, Rockford, IL, USA). Calponin protein expression was then measured as a normalization control for all blots. This protein is constitutively expressed in the rat myometrium in both pregnant and non-pregnant samples following RIPA lysis buffer protein extraction (White *et al.* 2005; Williams *et al.* 2005).

2.5 Immunofluorescence

Immunofluorescence detection was performed on samples obtained from normal pregnancy and unilateral pregnancy. All studies were repeated in triplicate with three independently collected samples (n=3). Slides containing tissue sections underwent several washes in xylene (3 X 100% for 5 min each), ethanol (1X 100%, 95%, 90%, 80%, 70% and 50% for 3 min each) and finally PBS (3 X for 7 min each) in order to de-wax and rehydrate the tissue sections. Two different types of epitope retrieval were then carried out in succession. First heat induced epitope retrieval using 0.01M sodium citrate buffer, pH 6.0 was performed. Slides were immersed for 10 minute periods in the solution that was preheated in a water bath at 95°C. After the 10 minute immersion,

slides were transferred to a new preheated solution for another 10 minute period. This was repeated two additional times for a total of 40 minutes of immersion. Then, a second epitope retrieval was performed with a 15 minute incubation of tissue sections in 1mg/mL trypsin in Tris buffer (4 mM $CaCl_2$, 200 mM Tris, pH 7.7) at room temperature.

Following epitope retrieval, tissue sections were then washed for 5 minutes in PBS followed by a 30 min block period with 5% normal goat serum/1% horse serum in PBS. Sections were then incubated overnight in a primary antisera, with shaking at 4 ^{o}C, or a non-immune IgG (negative control) of the same species as the primary antisera and utilized at the same concentration (Table 2.1). The next day, sections were washed in PBS (2 x 5min) and then incubated with the appropriate fluorescently-conjugated secondary antisera (Table 2.1) for 30 mins at room temperature with gentle agitation. Tissue sections examined by laser scanning confocal microscopy were also co-incubated with a TO-PRO®-3 nuclear stain (Invitrogen; T3605; 1:100) added to the secondary antisera solution. Sections were then washed with cold PBS containing 0.02% Tween-20 (2 x 5 mins) and then mounted with Vectashield (Vector Laboratories Inc., Burlington, Ontario, Canada), containing 4', 6-diamidino-2-phenylindole (DAPI) to stain nuclei. Either a Leica DMIRE2 microscope (Leica Microsystem (Canada) Inc., Richmond Hill, Ontario, Canada) equipped for epi-fluorescence and with a QImaging Retiga EXi Camera (QImaging, Surrey, British Columbia, Canada) or a FluoView 300 laser scanning confocal microscope (Olympus Optical, Melville, NY) was used to examine the slides and capture images. Images collected on the Leica DMIRE2 microscope were analyzed using Improvision Openlab software version 5.5 (PerkinElmer, Waltham, MA, USA).

2.6 Cell Culture

Dr. Ann Word (Southwestern Medical Center; Dallas, Texas) graciously donated hTERT-HM cells, which were used for all cell experiments. This cell line has derived from human myometrial cells obtained from women who had undergone a hysterectomy. This cell line possesses several characteristics of endogenous uterine smooth muscle cells such as expression of the key markers calponin, oxytocin receptor, α smooth muscle actin, and the oxytocin receptor in addition to its maintained responsiveness to 17β-estradiol. Also, hTERT-HM cells retain their elongated shape, central nucleus and their confluent sheet-like growth pattern. These similarities between the immortalized cell line and human myometrial smooth muscle cells make them an ideal model system to study myometrial development and function (Condon et al., 2002).

Dulbecco's modified Eagle's medium nutrient mixture F-12(Ham) 1X (DMEM/F12 1:1; Invitrogen, Burlington, ON, Canada) containing 10% fetal bovine serum (FBS; The Cell Culture Company, Oakville ON, Canada), 100U/ml penicillin and 100μg/ml streptomycin (Invitrogen, Burlington, ON, Canada) was used for cell cultivation. Cells were grown in 75 cm^2 flasks, in a 5% CO_2 incubator maintained at a constant temperature of 37^oC. Media was changed daily and cells grown until they reached approximately 80% confluency, after which they were either passaged into new 75cm^2 flasks to allow for further growth or they were used for various experiments. Cells were grown on 8 well chamber slides for immunofluorescence experiments and were grown on 6 well plates for transfection experiments. For immunofluorescence detection cells were seeded on chamber slides at approximately 10 000 cells per well and allowed

to grow for 48 h at 37˚C. The cells were then fixed in 4% PFA/PBS for immunofluorescence (n=3).

2.7 Plasmid Transformation

DH5α competent cells (Invitrogen, Burlington, ON, Canada) were thawed on ice prior to transformation. 50μL of cells were transferred to a 15 mL Falcon tube pre-chilled on ice, to which 5μL of pCMV6 Hsf1 (Origene: MD,USA) plasmid was added. This mixture was then chilled on ice for 30 minutes, followed by a 90 second heat shock at 42°C, and then re-chilled again for 2 minutes on ice. 1mL of pre-warmed cell culture media (without antibiotic) was then added to the mixture followed by shaking at 220rpm at 37°C for 1h. The mixture was then plated on pre-warmed agar plates with antibiotic (Kanamycin 25μg/mL), the plates inverted and incubated overnight at 37°C. Single colonies were then selected and added to 3mL of media with ampicillin in 15mL culture tubes. Cultures were left shaking overnight at 220 rpm at 37°C.

Plasmid DNA was isolated using a PureLink Quick Plasmid Miniprep Kit (Invitrogen, Burlington, ON, Canada) according to the manufacturer's protocol and DNA concentration then measured using a NanoDrop Spectrophotometer.

Samples were prepared for diagnostic restriction endonuclease digestion and agarose gel electrophoresis as follows; 1μg DNA, 10 μg/μL restriction enzyme, 1μL 10x buffer (chosen based on the restriction enzyme) and MilliQ water to make the solution up to 10μL. The mixtures were heated for 1h at 37°C in a water bath. The cDNA was inserted at the Sgfl/ Mlu I restriction sites of pCMV6 (Origene: MD,USA). This plasmid

was therefore verified using restriction enzymes Sgfl and Mlu I. Control restriction endonuclease digestions (i.e. uncut plasmids) were made using 0.5 μg of DNA, buffer and water, but in the absence of restriction endonucleases. Before loading samples in the agarose gel, 1μL of 6X Dye was added to each sample. The 1% agarose gel that had been prestained with SYBR safe. Agarose gel electrophoresis was run for 40 minutes at 100V, after which digestions were then analyzed.

Next a DNA GeneElute HP Plasmid Midiprep Kit (Sigma-Aldrich, MO, USA) was used to purify the plasmid DNA, according to manufacturer's instructions. To alleviate any contamination with ethanol, a mixture of 0.1 volume of 3 M sodium acetate and 0.7 volume isopropanol was added to each sample. The samples were subsequently washed with 70% ethanol and then DNA was precipitated according to the midiprep kit (Sigma Aldrich). The precipitated DNA concentration was then determined using a NanoDrop spectrophotometer after resuspension in deionized water. After determining the sample concentrations, samples were prepared for agarose gel electrophoresis as escribed above. Samples were heated at 37^{o}C for one hour, except for the uncut plasmids. Before loading samples onto the agarose gel 1μL of 6X Dye was added to each sample. Agarose gel was run for 40 minutes at 100V. The cDNA was inserted at restriction sites as described above.

2.8 Collection of cell protein lysates

For cell lysate preparation, these samples were rinsed in 5 mL of PBS, the PBS was aspirated, 0.5 mL of RIPA++ buffer was added to each flask, and flasks chilled on ice for 2-3 minutes until the containers were cool. Using a scraper, cells were scraped off the bottom of the dish and the mixture was placed into 1.5 mL microcentrifuge tubes. The samples were then centrifuged at 4°C for 15 minutes at 12 000 rpm. The supernatants were collected and placed in separate microcentrifuge tubes and stored at -80°C.

2.9 Optimization of Transfection

An Amaxa basic nucleofector kit for primary smooth muscle cells (Lonza, Mississauga, ON, Canada; Cat# VPI-1004) was used to determine which electroporation program would be optimal for transfection of hTERT-HM cells with the pmaxGFPTM expression vector provided. Cells were rinsed with 5 mL PBS and then incubated with 1 mL trypsin for 5 minutes at 37°C to detach cells from the culture dish. One millilitre of media was then added to each flask to inactivate the trypsin. Each flask was repeatedly rinsed for ~2-3 minutes with the media/trypsin mixture using a serological pipet to ensure optimal cell detachment and disassociation into single cells. The mixture was then collected and pooled with solutions from other flasks in a 15mL tube. Cells were then counted using a hemacytometer and a volume of the solution containing approximately 1 million cells was added to separate 15 mL tubes. Each tube was then centrifuged for 10 minutes at 700 rpm. Excess media was aspirated and the pellet was then resuspended in 100μL nucleofector solution (18 μL supplement + 82μL nucleofector solution). Then,

4μL of the pmaxGFPTM expression vector was added. The solution was then transferred to a cuvette and electroporation conducted using one of 6 programs (A-033, D-033, P-013, P-042, U-025, B-017). Cell solutions that did not undergo electroporation served as controls. Then 0.5mL of media was added to each cuvette and the total solution was added to a 25cm^3 flask containing 6mL of pre-warmed media. The flask was then incubated for 10 minutes at 37°C. After incubation, the media was equally distributed among 3 tissue culture wells of a 6-well plate so that each well contained 2mL of culture media. Cells were cultured for 72 hours and photographed every 24 hours to monitor the level of transfection and the amount of cell loss.

2.10 Transfection of Cells

A myc-DDK-tagged pCMV6 Hsf1 expression vector (True-Orf, Rockville, MD; RC200314) was transfected into hTERT-HM cells, when cells reached ~80% confluency. An Amaxa basic nucleofector kit for primary smooth muscle cells (Lonza, Mississauga, ON, Canada; Cat# VPI-1004) was used for these experiments. Transfections were conducted as described in section 2.9 using program A-033. Three separate transfections were conducted, all using a total of 2 μg of plasmid DNA; the no program control (2μg the pmaxGFPTM expression vector), GFP (2 μg the pmaxGFPTM expression vector), and Myc-DDK-tagged Hsf1 (1 μg of pcMV6 Hsf1 expression vector and 1 μg pEGFP-C3 expression vector). Cell solutions that did not undergo electroporation served as controls. Cells were cultured for 24-72 hours and photographed every 24 hours to monitor any observable changes resulting from the transfection.

Co transfections were also performed using the same Hsf1 expression vector and a FLAG-tagged human pcMV7 PARP-1 vector (obtained from Dr. Girish Shah, Laval University, Quebec, Canada). Transfections were conducted as previously described above (Section 2.9). In these experiments four separate transfections were conducted, three of which used 2 µg of plasmid DNA; the no program control (2 µg pmaxGFPTM expression vector), GFP (2 µg pmaxGFPTM expression vector), and FLAG-tagged PARP-1 (1µg of pcMV7 PARP-1 expression vector and 1µg pmaxGFPTM expression vector). The final sample, the co transfected sample, contained both 1µg of pCMV-Hsf1 and 1µg pCMV-PARP-1 and 0.5µg of pmaxGFPTM expression vector. Cells were cultured for 24-72 hours and photographed every 24 hours to monitor any observable changes resulting from the transfection. Once transfections were completed, either cell lysates were collected for protein analysis or a proliferation assay was performed.

2.11 MTS Cell Proliferation Assay

The MTS (3-(4,5-dimethylthiazol-2-yl)-5-(3-carboxymethoxyphenyl)-2-(4-sulfophenyl)-2H-tetrazolium) proliferation assay is used to measure the number of metabolically active cells remaining in a cell culture. The MTS is converted to soluble formazan by the dehydrogenase enzymes found in the metabolically active cells. The quantity of the formazan product is then measured by an absorbance reading at 490 nm, and the magnitude of the reading is directly proportional to the number of living cells in culture.

2.11.1 Preparation of MTS and PMS Solutions

To prepare the MTS solution, 21 mL of Hank's Balanced Salt Solution (HBSS), which contained no phenol, Mg^{+} or Ca^{2+}, was added to a light protected container. 42 mg of MTS Reagent powder (Promega, Madison, WI, USA) was then added to the HBSS solution and mixed at moderate speed on a magnetic stir plate for ~ 15 minutes, or until the MTS was completely dissolved. The pH of the solution was then adjusted to be within the range of 6.0-6.5 using 1N HCl or 1N NaOH. The MTS solution was then filter sterilized through a 0.2 μm filter into a sterile 50 mL falcon tube. The soluntion was then aliquoted into 2mL volumes and stored at -20°C until needed.

To make the phenazine methosulfate (PMS) solution, 9.2 mg of PMS (Sigma, St. Louis, MO, USA) was added to a 15mL tube containing 10mL of 1X PBS and then mixed by inversion. The solution was then aliquoted into 200μL volumes and stored at -20°C.

2.11.2 Proliferation Assay

A mixture of PMS and MTS was made by adding 100μL of PMS solution to a 2mL aliquot of MTS solution and mixed gently. Aliquots of 100μL were then added to each well of the 24 well plate containing hTERT-HM cells. The plate was then gently swirled to ensure a homogeneous media/MTS solution and was then returned to the 37°C incubator. To measure the amount of soluble formazan produced by the cellular reduction of the MTS, an ELISA plate reader was used to record the absorbance at

490nm. The absorbance readings were recorded at 30 minutes, 1 hour and 1.5 hour intervals.

2.12 Data Analysis

Densitometry on immunoblots was achieved using Scion Image Analysis software (Scion Image Corporation, Frederick, MD, USA). Densitometric values were normalized to the calponin loading control. GraphPad Instat version 3.0 (GraphPad Software, San Diego, CA, USA, www.graphpad.com) was used to carry out statistical analysis. Graphs were subsequently prepared using GraphPad Prism version 4.0 (GraphPad Software). All data from gestational profiles followed a Gaussian distribution as determined with a Brown-Forsythe test. Data from the gestational profile experiments were analyzed using a One-way analysis of variance (ANOVA) followed by Newman-Keuls post-hoc test. Data from unilateral pregnancy experiments were analyzed using a student t-test. A comparison was considered statistically significant if it had a p-value < 0.05.

Chapter Three

Results

3.1 Normal Pregnancy and Labour

3.1.1 Hsf1 Protein Expression Analysis

The expression of Hsf1 protein in the rat myometrium was studied using immunoblot analysis of both non pregnant (NP) and pregnant rat samples throughout the entire gestational period. Five complete independent sets of tissues were used for analysis (NP, d6, d12, d15, d17, d19, d21, d22, d23, PP). To confirm equal loading of proteins in the immunoblots, following electroblotting of polyacrylamide gels, a MemCode™ Reversible Protein Staining kit was used.

The blots were probed with anti-rabbit Hsf1 specific antisera while anti-mouse calponin specific antisera was used to detect calponin as a normalization control. Both Hsf1 and calponin were detected at their predicted molecular weights of 75kDa and 37kDa, respectively (Figure 3.1). The expression of total Hsf1 changed significantly throughout gestation (ANOVA $p<0.05$; $n=5$), being elevated in NP myometrium and highly expressed early in gestation at d6 and d12. Specifically, Hsf1 expression then significantly decreased at d15, d17, and d22 compared to d6 ($p<0.05$)..

3.1.2 Immunofluorescent Detection of Hsf1

Immunofluorescence was used to detect the spatial arrangement of Hsf1 throughout gestation. Analysis of both circular and longitudinal muscle layers demonstrated that throughout pregnancy total Hsf1 was primarily detected in the cytoplasm of myometrial cells (Figure 3.2-3.5) At all time points there was faint detection of Hsf1 in the cell nucleus, however this was minor compared to the amount

Figure 3.1 Representative immunoblot and densitometric analysis of total Hsf1 protein expression in rat myometrial tissue throughout gestation. Both Hsf1 and calponin were detected at their appropriate molecular weights of 75kDa and 34kDa, respectively. Representative immunoblots are shown. Densitometric analysis of Hsf1 expression was performed. The histogram shown displays the relative optical density of Hsf1 immunoblot data that has been normalized to the calponin loading control. Hsf1 expression was found to change significantly across gestation (one-way ANOVA; $p<0.05$; n=5). The data are shown as mean ±S.E.M, and were from 5 different complete experiments. Data indicated with symbols were found to be statistically significant ($p<0.05$ d6 versus d15, d17, d 22). The Hsf1 expression was elevated early in pregnancy and then decreased suddenly and remained low until d23, labour (L). The decrease in expression from early gestation to late gestation was significantly different between d6 and d15, d17 and d22. Defined abbreviations: NP= non-pregnant, PP= post-partum.

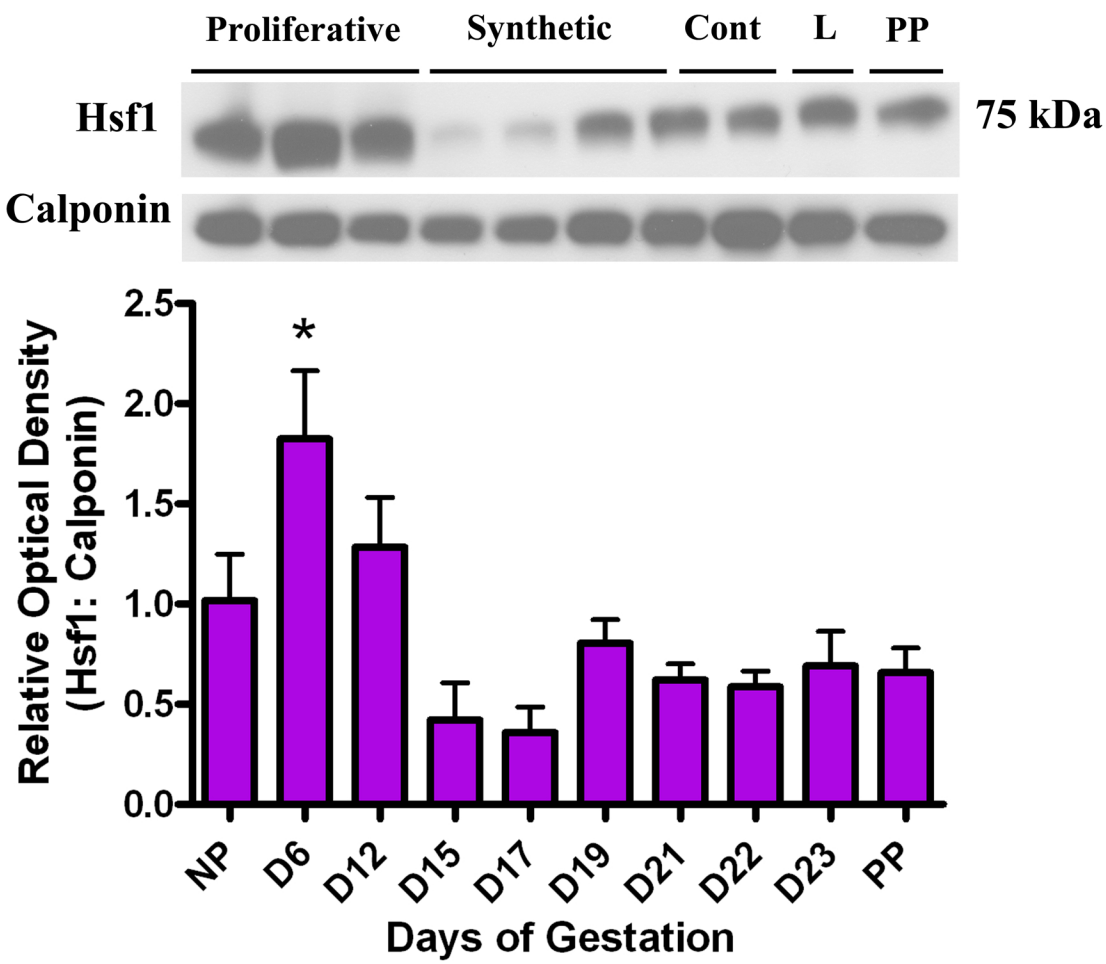
Proliferative
Synthetic
Cont
L
PP
Hsf1
75 kDa
Calponin
Relative Optical Density
(Hsf1: Calponin)
2.5
2.0
1.5
1.0
0.5
0.0
*
NP
D6
D12
D15
D17
D19
D21
D22
D23
PP
Days of Gestation

Figure 3.2 Immunofluorescent detection of Hsf1 in rat uterine longitudinal muscle tissue from non pregnant rats to d17 of gestation. Cross sections of myometrial tissue were mounted onto slides and then probed with anti-rabbit Hsf1 specific antisera for immunofluorescence analysis. Throughout gestation the detection levels of Hsf1 did not change significantly. At all time points Hsf1 was mostly detected in the cytoplasm of cells, with very faint detection in the nuclei. Defined abbreviations: NP= non-pregnant, Ctrl= control, tissue section incubated with a matched IgG instead of antisera as a control for antisera specificity. Scale bar = 50μm.

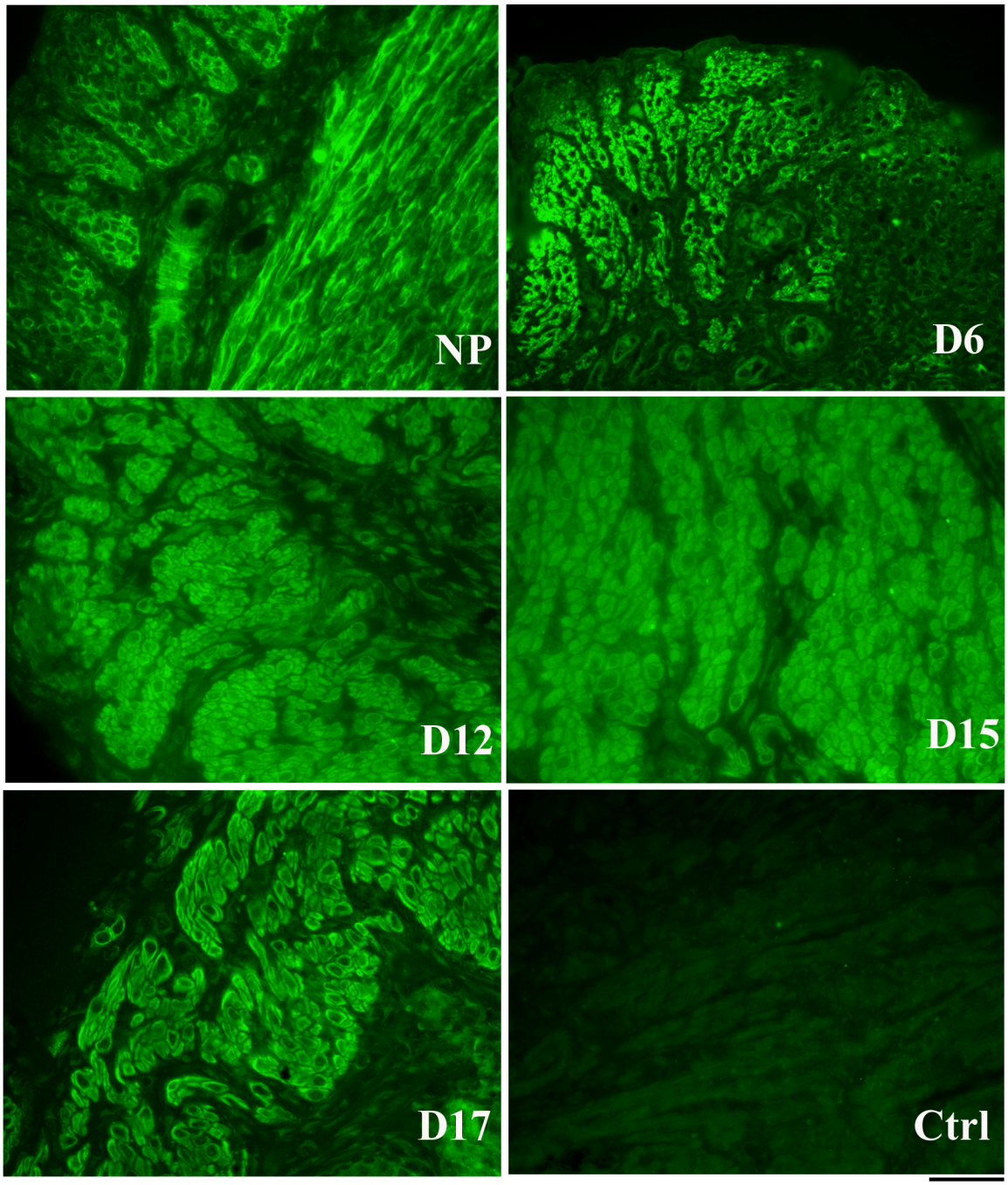
NP
D6
D12
D15
D17
Ctrl

Figure 3.3 Immunofluorescent detection of Hsf1 in rat uterine longitudinal muscle tissue from d19 to post-partum. Cross sections of myometrial tissue were mounted onto slides and then probed with anti-rabbit Hsf1 specific antisera for immunofluorescence analysis. Throughout gestation the detection levels of Hsf1 did not change significantly. At all time points Hsf1 was mostly detected in the cytoplasm of cells, with faint detection in the nuclei. Defined abbreviations: PP= Post-partum, Ctrl= control. Scale bar = 50μm.

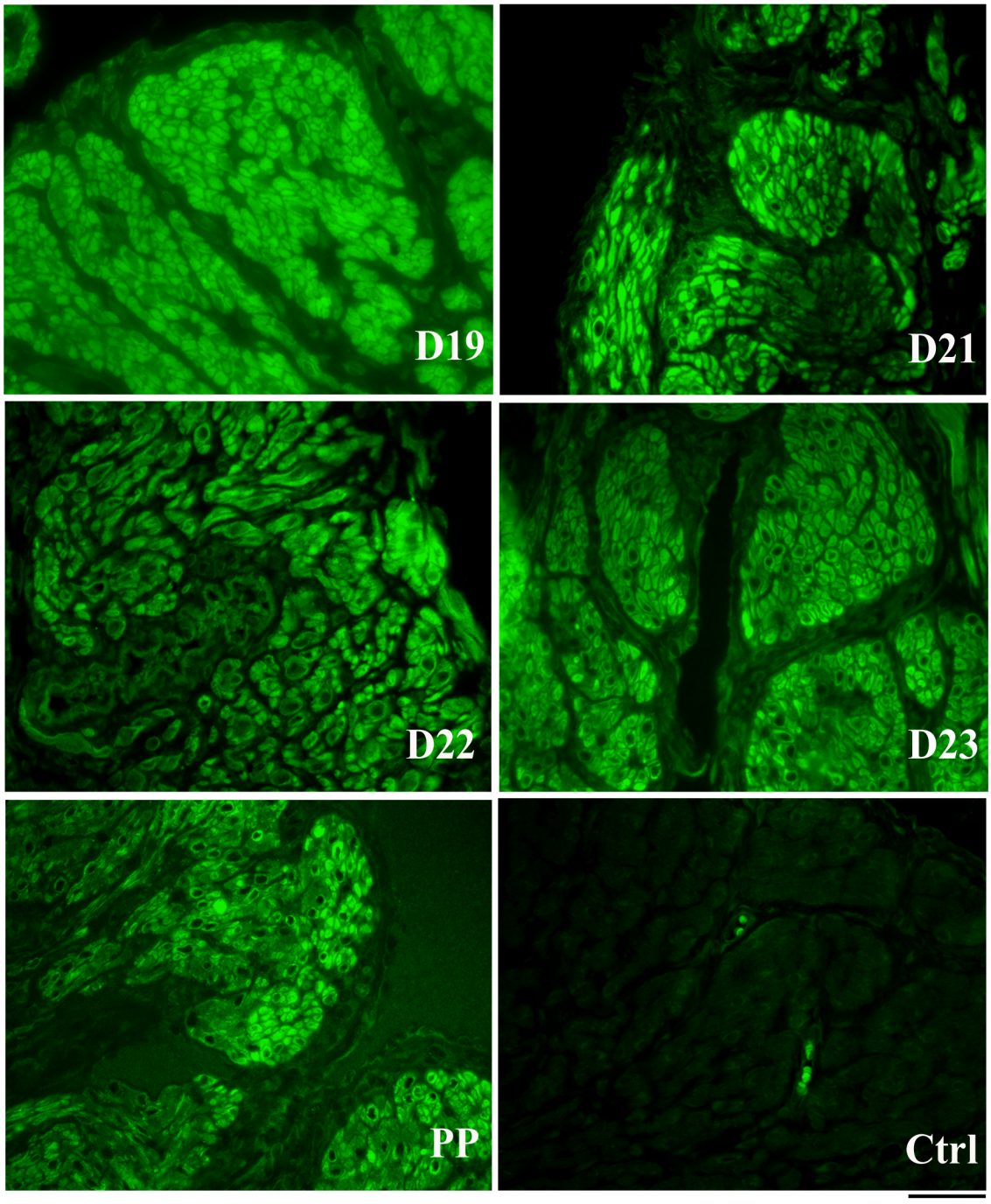
D19
D21
D22
D23
PP
Ctrl

Figure 3.4 Immunofluorescent detection of Hsf1 in rat uterine circular muscle tissue from non pregnant rats to d17 of gestation. Cross sections of myometrial tissue were mounted onto slides and then probed with anti-rabbit Hsf1 specific antisera for immunofluorescence analysis. Throughout gestation the detection levels of Hsf1 did not change significantly. At all time points Hsf1 was mostly detected in the cytoplasm of cells, with faint detection in the nuclei. Defined abbreviations: NP= non-pregnant, Ctrl= control, tissue section incubated with a matched IgG instead of antisera as a control for antisera specificity. Scale bar = 50μm.

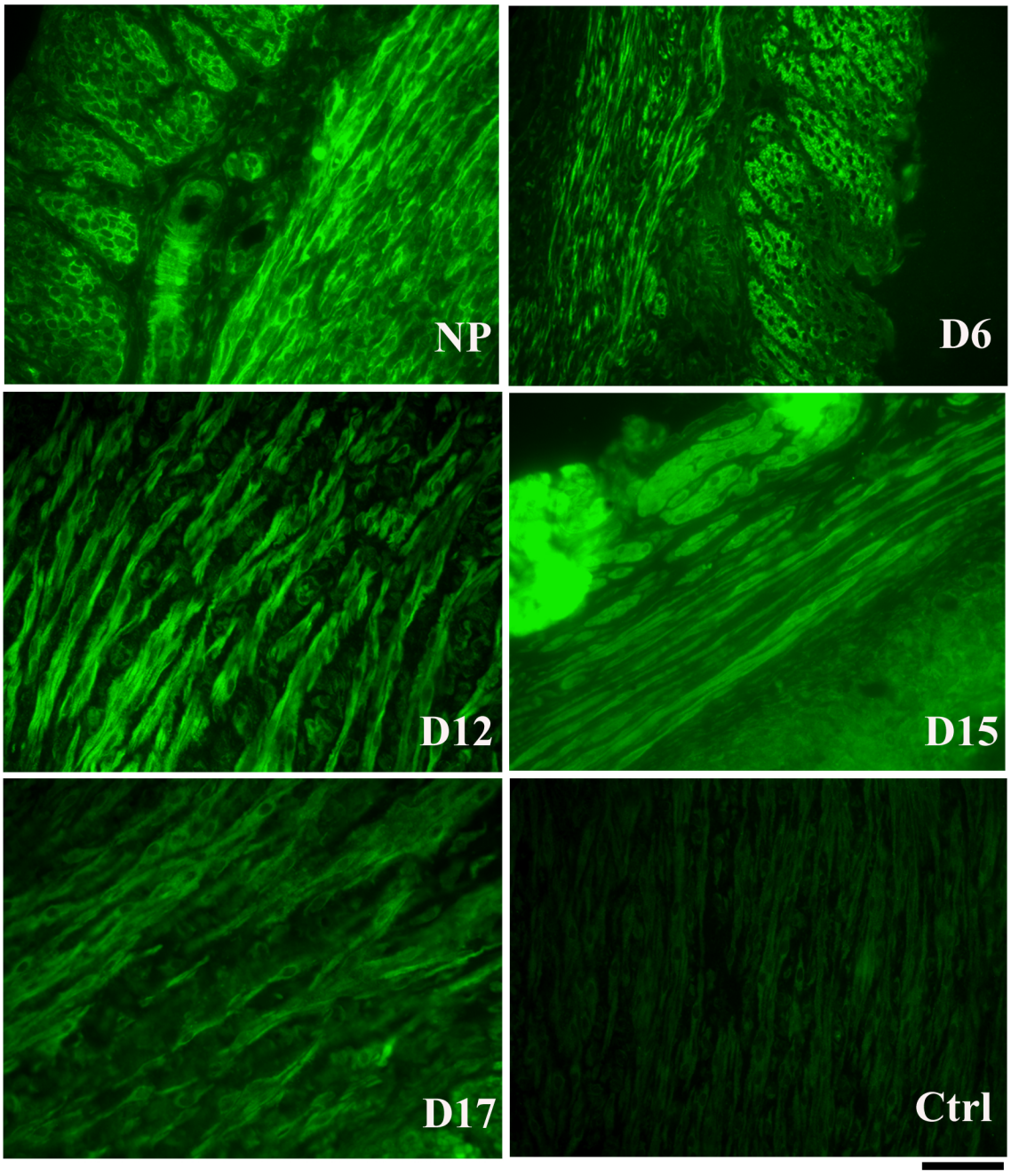
NP
D6
D12
D15
D17
Ctrl

Figure 3.5 Immunofluorescent detection of Hsf1 in rat uterine circular muscle tissue from d19 to post partum. Cross sections of myometrial tissue were mounted onto slides and then probed with anti-rabbit Hsf1 specific antisera for immunostaining. Throughout gestation the detection levels of Hsf1 did not change significantly. At all time points Hsf1 was primarily detected in the cytoplasm of cells, with very faint detection in the nuclei. Defined abbreviations: NP= Post-partum, Ctrl= control. Scale bar = 50μm.

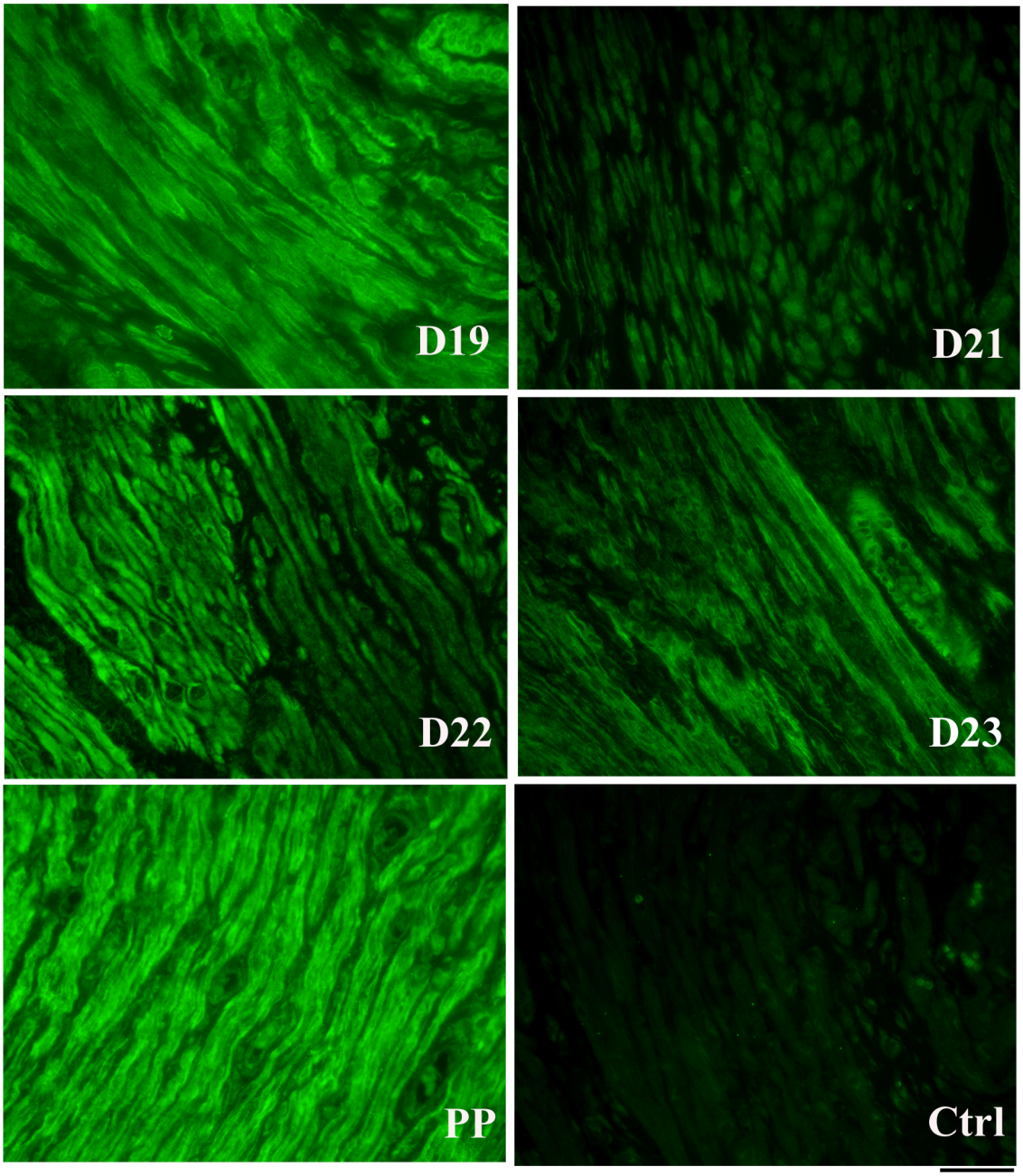
D19
D21
D22
D23
PP
Ctrl

observed in the cytoplasm. Qualitatively, Hsf1 detection did not change markedly over the course of gestation. Furthermore, Hsf1 was also immunolocalized to the blood vessel SMCs and virtually undetectable in stromal fibroblasts around muscle bundles.

To assess the quality of the Hsf1 antisera for immunofluorescence procedures, rat testis tissue sections were examined for localization of Hsf1 (Figure 3.6). Hsf1 protein expression was previously detected in rat testis, primarily in the cytoplasm by Akerfelt et. al (2010). Therefore, as a positive control, immunofluorescence was performed and confirmed that Hsf1 was localized to the cytoplasm of testicular cells.

3.1.3 Immunofluorescent Detection of Hsf1 with Laser Scanning Confocal Microscopy

To more specifically examine immunostained rat uterine tissue sections for Hsf1 nuclear staining, 1μm thick optical sections of myometrial tissue were imaged by laser scanning confocal microscropy. Cross sections of myometrial tissue were immuno-stained with an anti-rabbit Hsf1 specific antisera and TO-PRO®-3 nuclear stain. Hsf1 was still mostly detectable in the cytoplasm; however it was also detectable as speckles in the nuclei of myometrial cells throughout gestation (Figure 3.7; n=3).

3.2 Examination of pHsf1 (Ser 230) Expression

3.2.1 Evidence for Post-translational Modifications

Hsf1 can undergo a wide variety of post-translational modifications (Hietakangas et al., 2006; Knauf et al., 1996). Thus, immunoblot analysis of Hsf1 expression was performed with both non pregnant and pregnant rat myometrium tissue lysates throughout the entire gestational period using 8% acrylamide gels, instead of 15%, to resolve potential changes in MW due to post-translational modifications.

Figure 3.6 Verification of Hsf1 immunostaining with mouse testis. Cross sections of mouse testis were probed with anti-rabbit Hsf1 specific antisera for immunofluorescence analysis. Hsf1 expression was detected in the rat testis, primarily in the cytoplasm of cells. This confirmed the appropriateness of the antiserum for immunofluorescence analysis.

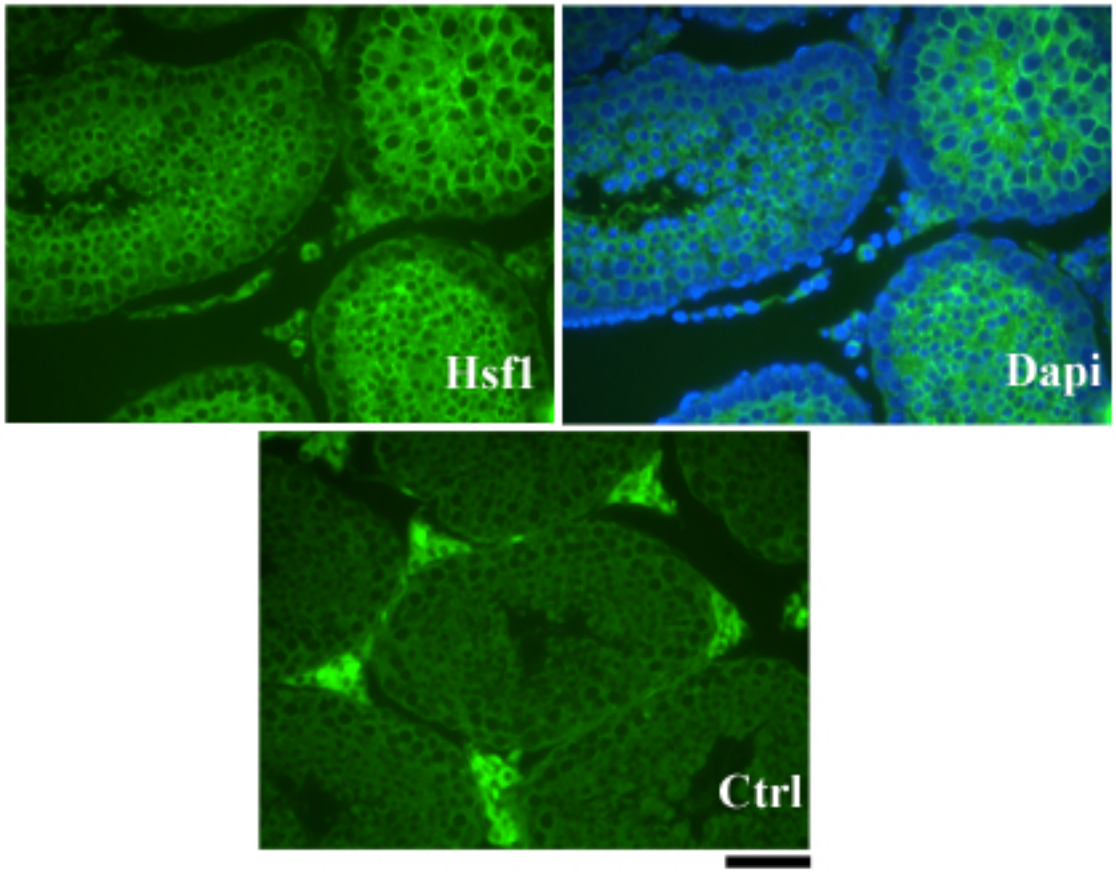
Hsf1
Dapi
Ctrl

Figure 3.7 Spatial detection of total Hsf1 in rat uterine smooth muscle tissue throughout gestation using laser scanning confocal microscopy. Five gestational time points are shown as representative images for the entire pregnancy. Hsf1 was detected in cell nuclei as speckles throughout gestation. Images shown are representative of three different experiments. Scale bar = 100μm. NP= non-pregnant, Ctrl= control.

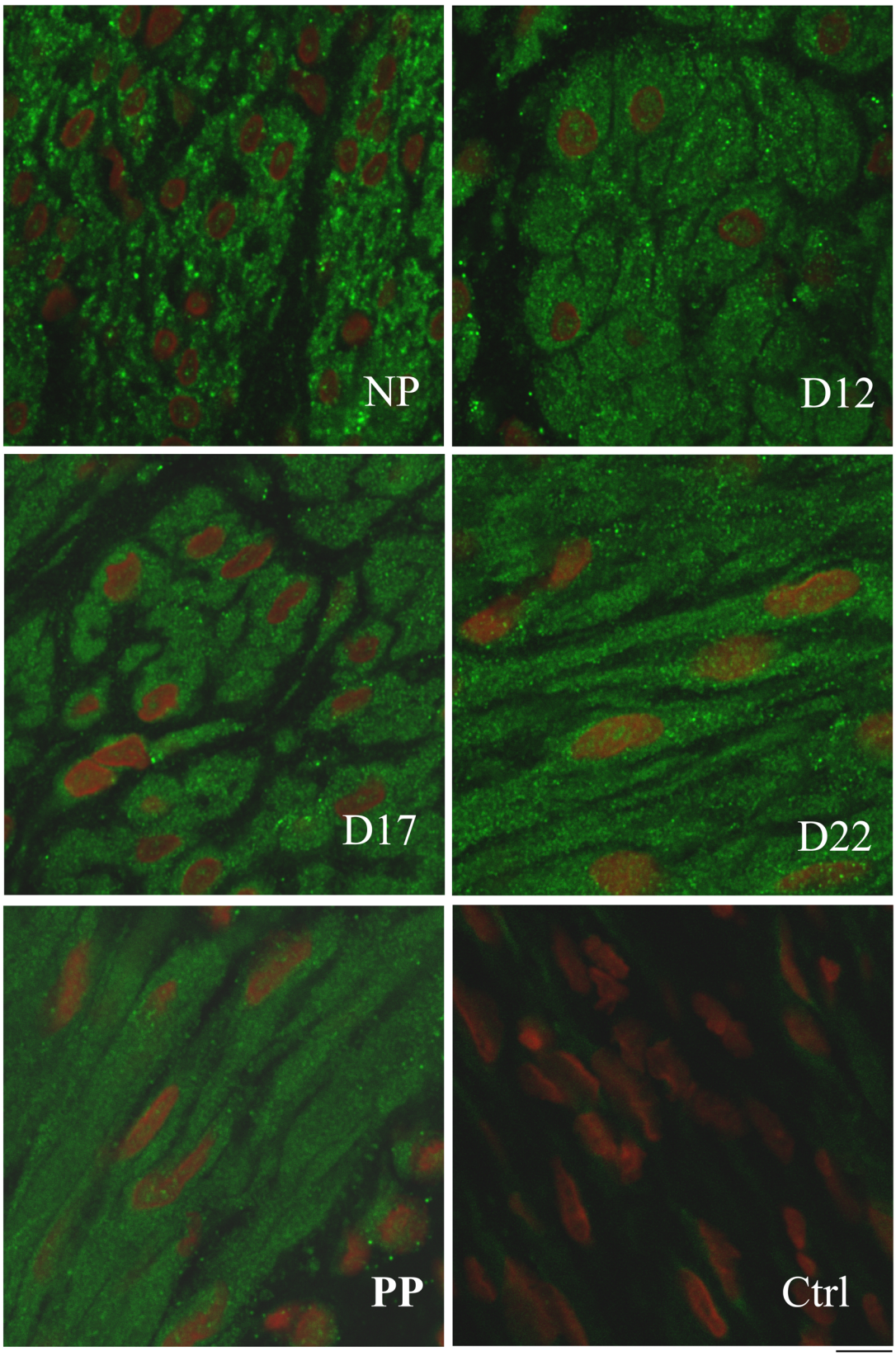
NP
D12
D17
D22
PP
Ctrl

The blot was probed with anti-rabbit Hsf1 specific antisera, and bands were detected in the ~60-75 kDa molecular weight range (Figure 3.8 A). The results indicated that myometrial Hsf1 may undergo a number of post-translational modifications which could account for the observed range in molecular weight.

3.2.2 pHsf1 Protein Expression Analysis

Hsf1 can be actively phosphorylated (p) on the serine (ser)-230 residue leading to Hsf1 transcriptional activation (Knauf et al., 1996). Thus, immunoblot analysis was performed with anti-rabbit pHsf1 (Ser-230) specific antisera using both non pregnant and pregnant rat myometrium tissue lysates to assess Hsf1 activation. pHsf1 was detected at a lower molecular weight than that of total Hsf1 (Figure 3.8 B). The expression of pHsf1 changed throughout gestation, being elevated at NP and early in gestation at d6 and d12, then steadily decreasing from d15 onward. Specifically, there was a significant increase in pHsf1 expression at d12 compared to d22 ($p<0.05$).

3.3 Unilateral Pregnancy Model

3.3.1 Expression of Hsf1 protein

It was possible that uterine stretch, which increasingly occurs from mid-pregnancy to term, might negatively regulate Hsf1 expression. A unilateral pregnancy model (Shynlova et al, 2007) was used to determine the effect of uterine stretch on Hsf1 expression at d15, d19 and d23. Myometrial tissue lysates from both the gravid (stretched) and non-gravid (non-stretched) uterine horns were used for immunoblot analysis, and probed with anti-rabbit Hsf1 antisera (Figures 3.9, 3.10). There were no statistically significant changes in myometrial Hsf1 expression between the gravid and non-gravid horns at any time point ($p>0.05$).

Figure 3.8 Hsf1 undergoes post-translational modification. **A)** Total Hsf1 expression in rat myometrial tissue throughout gestation resolved using an 8% acrylamide gel. A representative immunoblot is shown. Several bands can be seen in the 60-75kDa range as Hsf1 undergoes several forms of post-translational modifications. Defined abbreviations: NP= non-pregnant, PP= post-partum. **B)** Phosphorylated (Ser-230) Hsf1 expression in rat myometrial tissue throughout gestation. Both pHsf1 and calponin were detected at the molecular weights of ~60kDa and 34kDa, respectively. Representative immunoblots are shown. At 10 different gestational time points, densitometric analysis of pHsf1 was performed. The histogram shown displays the relative optical density of pHsf1 that has been normalized to the calponin loading control. pHsf1 expression was found to change significantly across gestation (one-way ANOVA; $p<0.05$; $n=4$). The data is shown as mean ±S.E.M, and came from 4 different experiments. Data indicated with symbols were found to be statistically different after post hoc statistical tests were performed ($p<0.05$ d12 versus d22). The pHsf1 expression was elevated early in pregnancy and then decreased gradually until d23 labour (L). The data showed there was a significant increase in pHsf1 expression at d12 compared to d22. Defined abbreviations: NP= non-pregnant, Cont= Contractile Phase, PP= post-partum.

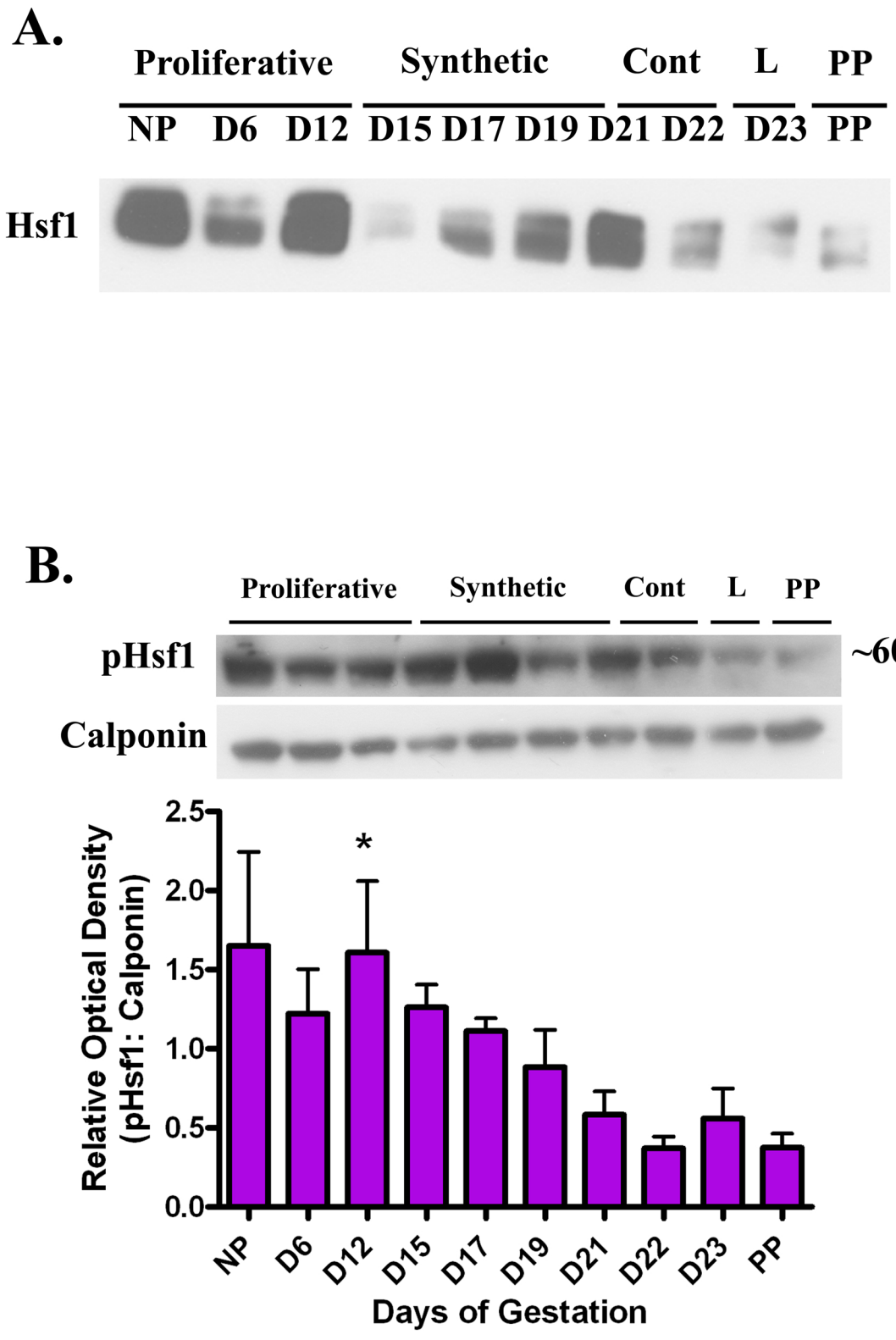
A.
Proliferative
Synthetic
Cont
L
PP
NP
D6
D12
D15
D17
D19
D21
D22
D23
PP
Hsf1
B.
Proliferative
Synthetic
Cont
L
PP
pHsf1
~60 kDa
Calponin
Relative Optical Density
(pHsf1: Calponin)
2.5
2.0
1.5
1.0
0.5
0.0
*
NP
D6
D12
D15
D17
D19
D21
D22
D23
PP
Days of Gestation

Figure 3.9 Representative immunoblot and densitometric analysis of Hsf1 at d15 and d19 in both gravid and non-gravid horns. Uterine stretch had no significant effect on total Hsf1 expression. There were no significant differences in myometrial Hsf1 expression between the gravid and non-gravid horn at d15 or d19 of gestation (d15 p=0.97 D19 p=0.96). **A)** A representative immunoblot is shown that detected Hsf1 and calponin at d15 of pregnancy and at their respective molecular weights of 75kDa and 34kDa. The histogram shown displays the relative optical density of Hsf1 that has been normalized to the calponin loading control. The data are shown as mean ± S.E.M, and are from 4 different experiments (n=4) at d15. **B)** A representative immunoblot is shown that detected Hsf1 and calponin at d19 of pregnancy. The histogram shown displays the relative optical density of Hsf1 that has been normalized to the calponin loading control. The data are shown as mean ± S.E.M, and are from 4 different experiments (n=4) at d19. Defined abbreviations: G= gravid (stretched), NG= non-gravid (non-stretched).

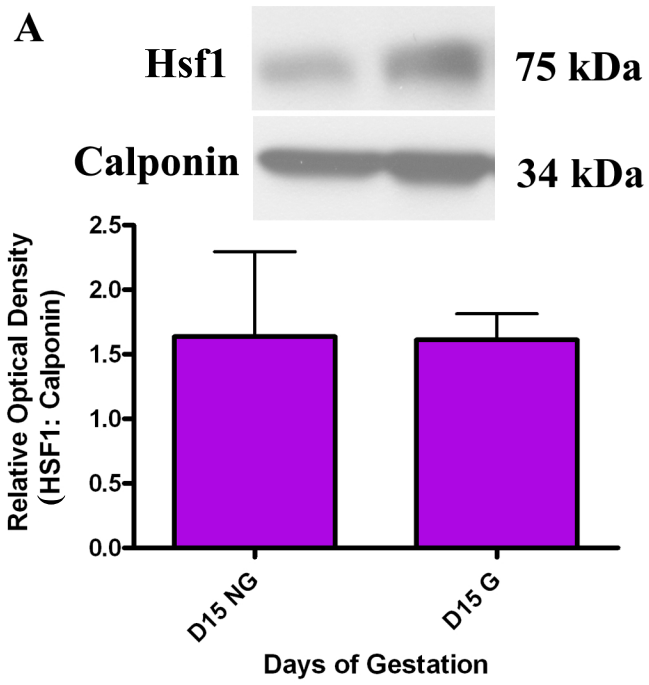
A
Hsf1
75 kDa
Calponin
34 kDa
Relative Optical Density
(HSF1: Calponin)
2.5
2.0
1.5
1.0
0.5
0.0
D15 NG
D15 G
Days of Gestation

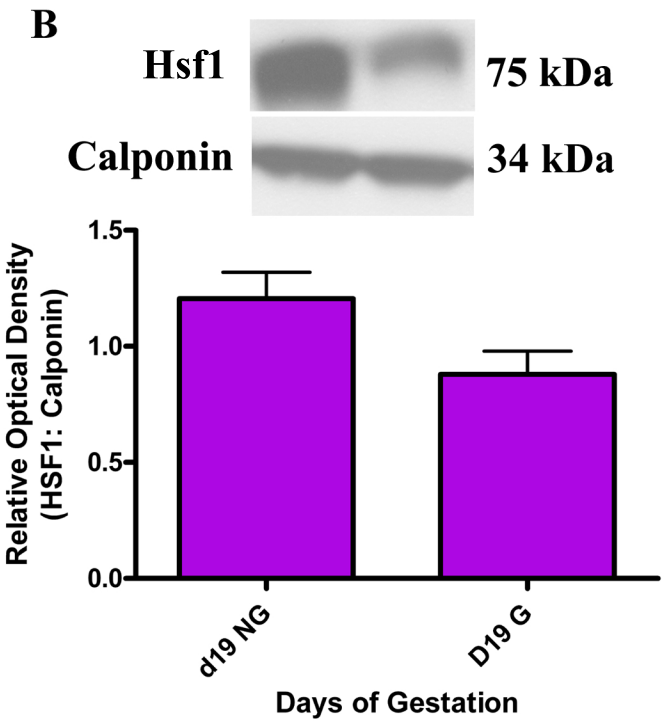
B
Hsf1
75 kDa
Calponin
34 kDa
Relative Optical Density
(HSF1: Calponin)
1.5
1.0
0.5
0.0
d19 NG
D19 G
Days of Gestation

Figure 3.10 Representative immunoblot and densitometric analysis of Hsf1 at d23 in both gravid and non-gravid horns. Uterine stretch had no significant effect on total Hsf1 expression. There were no significant differences in myometrial Hsf1 expression between the gravid and non-gravid horn at d23 of gestation. A representative immunoblot is shown and the histogram displays the relative optical density of Hsf1 that has been normalized to the calponin loading control. The data are shown as mean ± S.E.M, and were from 4 different experiments (n=4) at d23. Defined abbreviations: G= gravid (stretched), NG= non-gravid (non-stretched).

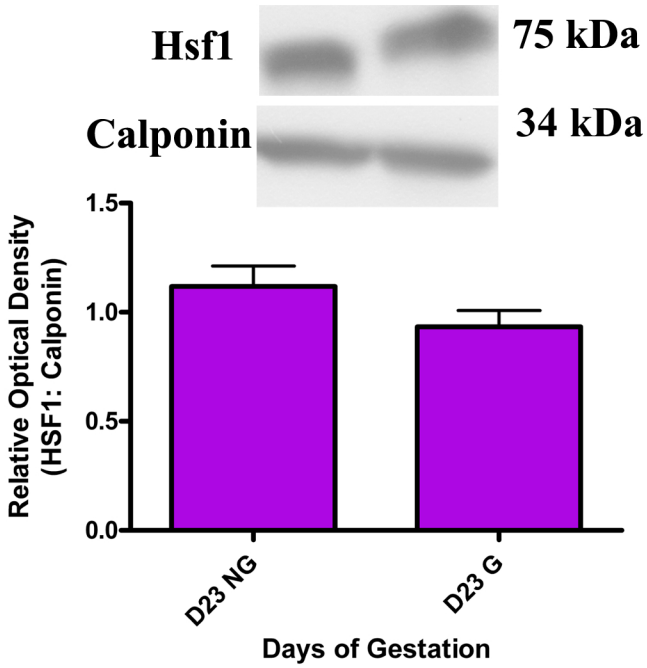
Hsf1
75 kDa
Calponin
34 kDa
Relative Optical Density
(HSF1: Calponin)
1.5
1.0
0.5
0.0
D23 NG
D23 G
Days of Gestation

3.3.2 Immunofluorescent Detection of Hsf1

Immunofluorescence was used to detect the spatial arrangement of Hsf1 in both gravid and non-gravid uterine tissue. Analysis of both circular and longitudinal muscle layers demonstrated that total Hsf1 was similarly detected in both gravid and non-gravid tissues and was primarily detected in the cytoplasm of myometrial cells (Figures 3.11, 3.12). In all tissue sections there was faint detection of Hsf1 in the cell nucleus; however, this was minor compared to the amount observed in the cytoplasm. Furthermore, Hsf1 was immunolocalized to blood vessel SMCs and virtually undetectable in stromal fibroblasts around muscle bundles.

3.3.3 Expression of pHsf1 protein

Since pSer-230 Hsf1 is the transcriptionally active form of Hsf1, it was possible that uterine stretch might specifically regulate its expression. The same unilateral pregnancy model (Shynlova et al, 2007) was used to determine the effect of uterine stretch on pSer-230 Hsf1 expression at d15, d19 and d23. Myometrial tissue lysates of both the gravid (stretched) and non-gravid (non-stretched) uterine horns were used for immunoblot analysis and probed with anti-rabbit pSer-230 Hsf1 (Figures 3.13, 3.14). There were no statistically significant changes in pHsf1 expression between the gravid and non-gravid horns at any time point ($p>0.05$).

3.4 Examination of Hsf2 Expression

3.4.1 Hsf2 Protein Expression Analysis

Hsf2 can form hetero-trimers with Hsf1 and it is involved in several developmental processes such as spermatogenesis (Akerfelt et al., 2007). Thus,

Figure 3.11 Immunofluorescent detection of total Hsf1 in rat uterine longitudinal muscle tissue in both gravid and non gravid horns at d19 and d23 of gestation. Cross sections of myometrial tissue were mounted onto slides and then probed with anti-rabbit Hsf1 specific antisera for immunofluorescence analysis. Hsf1 was robustly detectable in the cytoplasm of cells, with very faint detection in the nuclei at all timepoints. The detection levels of Hsf1 were also not altered. Defined abbreviations: Ctrl= control. Scale bar = 50μm.

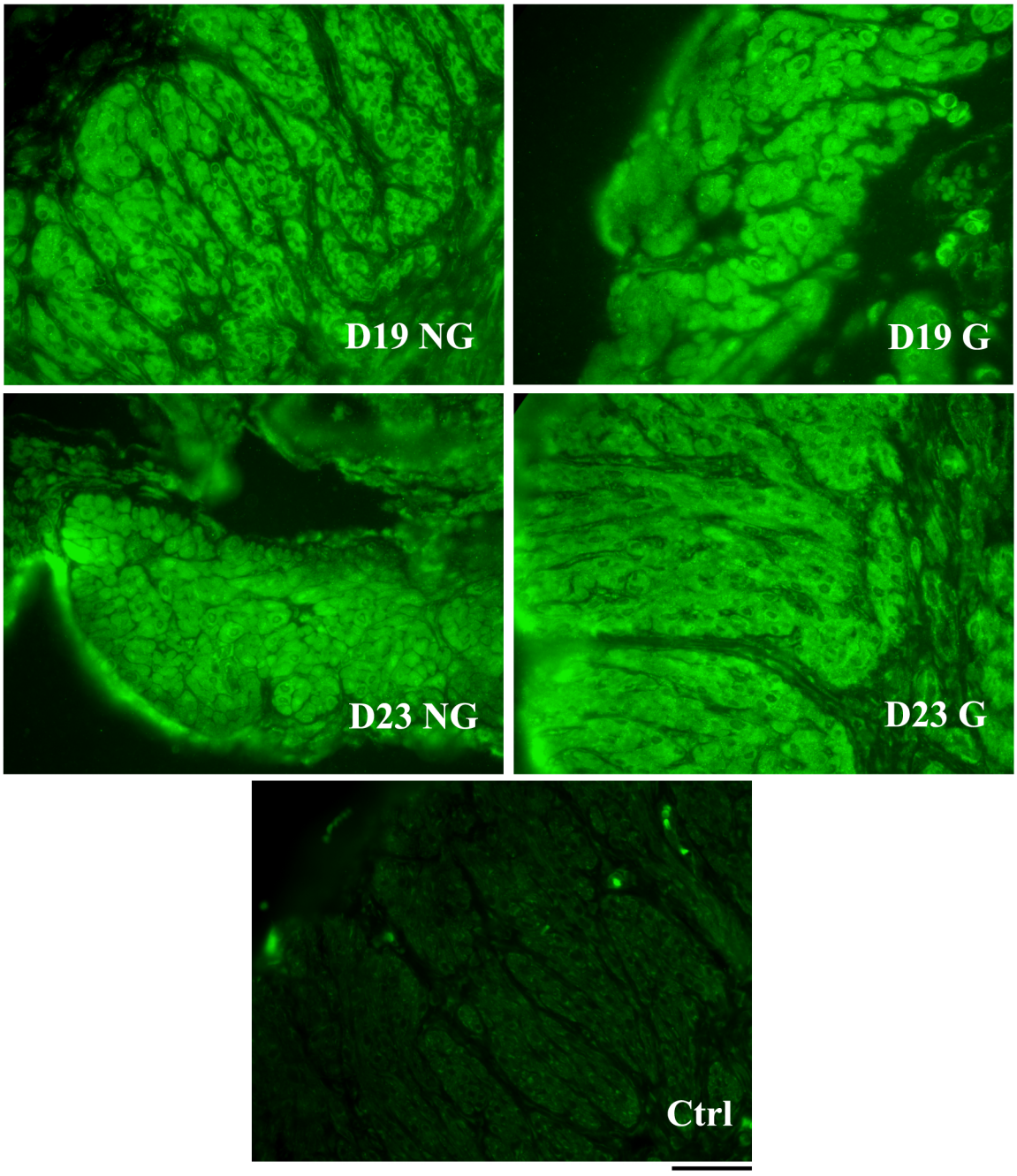
D19 NG
D19 G
D23 NG
D23 G
Ctrl

Figure 3.12 Immunofluorescent detection of total Hsf1 in rat uterine circular muscle tissue in both gravid and non gravid horns at d19 and d23 of gestation. Cross sections of myometrial tissue were mounted onto slides and then probed with anti-rabbit Hsf1 specific antisera for immunofluorescence analysis. Hsf1 was robustly detectable in the cytoplasm of cells, with very faint detection in the nuclei at all timepoints. The detection levels of Hsf1 were also not altered. Defined abbreviations: Ctrl= control. Scale bar = 50μm.

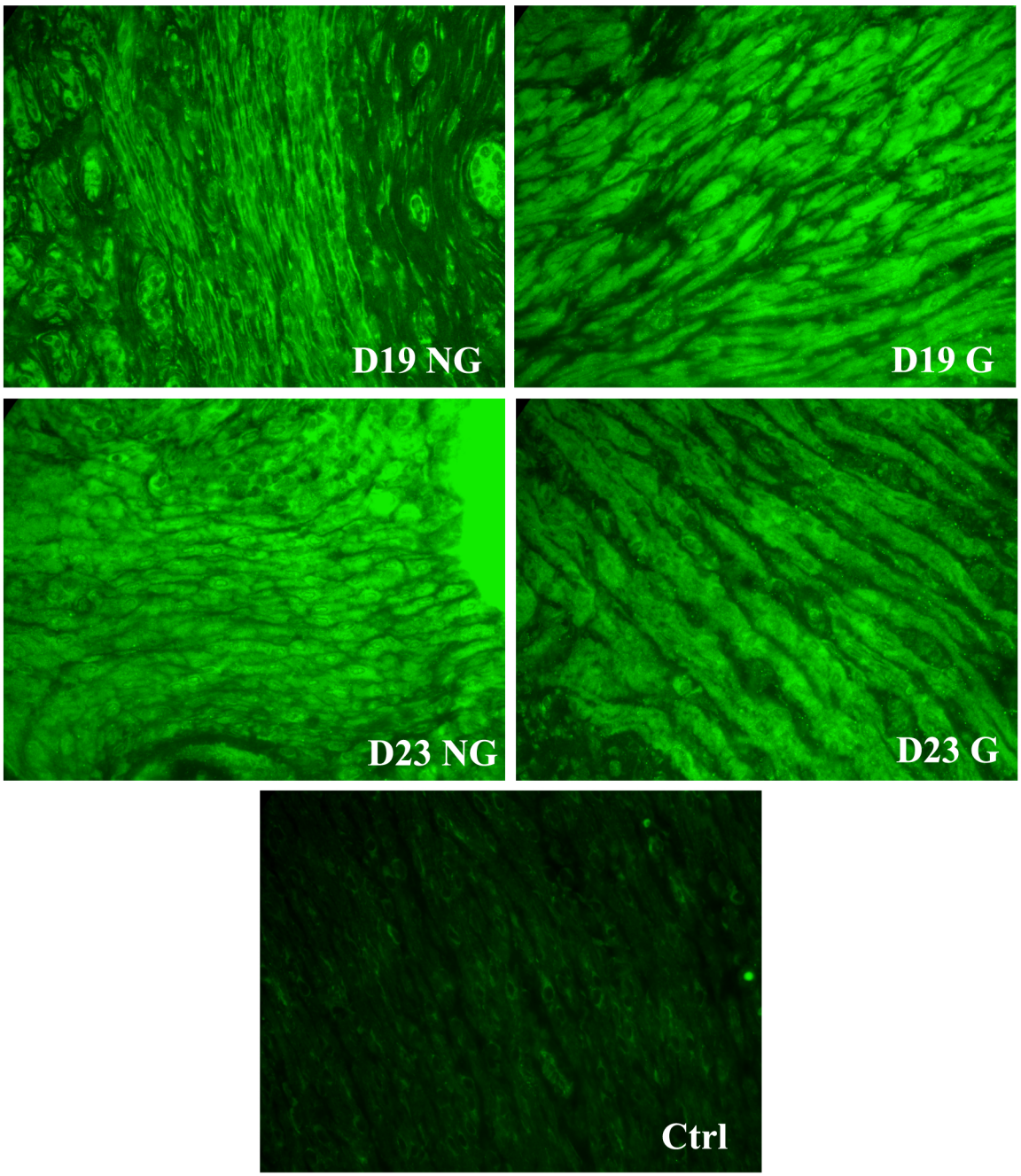
D19 NG
D19 G
D23 NG
D23 G
Ctrl

Figure 3.13 Representative immunoblot and densitometric analysis of pSer-230 Hsf1 at d15 and d19 in both gravid and non-gravid horns. Uterine stretch had no significant effect on pSer-230 Hsf1 expression. At d15 and d19 of gestation there were no differences in Hsf1 expression between the gravid and non-gravid horn. **A)** Representative immunoblots are shown demonstrating detection of pSer-230 Hsf1 and calponin at d15 of pregnancy. The histogram below the immunoblots displays the relative optical density of Hsf1 that has been normalized to the calponin loading control. **B)** Representative immunoblots are shown demonstrating detection of Hsf1 and calponin at d19 of pregnancy. The histogram shown below the immunoblots displays the relative optical density of Hsf1 that has been normalized to the calponin loading control. All data shown in A) and B) represent means ± S.E.M and are from 4 different experiments (n=4) at each timepoint. Defined abbreviations: G= gravid (stretched), NG= non-gravid (non-stretched).

A

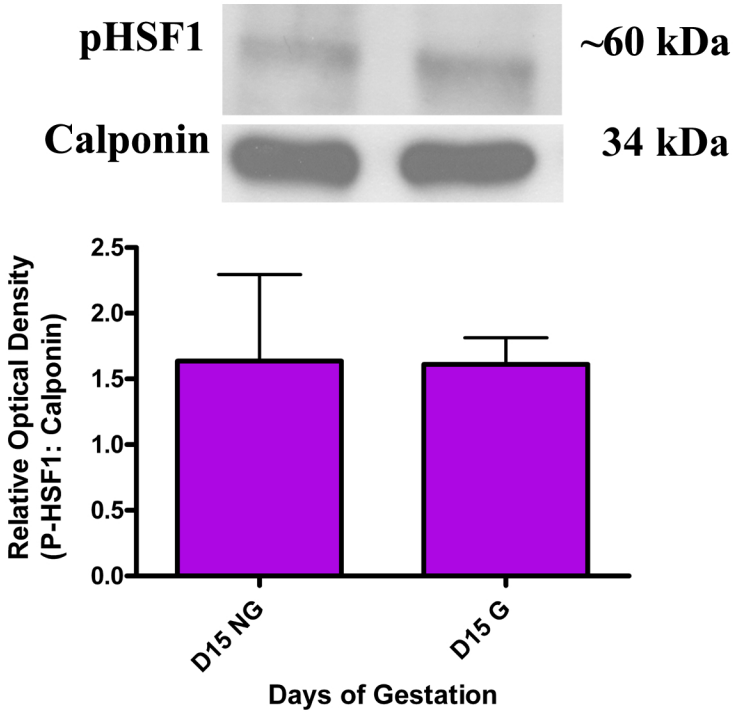
pHSF1
~60 kDa
Calponin
34 kDa
Relative Optical Density
(P-HSF1: Calponin)
2.5
2.0
1.5
1.0
0.5
0.0
D15 NG
D15 G
Days of Gestation

B

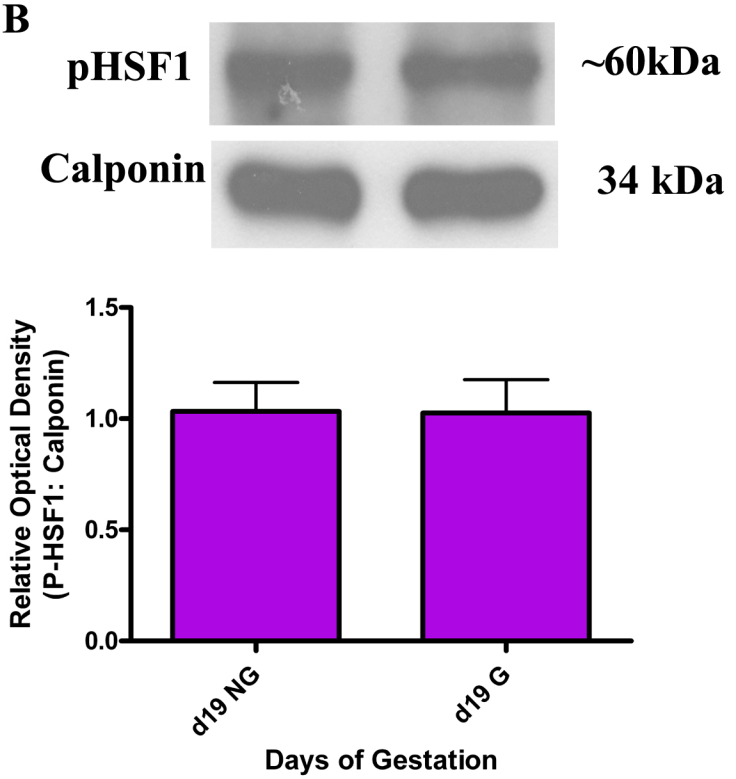
pHSF1
~60kDa
Calponin
34 kDa
Relative Optical Density
(P-HSF1: Calponin)
1.5
1.0
0.5
0.0
d19 NG
d19 G
Days of Gestation

Figure 3.14 Representative immunoblot and densitometric analysis of pSer-230 Hsf1 at d23 in both gravid and non-gravid horns. Uterine stretch did not alter pSer-230 Hsf1 expression at d23 of pregnancy. Representative immunoblots are shown for Hsf1 and calponin. The histogram shown below the blots displays the relative optical density of Hsf1 that has been normalized to the calponin loading control. The data are shown as mean ± S.E.M, and were from 4 different experiments (n=4). Defined abbreviations: G= gravid (stretched), NG= non-gravid (non-stretched).

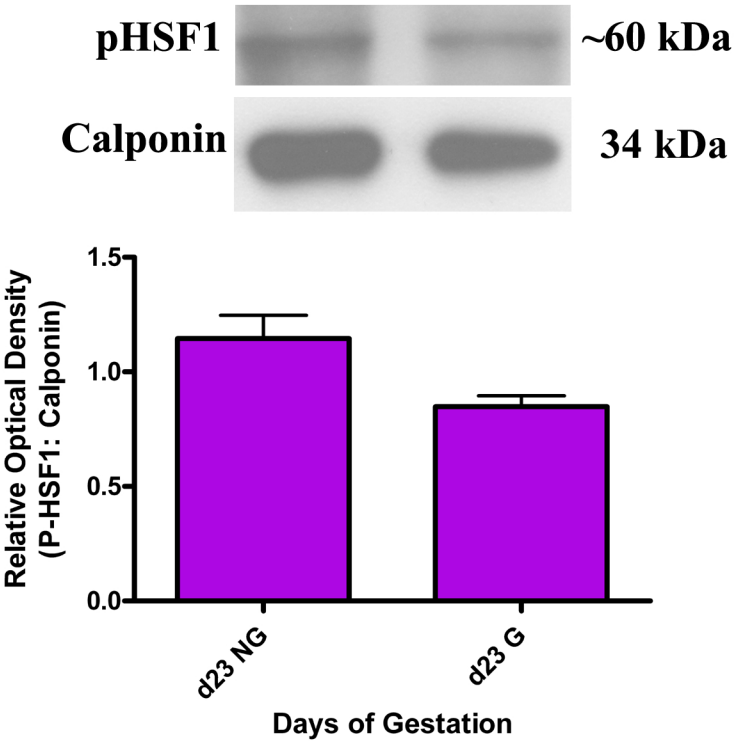
pHSF1
~60 kDa
Calponin
34 kDa
Relative Optical Density
(P-HSF1: Calponin)
1.5
1.0
0.5
0.0
d23 NG
d23 G
Days of Gestation

immunoblot analysis of Hsf2 protein expression in both non pregnant and pregnant rat myometrium tissue lysates was performed.

Blots were probed with anti-rabbit Hsf2 specific antisera and anti-mouse calponin specific antisera. Hsf2 was detected at ~75kDa as expected and appeared to be constitutively expressed (Figure 3.15). No significant changes in Hsf2 protein expression were noted throughout gestation ($p>0.05$).

3.4.2 Immunofluorescent Detection of Hsf2

Immunofluorescence was used to detect the spatial expression of Hsf2 in myometrial cells throughout gestation. Analysis of both circular and longitudinal muscle layers demonstrated that throughout pregnancy total Hsf2 was primarily detected in the cytoplasm of myometrial cells and Hsf2 detection did not change markedly over the course of this period (Figures 3.16-3.19).

3.5 Examination of PARP-1 Expression

3.5.1 PARP-1 Protein Expression Analysis

PARP-1 mediates nucleosome dissociation on target genes of Hsf1, allowing for their transcription (Petesch et al., 2008). It is also known to be involved in processes such as proliferation, differentiation and tumor cell transformation, which are similar to those of Hsf1 (Petesch et al., 2008). Knowing this, immunoblot analysis was performed to assess PARP-1 expression in both non pregnant and pregnant rat myometrium tissue lysates throughout the entire gestational period.

Blots were probed with anti-mouse PARP-1 specific antisera and anti-mouse calponin specific antisera. PARP-1 was detected at 115kDa and expression showed a

Figure 3.15 Representative immunoblot and densitometric analysis of total Hsf2 protein expression. Representative immunoblots are shown and demonstrate detection of Hsf2 and calponin at appropriate molecular weights. At 10 different gestational time points, densitometric analysis of Hsf2 immunoblots was performed. The histogram shown displays the relative optical density of Hsf2 that has been normalized to the calponin loading control. Hsf2 expression did not significantly change throughout gestation (one-way ANOVA; $p>0.05$; $n=4$). The data are shown as mean ±S.E.M, and were from 4 different experiments. Defined abbreviations: NP= non-pregnant, PP= post-partum, L= labour (d23).

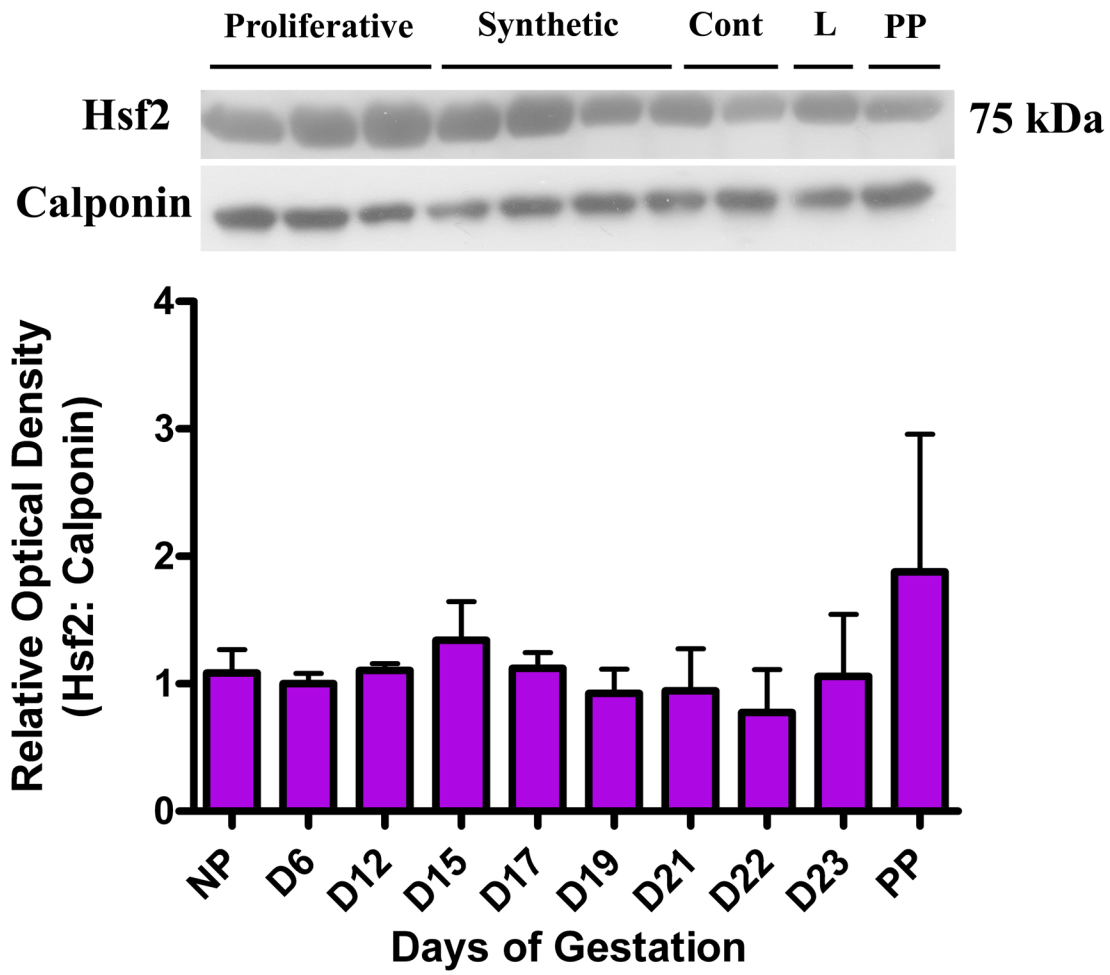
Proliferative
Synthetic
Cont
L
PP
Hsf2
75 kDa
Calponin
Relative Optical Density
(Hsf2: Calponin)
0
1
2
3
4
NP
D6
D12
D15
D17
D19
D21
D22
D23
PP
Days of Gestation

Figure 3.16 Immunofluorescent detection of total Hsf2 in rat uterine longitudinal muscle tissue from non pregnant rats to d17 of pregnancy. Cross sections of myometrial tissue were mounted onto slides and then probed with anti-rabbit Hsf2 specific antisera for immunofluorescence analysis. Throughout gestation the detection levels of Hsf2 did not change significantly. At all time points Hsf2 was detected in the cytoplasm of cells, with very faint detection in the nuclei. Defined abbreviations: NP= non-pregnant, Ctrl= control, tissue section incubated with a matched IgG instead of antisera as a control for antisera specificity. Scale bar = 50μm.

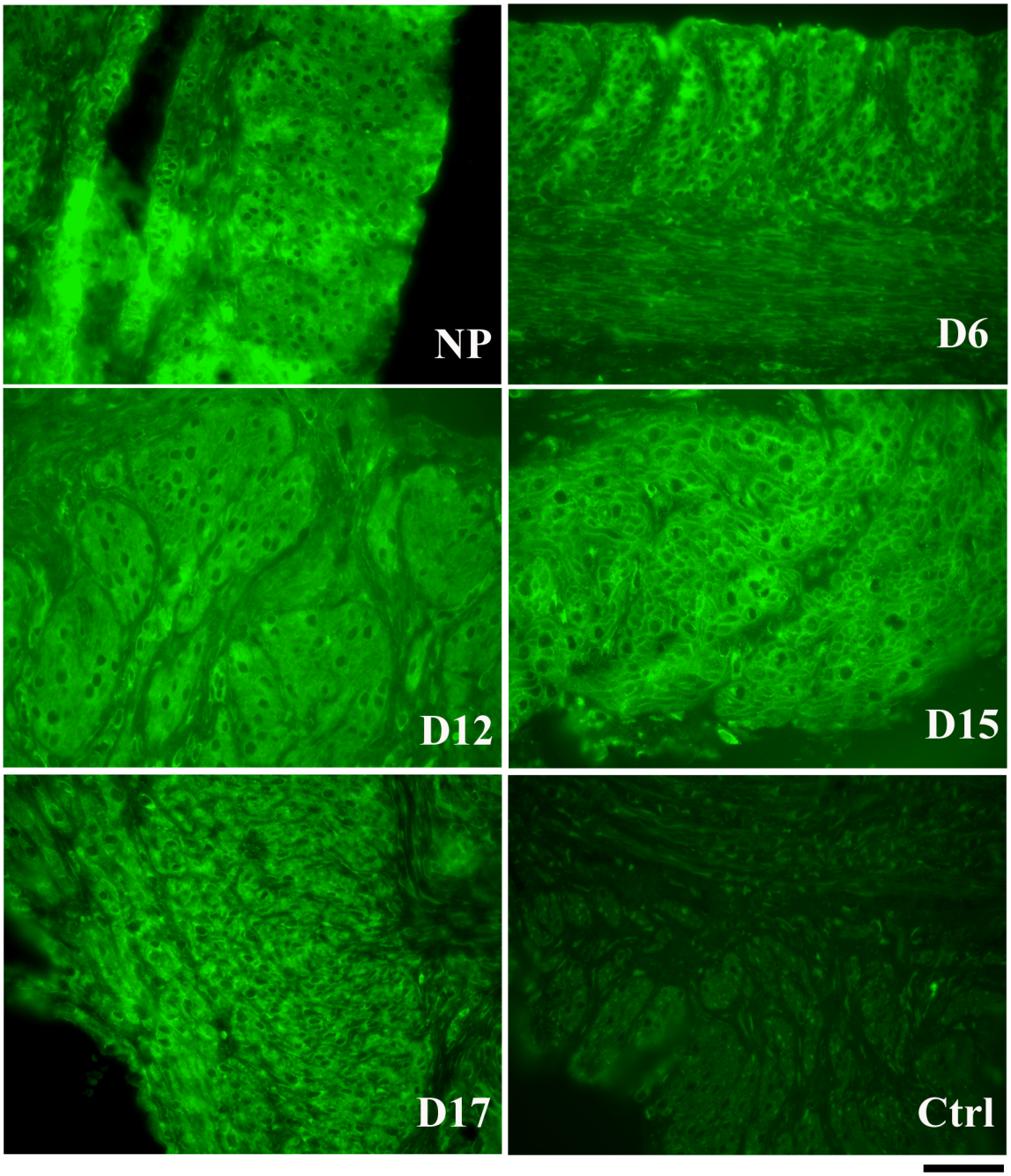
NP
D6
D12
D15
D17
Ctrl

Figure 3.17 Immunofluorescent detection of total Hsf2 in rat uterine longitudinal muscle tissue from d19 of pregnancy to post partum. Cross sections of myometrial tissue were mounted onto slides and then probed with anti-rabbit Hsf2 specific antisera for immunofluorescence analysis. Throughout gestation the detection levels of Hsf2 did not change significantly. At all time points Hsf2 was mostly detected in the cytoplasm of cells, with faint detection in the nuclei. Defined abbreviations: PP= Post-partum, Ctrl= control. Scale bar = 50μm.

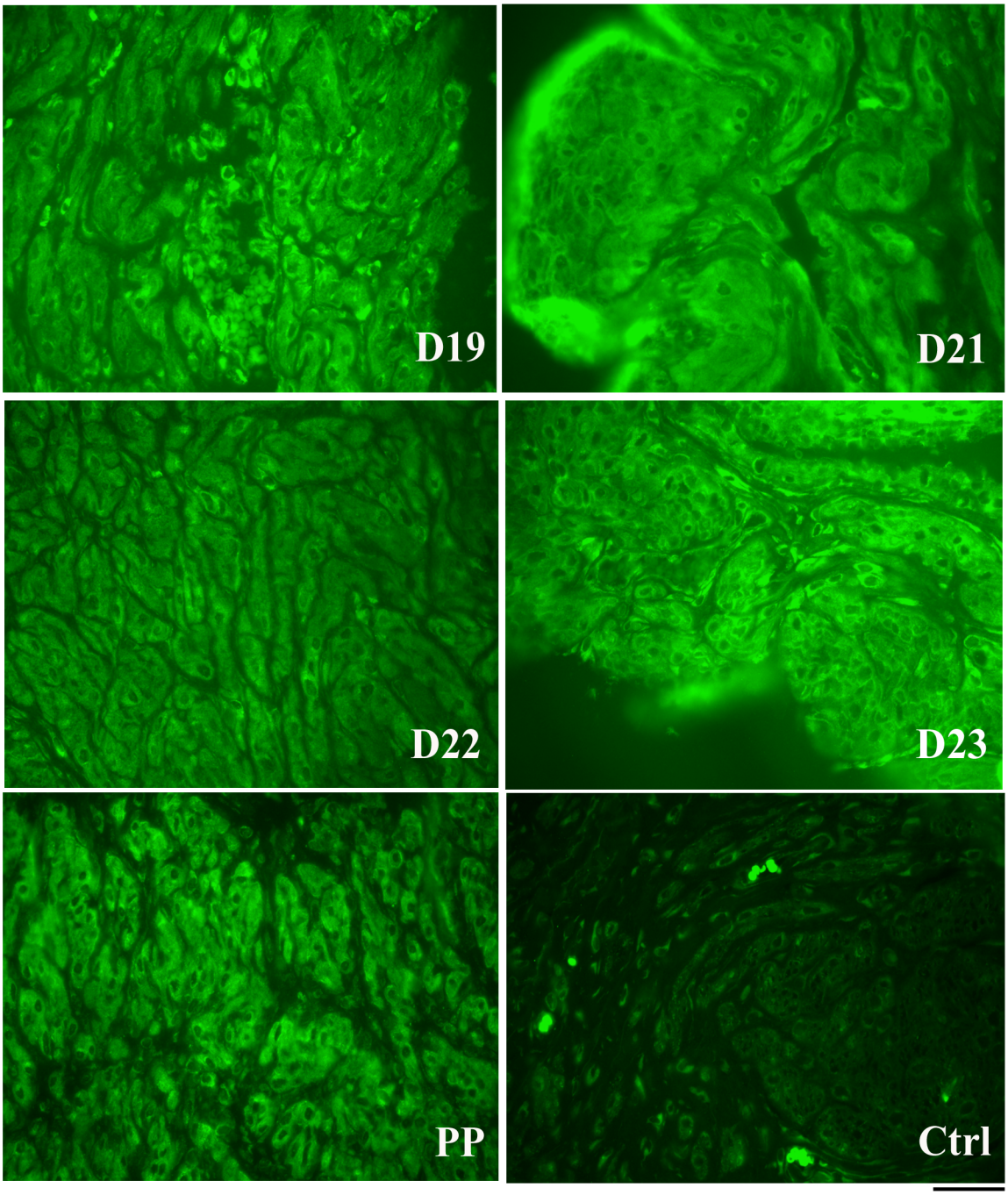
D19
D21
D22
D23
PP
Ctrl

Figure 3.18 Immunofluorescent detection of total Hsf2 in rat uterine circular muscle tissue from non pregnant rats to d17 of pregnancy. Cross sections of myometrial tissue were mounted onto slides and then probed with anti-rabbit Hsf2 specific antisera for immunofluorescence analysis. Throughout gestation the detection levels of Hsf2 did not change significantly. At all time points Hsf2 was mostly detected in the cytoplasm of cells, with faint detection in the nuclei. Defined abbreviations: NP= non-pregnant, Ctrl= control, tissue section incubated with a matched IgG instead of antisera as a control for antisera specificity. Scale bar = 50μm.

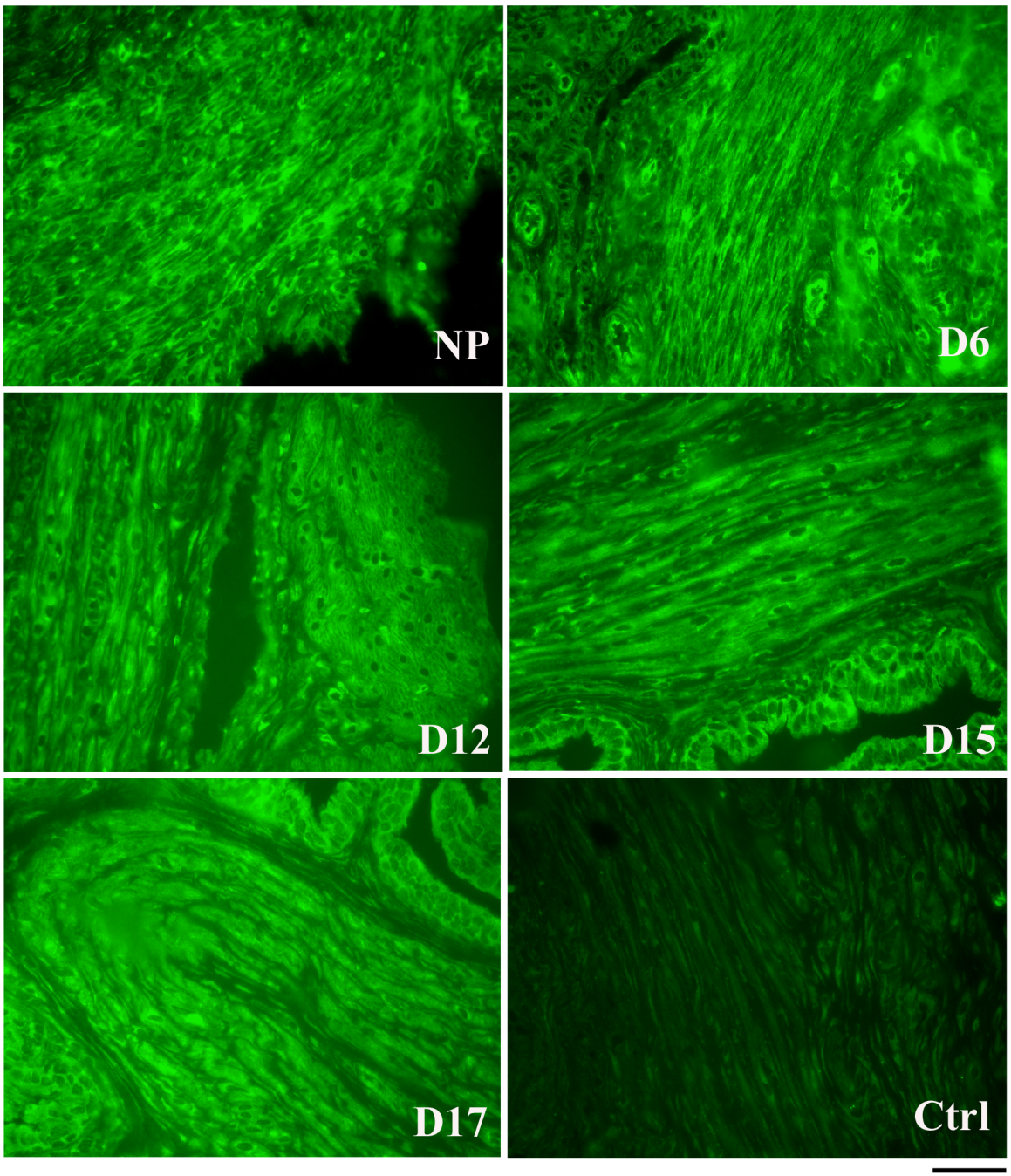
NP
D6
D12
D15
D17
Ctrl

Figure 3.19 Immunofluorescent detection of total Hsf2 in rat uterine circular muscle tissue from d19 of rat pregnancy to post-partum. Cross sections of myometrial tissue were mounted onto slides and then probed with anti-rabbit Hsf2 specific antisera for immunofluorescence analysis. Throughout gestation the detection levels of Hsf2 did not change significantly. At all time points Hsf2 was primarily detected in the cytoplasm of cells, with faint detection in the nuclei. Defined abbreviations: NP= Non= pregnant, L= Labour (d23), PP= Post-partum, Ctrl= control. Scale bar = 50μm.

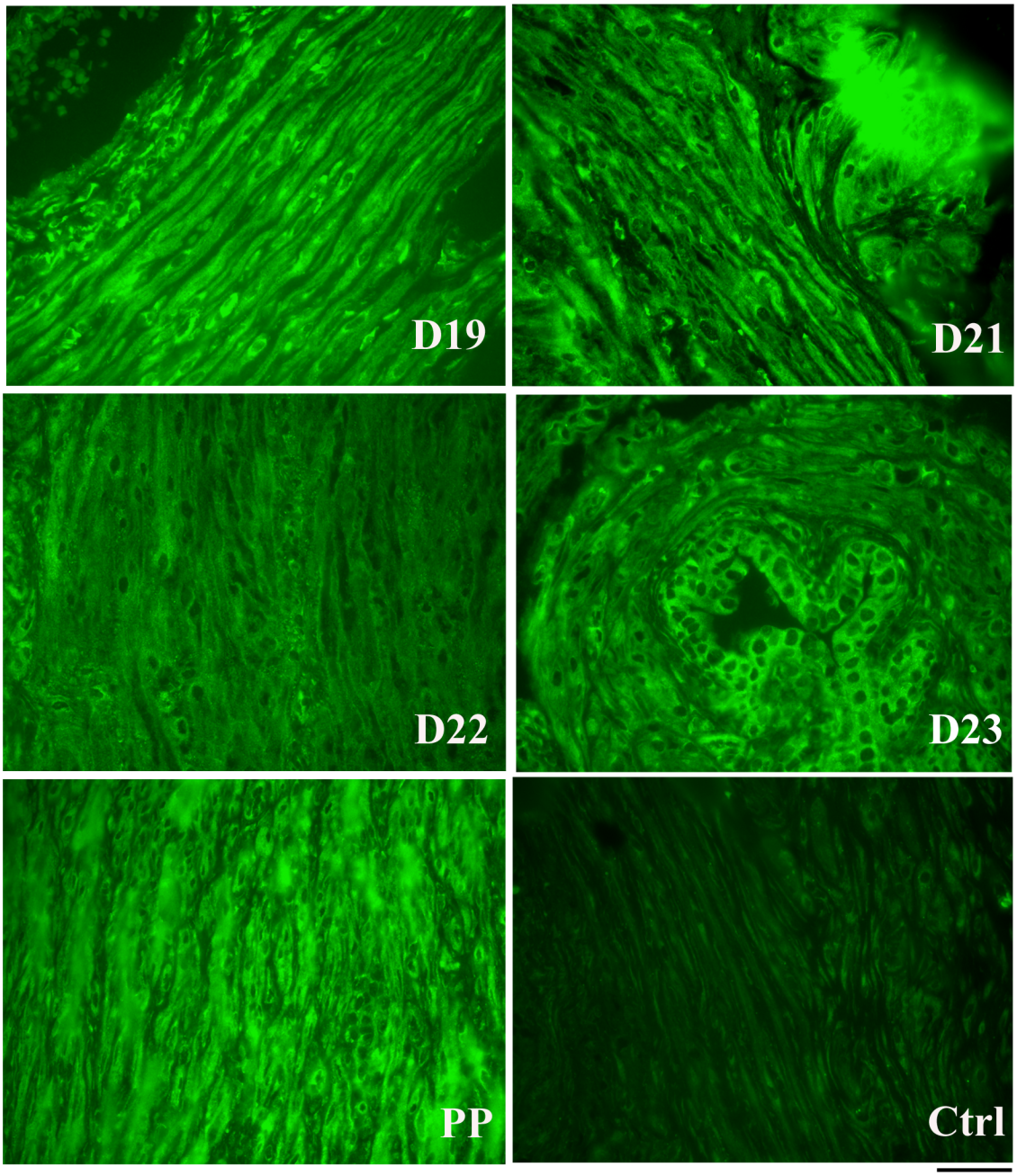
D19
D21
D22
D23
PP
Ctrl

significant decrease at d 12, 15, 17 and 19 when compared to NP, PP and d 6, 21, 22, and 23 (Figure 3.20).

3.6 Exogenous Expression of Hsf1 in hTERT-HM Cells

3.6.1 Restriction Endonuclease Digestion of pCMV6-Hsf1 Vector

Before transient transfection of hTERT-HM cells with a pCMV6-Hsf1 vector could be performed, restriction endonuclease digestion was conducted to verify the identity of the purified pCMV6-Hsf1 expression vector. The cDNA was inserted into the AsiSI/ Mlu I restriction sites of pCMV6 (Origene: MD, USA) and was therefore verified using these restriction enzymes . The uncut plasmid displayed two bands following electrophoresis representing supercoiled and relaxed circular forms of DNA, respectively. Following digestion of the vector using AsiSI/Mlu1, two expected DNA bands were visible, with an expected size of ~1600 bp, representing the insert, and ~12 000 bp, representing the pcMV6 expression vector (Figure 3.21). The same restriction endonuclease digestions of the expression vector were performed following midi preparation of the vector and DNA purification.

3.6.2 Optimization of Transfection Efficiency of hTERT-HM Cells

hTERT-HM cells were transfected using an Amaxa Nucleofector system. Prior to any transfections, experiments were conducted in triplicate to optimize the transfection efficiency. An Amaxa basic nucleofector kit for primary smooth muscle cells (Lonza) was used to transiently transfect hTERT-HM cells with the pEGFP-C3 expression vector capable of expressing green fluorescent protein. Six different programs were tested for

Figure 3.20 PARP-1 expression in rat myometrial tissue throughout gestation. **A)** Both PARP-1 and calponin were detected at the molecular weights of 115kDa and 34kDa, respectively. Representative immunoblots are shown that demonstrate their molecular weights. At 10 different gestational time points, densitometric analysis of PARP-1 was performed. The histogram shown displays the relative optical density of PARP-1 that has been normalized to the loading control, calponin, which accounts for any discrepancies, which may have occurred in loading the samples. PARP-1 expression was found to change significantly across gestation, following one-way ANOVA ($p<0.05$; $n=4$). The data is shown as mean ±S.E.M, and came from 4 different complete experiments. Data indicated with symbols were found to be statistically different after a post hoc Newman Keuls was performed ($p<0.05$). The PARP-1 expression was elevated early and late in pregnancy and then decreased in expression mid gestation. The data showed there was a significant decrease in expression at d12, 15, 17 and 19 when compared to all other time points throughout gestation. Defined abbreviations: NP= non-pregnant, PP= post-partum.

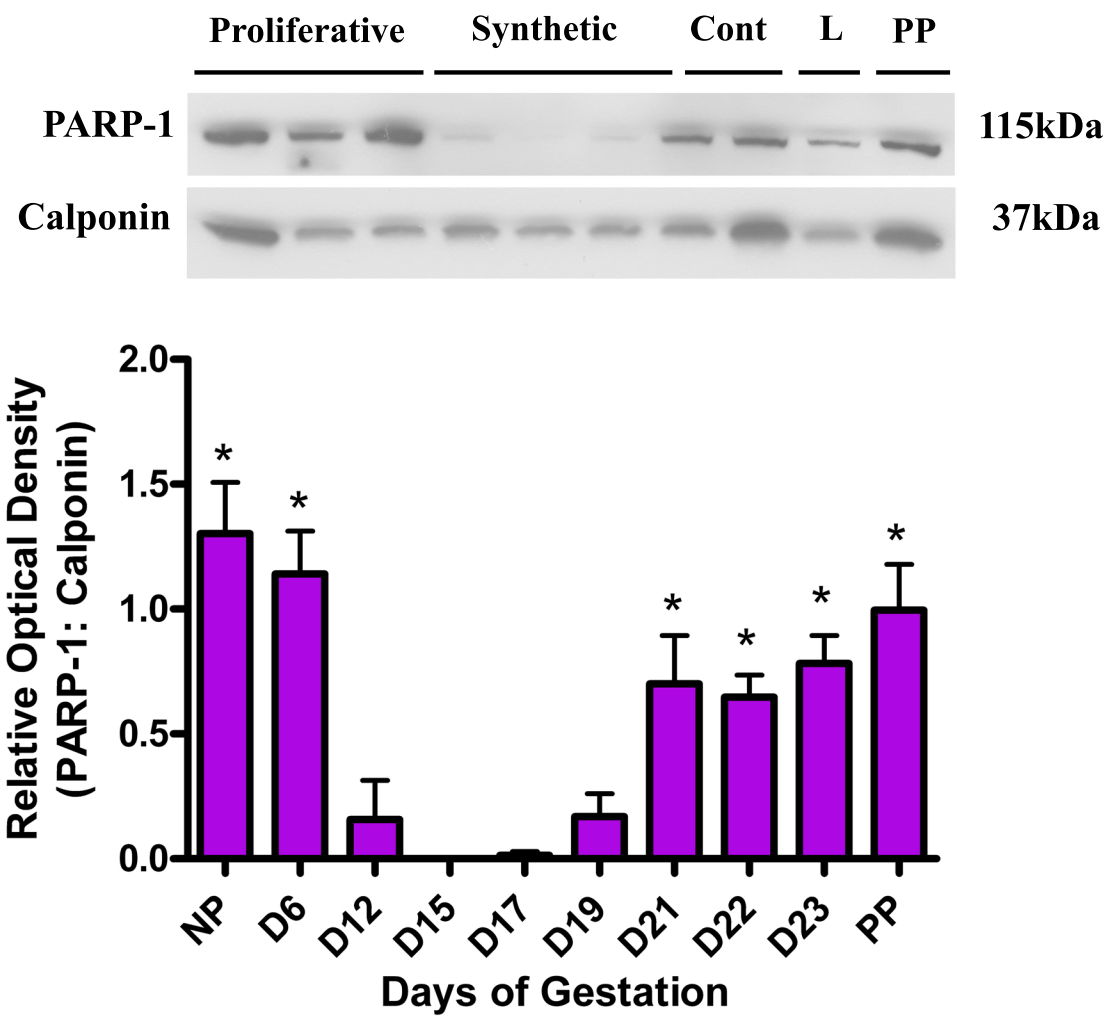
Proliferative
Synthetic
Cont
L
PP
PARP-1
115kDa
Calponin
37kDa
Relative Optical Density
(PARP-1: Calponin)
2.0
1.5
1.0
0.5
0.0
*
NP
D6
D12
D15
D17
D19
D21
D22
D23
PP
Days of Gestation

Figure 3.21 Representative restriction endonuclease digestion of the pCMV6 expression vector encoding a Myc-DDK tagged human Hsf1 cDNA construct. PureLink Quick Plasmid Miniprep Kit was used for DNA plasmid purification. For each enzyme, the vector was digested at 37°C in a water bath for 1 hour and the product compared to uncut pCMV6 Hsf1 plasmid DNA. Digestions were run on a 1% agarose gel that was prestained with SYBR Safe DNA gel stain. Lane 1, 1kb DNA Ladder; lane 2, uncut pCMV6 Hsf1 vector sample 1; lane 3, DNA digestion using AsiSI/MluI; lane 4, DNA digestion using MluI; lanes 5, 6 and 7 are the same as lanes 2, 3 and 4 except for pCMV6 Hsf1 vector sample 2 was used. Two bands are visible in the uncut plasmid lane since the circular DNA runs as two forms which migrate differently on a gel: a supercoiled and relaxed circular form. Digestion using both restriction enzymes was able to release the insert from the plasmid. Following digestion with only MluI, only one band was observed representing linearized plasmid DNA.

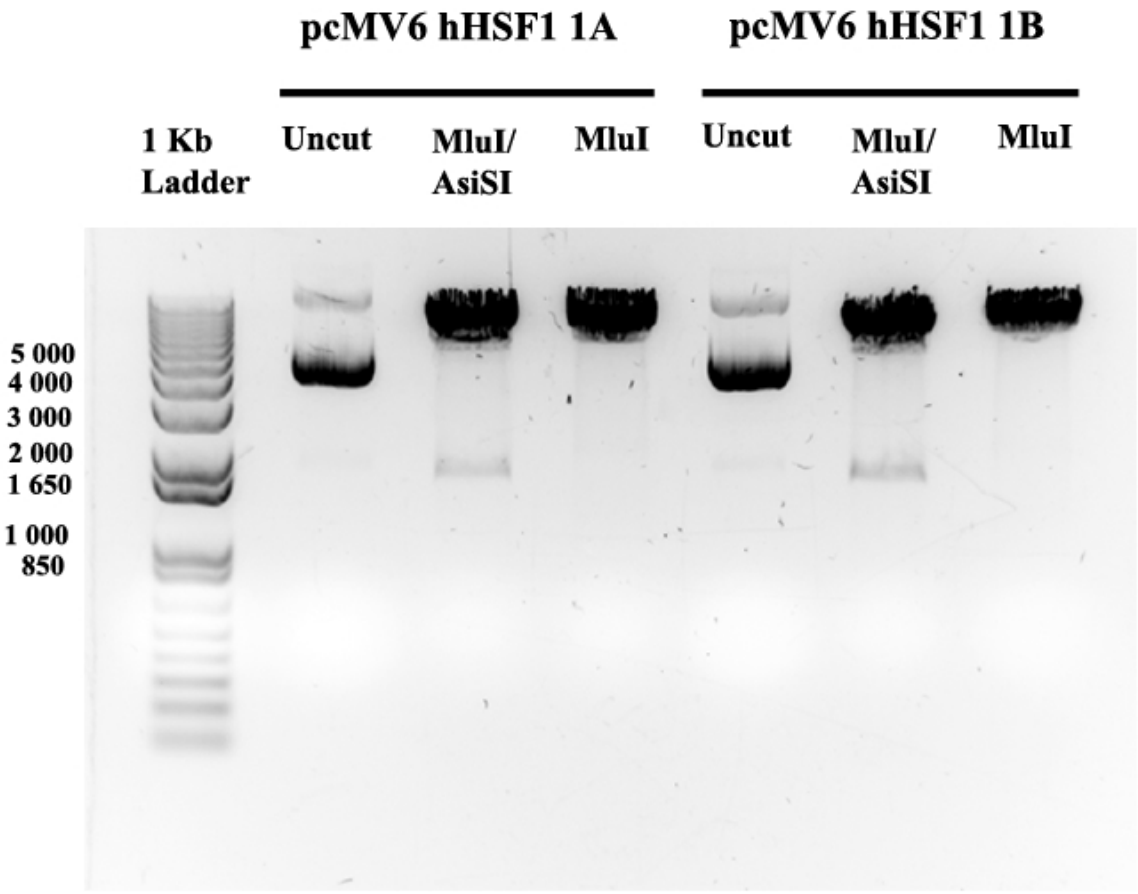
pcMV6 hHSF1 1A
pcMV6 hHSF1 1B
1 Kb Ladder
Uncut
MluI/ AsiSI
MluI
Uncut
MluI/ AsiSI
MluI
5 000
4 000
3 000
2 000
1 650
1 000
850

optimal transfection efficiency of the cells; A-033, D-033, P-013, P-042, U-025, B-017 or no program (control) and were examined at 24 and 48 hours (Figures 3.22, 3.23). This optimization of transfection was repeated with programs A-033 and U-025, which were the programs that showed the highest transfection efficiency and the lowest amount of cell loss. Consultation with Lonza also resulted in the testing of an additional program B-017 at two different time-points of 24 and 48 hours (Figures 3.24, 3.25). A-033 appeared to have the highest transfection efficiency and the least amount of hTERT-HM cell loss, and therefore was utilized for all further transfection experiments.

3.6.3 Transfection of hTERT-HM Cells with pCMV6-Hsf1 Vector

hTERT-HM cells were transiently co-transfected with a pCMV6-Hsf1 expression vector as well as a pEGFP-C3 expression vector to assess the effect of exogenous Hsf1 expression on these myometrial cells. As controls, additional cells were transfected with a pEGFP-C3 expression vector alone or not transfected (No Program). Phase contrast and fluorescent images were taken 24 hours, 48 hours and 72 hours following transfection. A representative image is shown at 72 hours, which also reflects the results seen at 24 and 48 hours. (Figure 3.26).

Protein lysates were also collected from hTERT-HM cells at both 24 and 72 hours post transfection with the pCMV6-Hsf1 expression vector. Immunoblot analysis was performed using a FLAG-tag specific antibody (Table 2.1) to recognize FLAG-tagged Hsf1 and confirm the transfection was successful. The analysis showed Hsf1 at ~75kDa only in cells transfected with pCMV6-Hsf1 (Figure 3.27 A). Immunoblot analysis was performed again with an Hsf1 specific antibody (Table 2.1) and this analysis detected

Figure 3.22 Examination of optimal transfection efficiency of hTERT-HM cells with pEGFP-C3 vector 24 h post-transfection. Experiments were conducted to determine which electroporation program (A-033, D-033, P-013, P-024, U-025), would provide the highest percentage of transfected cells with the least amount of cell death in hTERT-HM cells. Experiments were conducted with a basic nucleofector kit for smooth muscle cells. Images in the left hand column represent phase contrast micrographs, and images on the right hand column represent immunofluorescence micrographs showing which cells have been transiently transfected with the pEGFP-C3 expression vector. Images were taken 24 hours after transfection.

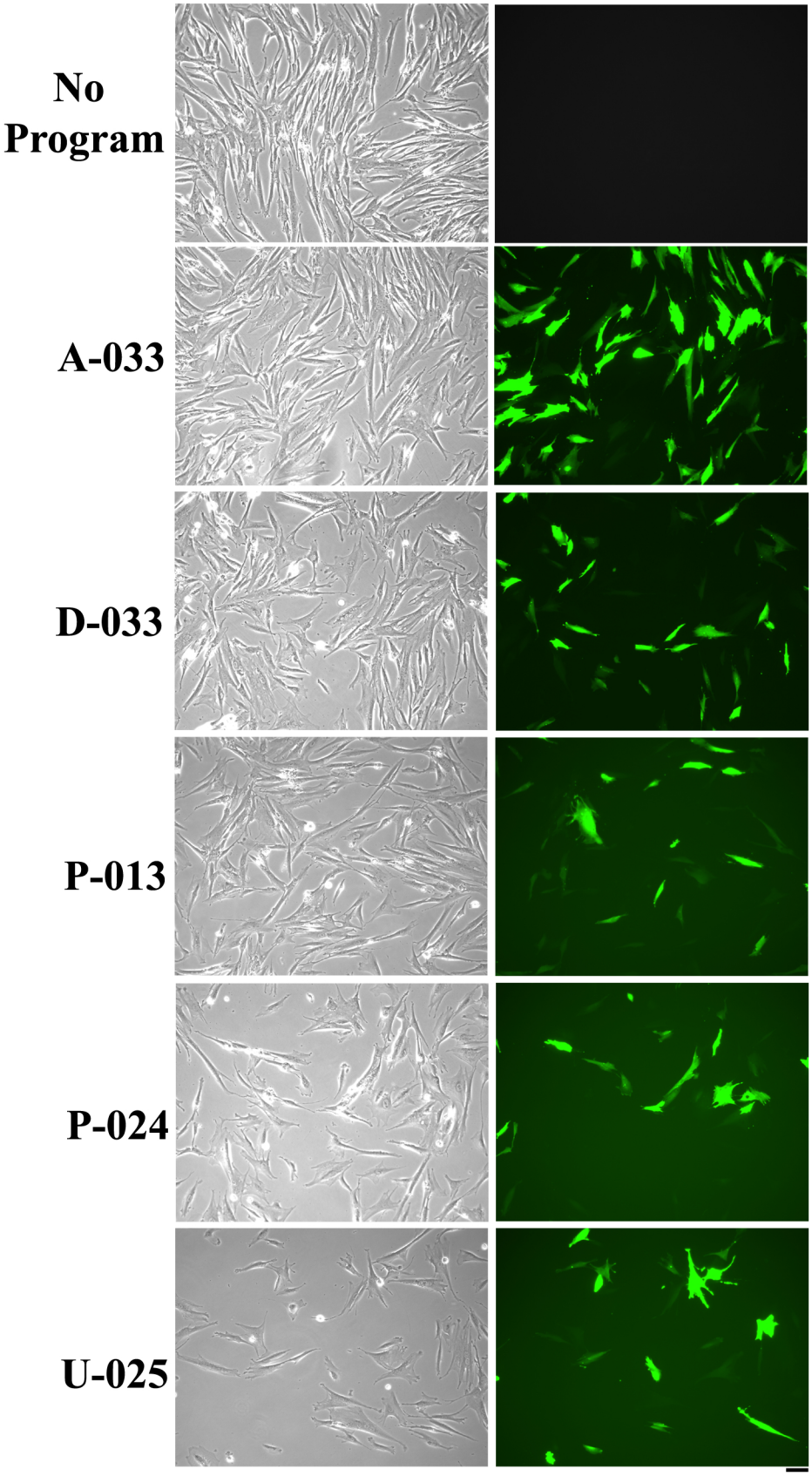
No Program
A-033
D-033
P-013
P-024
U-025

Figure 3.23 Examination of optimal transfection efficiency of hTERT-HM cells with pEGFP-C3 vector 48 h post-transfection. Experiments were conducted to determine which electroporation program (A-033, D-033, P-013, P-024, U-025), would provide the highest percentage of transfected cells with the least amount of cell death in hTERT-HM cells. Experiments were conducted with a basic nucleofector kit for smooth muscle cells. Images in the left hand column represent phase contrast micrographs, and images on the right hand column represent immunofluorescence micrographs showing which cells have been transiently transfected with the pEGFP-C3 expression vector. Images were taken 48 hours after transfection.

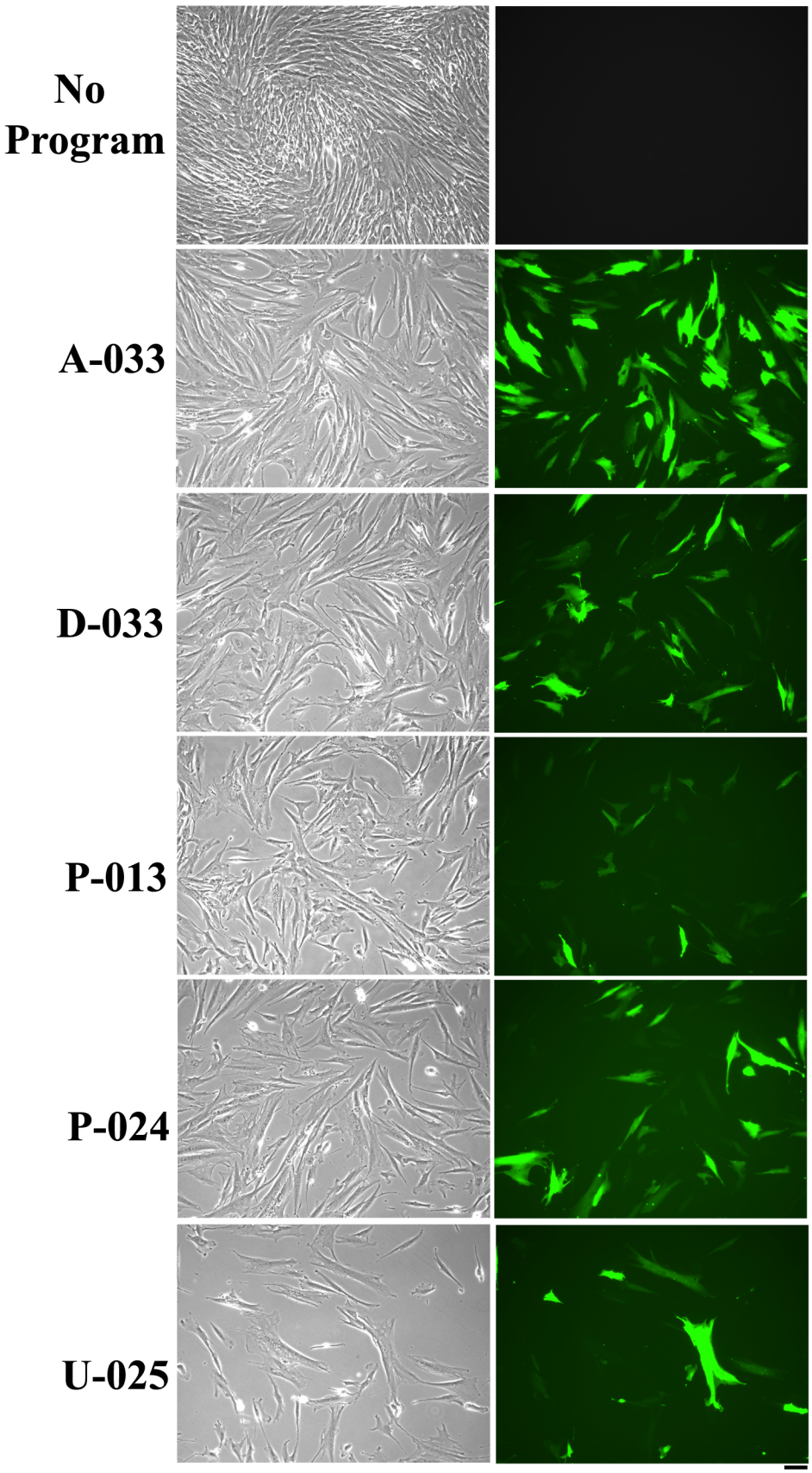
No Program
A-033
D-033
P-013
P-024
U-025

Figure 3.24 Optimization of transfection efficiency of hTERT-HM cells with programs A-033, U-025, and B-017 24 h post-transfection. An experiment was conducted focusing on two previously used transfection programs, A-033 and U-025, which previously appeared to be optimal for hTERT-HM cells. A third program, B-017, was suggested by the Nucleofector Company Lonza, and thus examined as well. Images in the left hand column represent phase contrast micrographs, and images on the right hand column represent immunofluorescence micrographs showing which cells have been transiently transfected with the pEGFP-C3 expression vector. Images were taken 24 hours after transfection.

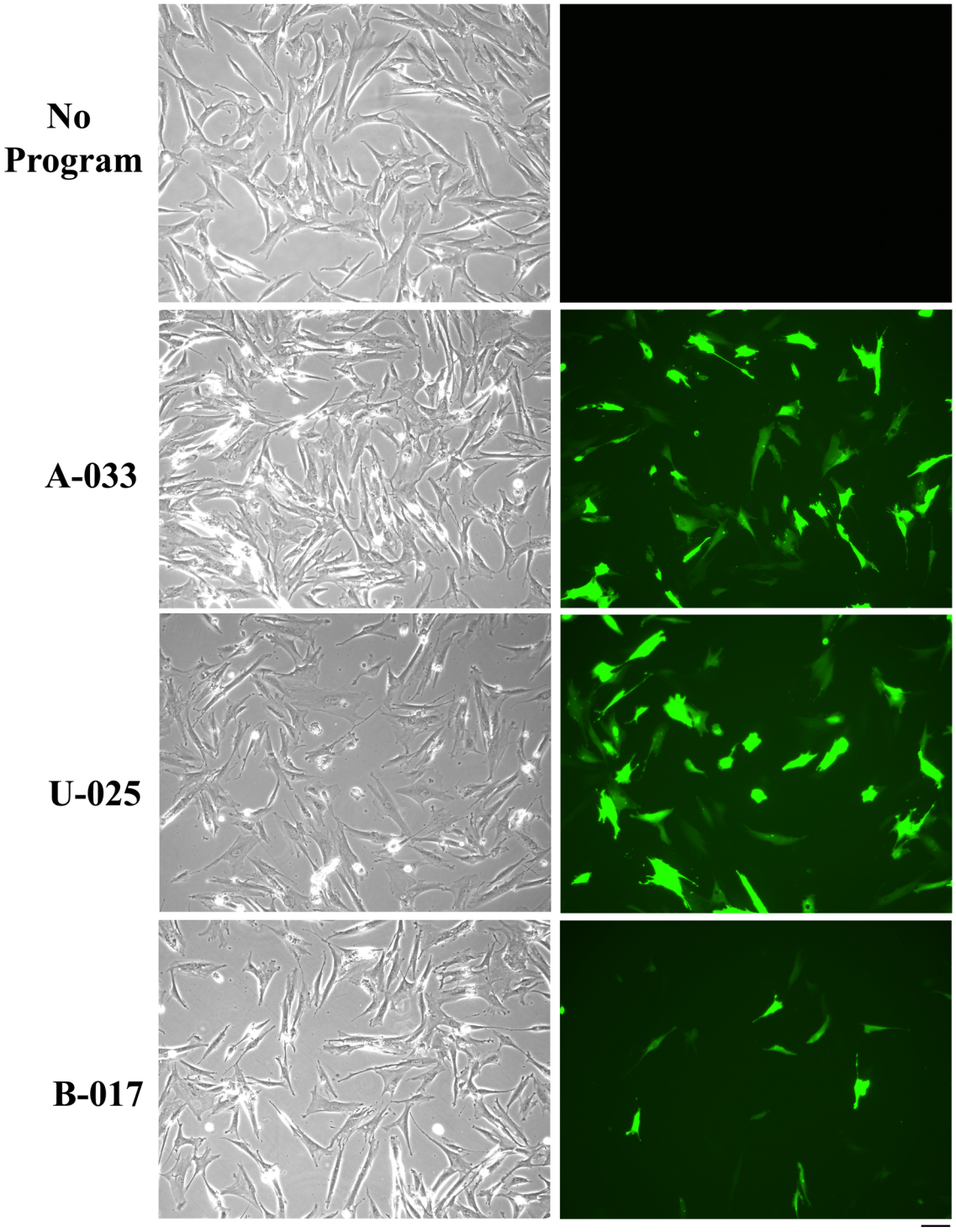
No Program
A-033
U-025
B-017

Figure 3.25 Optimization of transfection efficiency of hTERT-HM cells with programs A-033, U-025, and B-017 48 h post-transfection. An experiment was conducted focusing on two previously used transfection programs, A-033 and U-025, which previously appeared to be optimal for hTERT-HM cells. A third program, B-017, was suggested by the Nucleofector Company Lonza, and thus examined as well. Images in the left hand column represent phase contrast micrographs, and images on the right hand column represent immunofluorescence micrographs showing which cells have been transiently transfected with the pEGFP-C3 expression vector. Images were taken 48 hours after transfection.

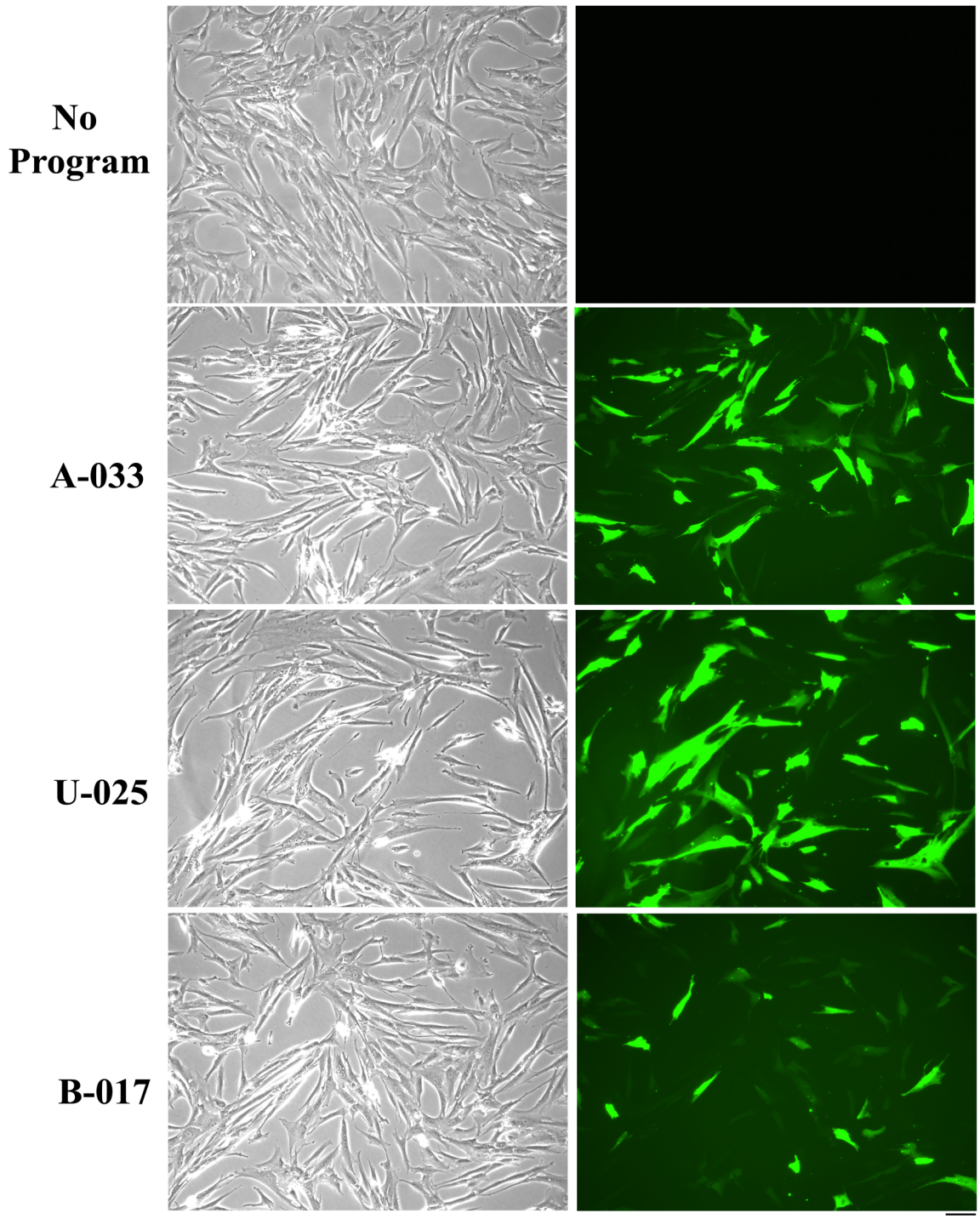
No Program
A-033
U-025
B-017

Figure 3.26 Transient co-transfection of hTERT-HM cells with pCMV6-Hsf1 and pEGFP-C3. hTERT-HM cells were either mixed with pEGFP-c3 expression vector but did not undergo electroporation (No program control), transfected with pEGFP-C3 alone (GFP), or co-transfected with pEGFP-C3 and pCMV6-Hsf1 mammalian expression vectors (Hsf1). The pCMV6-Hsf1 vector contained a myc-DDK-tagged human Hsf1 cDNA. Program A-033 was used for all transfections and images were taken 72 hours after transfection. Scale bar = 100 μm

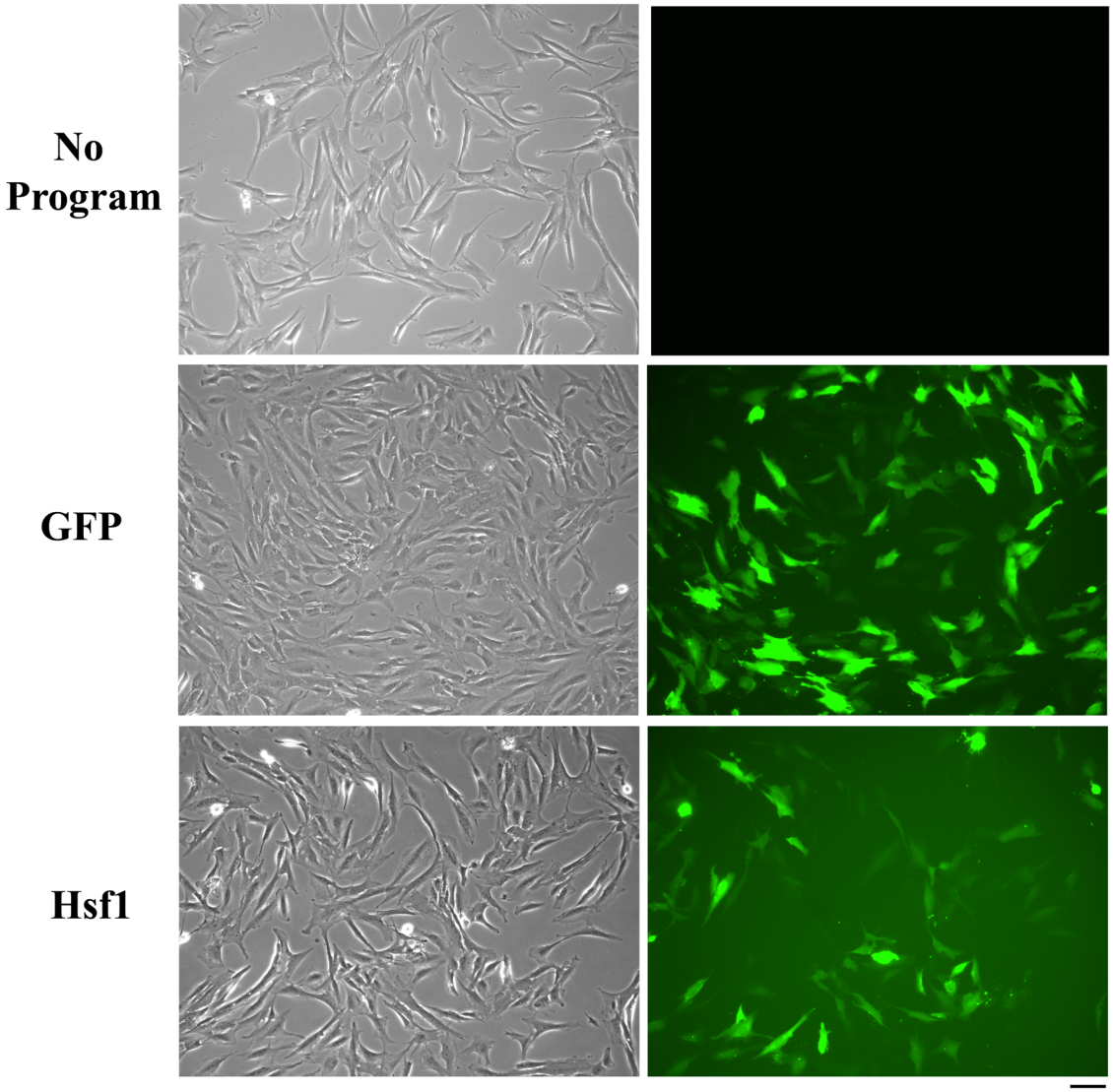
No Program
GFP
Hsf1

Figure 3.27 Confirmation of FLAG-tagged Hsf1 protein expression in transfected hTERT-HM cells 72h post transfection. hTERT-HM cells were transiently transfected with FLAG (DDK)-tagged pCMV6-Hsf1. To verify transfection, transfected cells were collected for protein extraction, SDS-PAGE, and electroblotting. Immunoblots were probed with a mouse monoclonal FLAG specific antisera (A) or rabbit polyclonal Hsf1 specific antisera (B) and subsequently a rabbit specific GAPDH antisera. The first lane represents a no program control where cells did not undergo transfection with pEGFP-C3 expression vector. The second lane represents a GFP control, where cells were transiently transfected with pEGFP-C3 alone. The third lane represents cells that were transfected with both FLAG-tagged pCMV6-Hsf1 and pEGFP-C3.

A

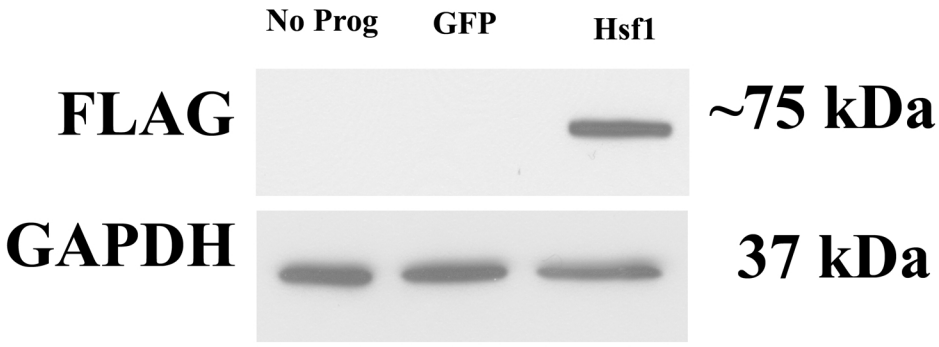
No Prog
GFP
Hsf1
FLAG
~75 kDa
GAPDH
37 kDa

B

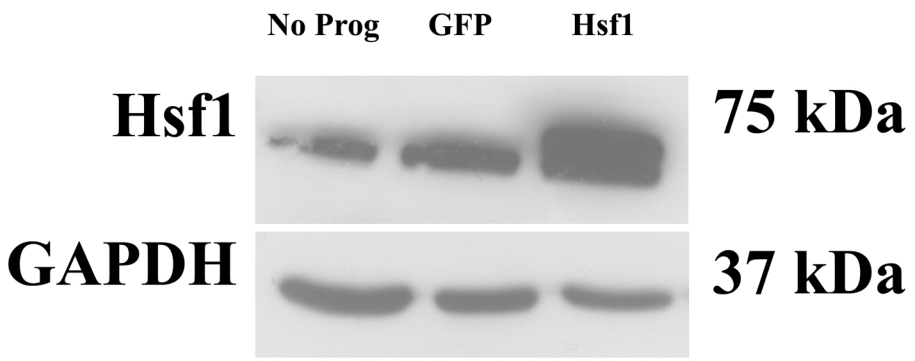
No Prog
GFP
Hsf1
Hsf1
75 kDa
GAPDH
37 kDa

endogenous Hsf1 at 75kDa in all cells. FLAG-tagged Hsf1 was also detected slightly above 75kDa in pCMV6-Hsf1 transfected cells both at 24 h (data not shown) and 72 h post transfection (Figure 3.27 B).

The same protein lysates collected at 24 and 72 hours post transfection were used in subsequent immunoblot analyses to assess whether exogenous expression of Hsf1 caused an increase in Hsf1 target gene expression (Table 2.1). Exogenous expression of Hsf1 did not increase Hsp 70, HspB1, PARP or HspB8 protein expression in the myometrium at 24 hours (Hsp70 only) or 72 hours post-transfection (HspB1, PARP-1, HspB8) (Figure 3.28).

3.6.4 Transfection of hTERT-HM Cells with pCMV6-Hsf1 and pCMV7-PARP-1 Vectors

hTERT-HM cells were transiently co-transfected with a pCMV7-PARP-1 and pEGFP-C3 expression vectors to assess the effect of exogenous PARP-1 expression in these myometrial cells. Finally, a co-transfection of pCMV6-Hsf1 and pCMV7-PARP-1 expression vectors with pEGFP-C3 was performed in order to assess the effect of expressing both exogenous proteins on target protein expression. hTERT-HM cells that were not transfected (No Program) served as a negative control. Phase contrast and fluorescent images were taken 24 hours, 48 hours and 72 hours following transfection. A representative image is shown at 72 hours, which also reflects the results seen at 24 and 48 hours. (Figure 3.29).

Twenty four and 72 hours post transfection of hTERT-HM cells, protein lysates were collected for subsequent immunoblot analyses. Blots were probed with a FLAG

Figure 3.28 Examination of expression of Hsf-1 inducible gene products following Hsf1 overexpression. Twenty four hours, or 72 hours post transfection, cells were lysed, protein extracted and SDS-PAGE and electroblotting completed. **A)** Hsp 70 protein expression in hTERT-HM cells 24h post transfection with FLAG-tagged pCMV6Hsf1. Immunoblots were probed with mouse monoclonal Hsp70 specific antisera and a rabbit polyclonal GAPDH specific antisera. **B)** HspB1 protein expression in hTERT-HM cells 72h post transfection. Immunoblots were probed with a mouse monoclonal HspB1 specific antisera and a rabbit polyclonal GAPDH specific antisera.. **C)** PARP-1 protein expression in hTERT-HM cells 72h post transfection. Immunoblots were probed with a mouse monoclonal PARP-1 specific antisera and a rabbit polyclonal GAPDH specific antisera. **D)** HspB8 protein expression in hTERT-HM cells 72h post transfection. Immunoblots were probed with a rabbit polyclonal HspB8 specific antisera and a rabbit polyclonal GAPDH specific antisera. In all blots, the first lane represents a no program control where cells did not undergo transfection after addition of pEGFP-C3 expression vector to the cells. The second lane represents a GFP control, where cells were transiently transfected with pEGFP-C3 alone. The third lane represents cells that were co-transfected with FLAG-tagged pCMV6Hsf1 and pEGFP-C3. In all cases, there appeared to be no increase in Hsp70, HspB1, PARP-1 or HspB8 protein expression upon over- expression of Hsf1 in hTERT-HM cells when compared to the GFP control ($p>0.05$, $n=3$).

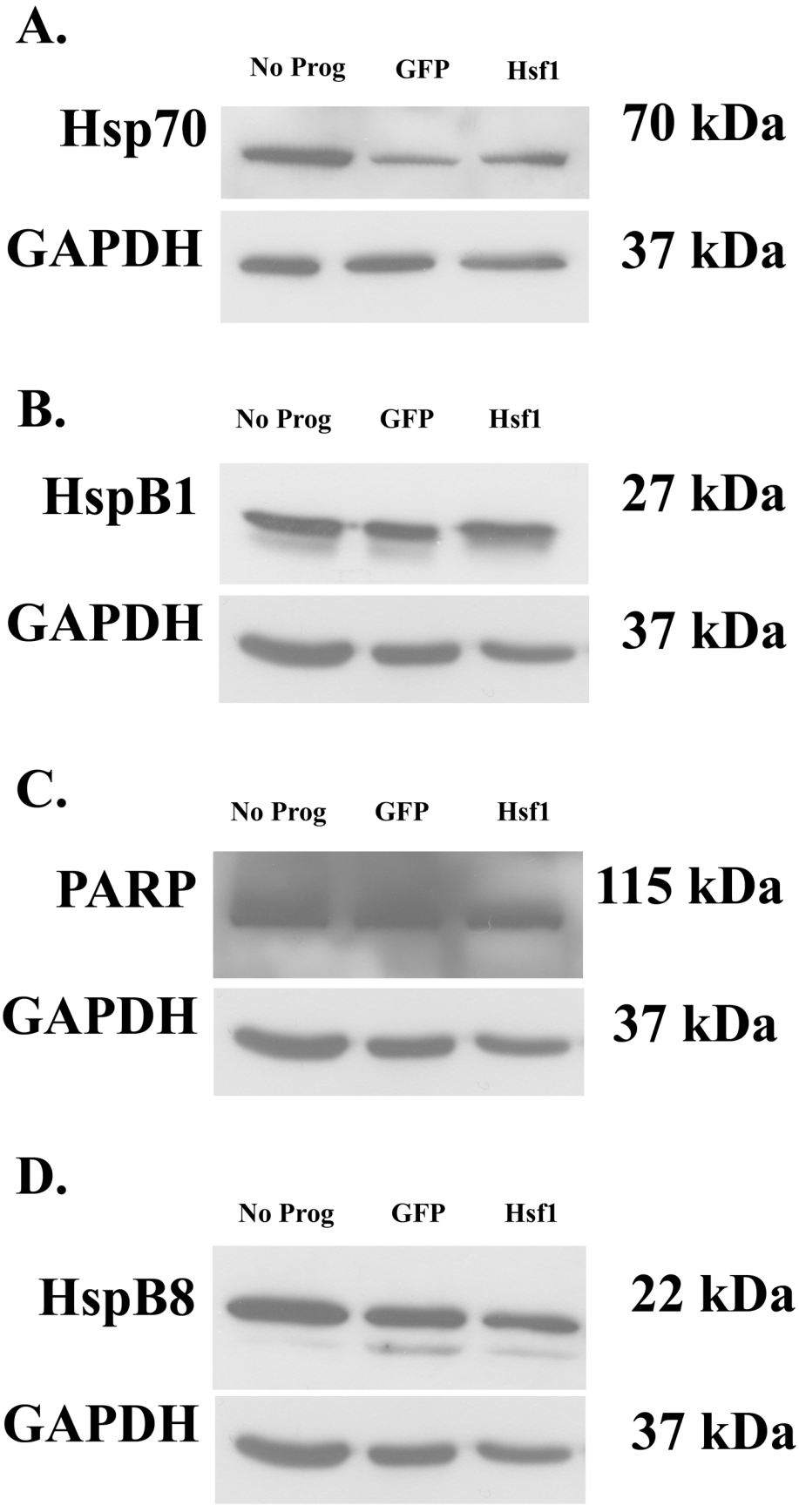
A.
No Prog
GFP
Hsf1
Hsp70
70 kDa
GAPDH
37 kDa
B.
No Prog
GFP
Hsf1
HspB1
27 kDa
GAPDH
37 kDa
C.
No Prog
GFP
Hsf1
PARP
115 kDa
GAPDH
37 kDa
D.
No Prog
GFP
Hsf1
HspB8
22 kDa
GAPDH
37 kDa

Figure 3.29 Assessment of transfection efficiency following PARP-1 and Hsf1 overexpression. Representative images from phase contrast micrographs and wide-field epi-fluorescence detection of hTERT-HM cells after co-transfection with mammalian expression vectors encoding hHsf1, hPARP-1, and EGFP cDNA. hTERT-HM cells were either mixed with mammalian expression vectors but did not undergo electroporation (No program control), transfected with pEGFP-C3 alone (GFP), co-transfected with pEGFP-C3 and pCMV7- PARP-1 (pCMV7-PARP-1/GFP) or co-transfected with pEGFP-C3, pCMV7- PARP-1 and pCMV6-Hsf1 mammalian expression vectors (pCMV7-PARP-1/pCMV6-Hsf1/GFP). Images were taken 72h hours after transfection but similar results were also observed at 24h and 48 h (data not shown). Scale bar = 100 μm.

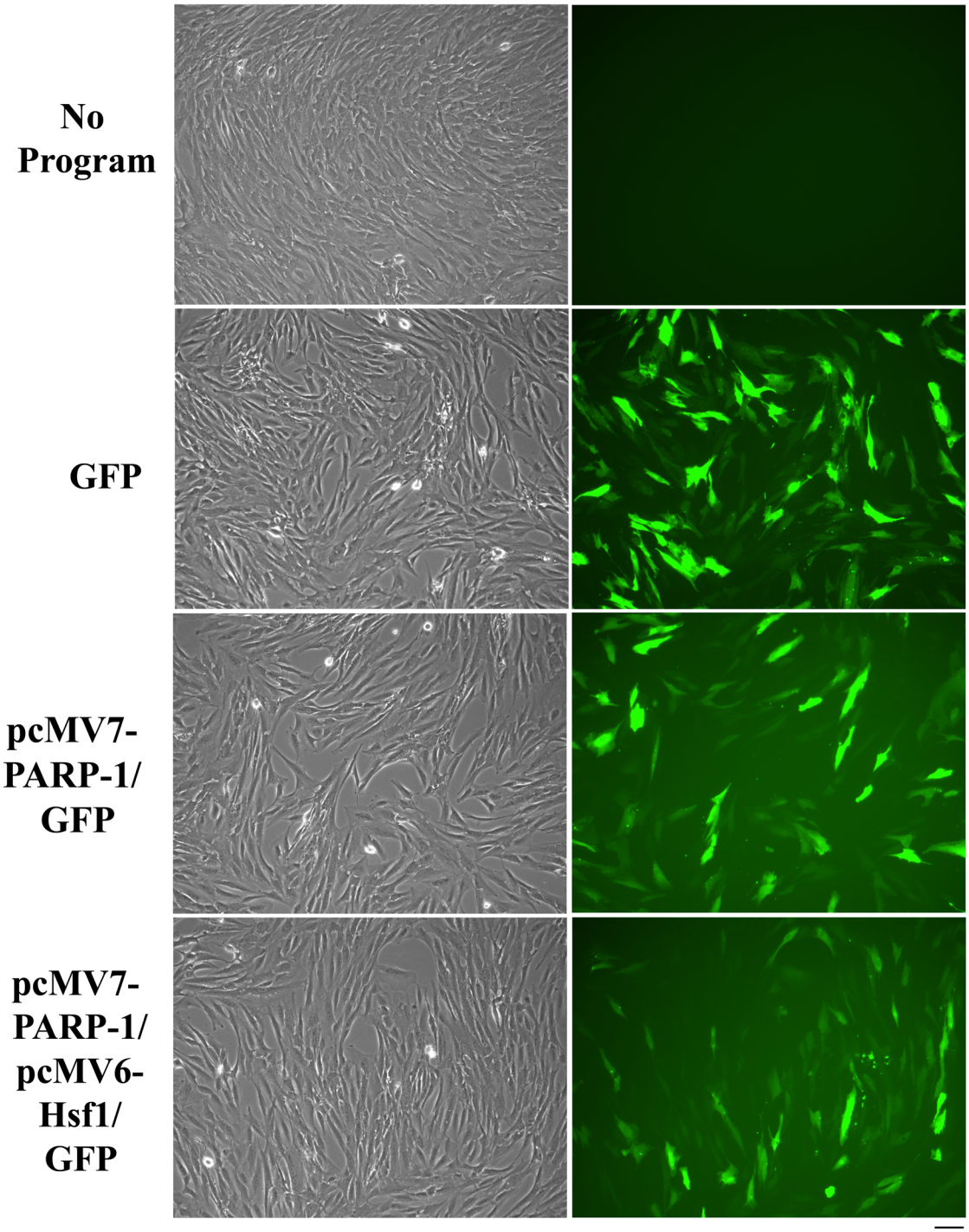
No Program
GFP
pcMV7-PARP-1/ GFP
pcMV7-PARP-1/ pcMV6-Hsf1/ GFP

specific antisera and confirmed the expression of both FLAG-tagged Hsf1 and FLAG-tagged PARP-1 at 24 hours (Table 2.1; Figure 3.30). Similar results were also seen at 72 hours. Subsequent immunoblot analysis was also performed using Hsf1 or PARP-1 specific antisera (Table 2.1). Endogenous Hsf1 and PARP-1 proteins were again detected in all lanes at their expected molecular weights of 75kDa and 115kDa, respectively. In the lanes where cells expressed exogenous levels of Hsf1, a band slightly higher than 75kDa was observed, representing the FLAG-tagged form of the Hsf1 protein (Figure 3.31). A similar doublet was not as resolvable for PARP-1 due to the higher molecular weight of PARP-1 and the percentage of acrylamide gel used for electrophoresis.

The same protein lysates collected at 24 and 72 hours post transfection were used in subsequent immunoblot analyses to determine whether exogenous co-expression of Hsf1 and PARP-1 resulted in an increase in target gene expression (Table 2.1). Results showed that exogenous co-expression of Hsf1 and PARP-1 did not increase Hsp70, Hsp90 or HspB1 expression in the myometrium (Figures 3.32).

3.6.5 Assessment of Proliferation Post Transfection with pCMV6-Hsf1 and pCMV7-PARP-1 Expression Vectors

hTERT-HM cells were grown as previously described in section 2.6. Cells were then transfected with pCMV6-Hsf1, pCMV7-PARP-1 or both expression vectors. Since both Hsf1 and PARP-1 are involved in cell proliferation, it was expected that cell proliferation would increase in hTERT-HM cells post transfection with these vectors. Following an MTS proliferation assay, it was demonstrated that cell proliferation (shown as percent cell survival) only significantly increased in hTERT-HM cells transfected with

Figure 3.30 Confirmation of FLAG-tagged PARP-1 and Hsf1 protein expression in hTERT-HM cells 24h post transfection. hTERT-HM cells were transiently transfected with FLAG (DDK)-tagged pCMV6-Hsf1 and FLAG-tagged pcMV7PARP-1. To verify transfection, transfected cells were collected for protein extraction, SDS-PAGE, and electroblotting. Immunoblots were probed with a mouse monoclonal FLAG specific antisera and subsequently a rabbit specific GAPDH antisera. Bands were detected at ~75kDa, ~115kDa and 37kDa, respectively, representing the FLAG-tagged Hsf1, FLAG-tagged PARP-1 and the GAPDH control. The first lane represents a no program control where cells did not undergo transfection with pEGFP-C3 expression vector. The second lane represents a GFP control, where cells were transiently transfected with pEGFP-C3 alone. The third lane represents cells that were transfected with both FLAG-tagged pCMV7-PARP-1 and pEGFP-C3. The final lane represents those cells that were co-transfected with FLAG-tagged pCMV7-PARP-1 and FLAG-tagged pCMV6-Hsf1.

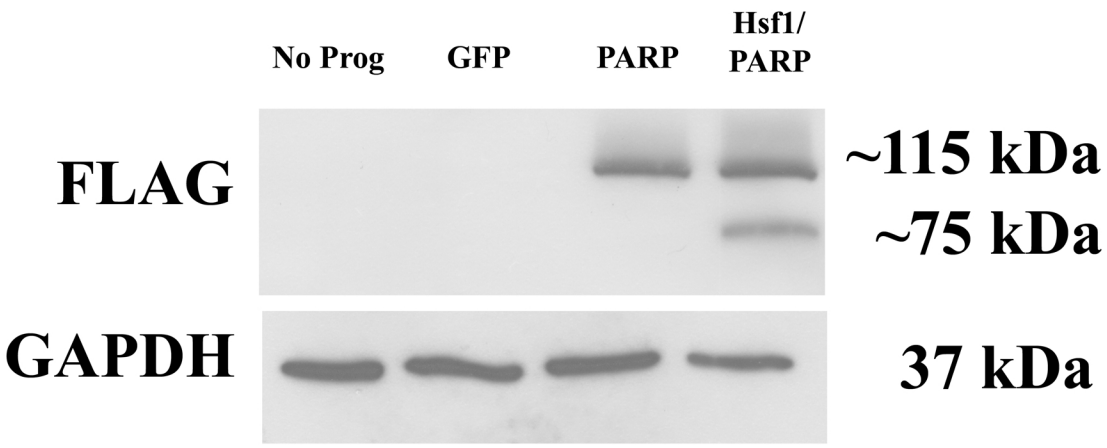
No Prog
GFP
PARP
Hsf1/
PARP
FLAG
~115 kDa
~75 kDa
GAPDH
37 kDa

Figure 3.31 Confirmation of Hsf1 and PARP-1 overexpression in transfected hTERT-HM cells. **A)** Hsf1 protein expression in hTERT-HM cells 24 h post co-transfection. hTERT-HM cells were transiently transfected with pEGFP-C3 alone, FLAG-tagged pCMV7-PARP-1 alone, or FLAG-tagged pCMV6-Hsf1 and FLAG-tagged pCMV7-PARP-1. To verify transfection, transfected cells were collected for protein extraction, SDS-PAGE, and electroblotting. Immunoblots were probed with a rabbit polyclonal Hsf1 specific antisera and subsequently a rabbit polyclonal GAPDH specific antisera. Bands were detected in all lanes at 75kDa and 37kDa, respectively, representing the Hsf1 and the GAPDH control. In the fourth lane, a second band at a slightly higher molecular weight was observed, which represents the FLAG-tagged form of Hsf1. The first lane represents a no program control where cells did not undergo transfection after addition of mammalian expression vectors to the cells. **B)** PARP-1 protein expression in hTERT-HM cells 24 h post co-transfection. hTERT-HM cells were transiently transfected and cell lysates and immunoblots prepared as described above. Immunoblots were probed with a mouse monoclonal PARP-1 specific antisera and subsequently a rabbit polyclonal GAPDH specific antisera. Bands were detected in all lanes at 115kDa and 37kDa representing PARP-1 and GAPDH, respectively. In the fourth lane, a second band, representig the FLAG-tagged form of PARP-1, was not observed. This was expected since the endogenous and Flag tagged PARP-1 were difficult to resolve within the SDS-PAGE utilized. The first lane represents a no program control where cells did not undergo transfection after the expression vectors were added to cells.

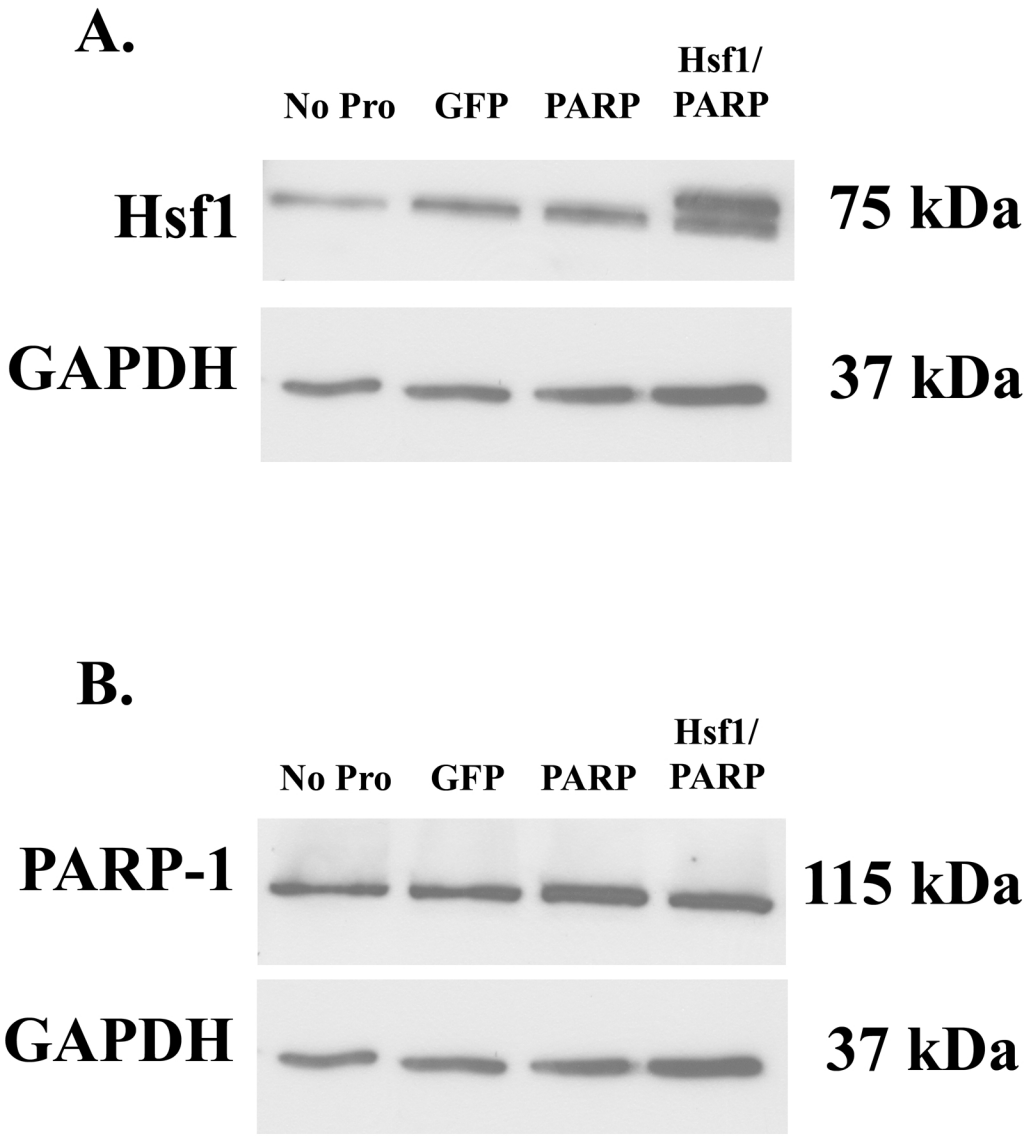
A.
No Pro
GFP
PARP
Hsf1/
PARP
Hsf1
75 kDa
GAPDH
37 kDa
B.
No Pro
GFP
PARP
Hsf1/
PARP
PARP-1
115 kDa
GAPDH
37 kDa

Figure 3.32 Examination of expression of Hsf-1 inducible gene products following Hsf1 and PARP-1 overexpression. **A)** Hsp70 protein expression in hTERT-HM cells 24 h post co-transfection. hTERT-HM cells were transiently transfected with pEGFP-C3, FLAG-tagged pCMV7-PARP-1, or both FLAG-tagged pCMV6-Hsf1 and FLAG-tagged pCMV7-PARP-1. Immunoblots were probed with an mouse monoclonal Hsp70 specific antisera and then a rabbit polyclonal GAPDH specific antisera. **B)** Hsp90 protein expression in hTERT-HM cells 24 h post co-transfection. hTERT-HM cells were transiently transfected as described above. Immunoblots were probed with an mouse monoclonal Hsp90 specific antisera and a then a rabbit polyclonal GAPDH specific antisera. **C)** HspB1 protein expression in hTERT-HM cells 24 h post co-transfection. hTERT-HM cells were transiently transfected as described above. Immunoblots were probed with an mouse monoclonal HspB1 specific antisera and then a GAPDH specific antisera. In all blots, the first lane represents a no program control where cells did not undergo transfection following addition of expression vectors to the cells. The second lane represents a GFP control, where cells were transiently transfected with pEGFP-C3. The third lane represents cells that were transfected with both FLAG-tagged pCMV7-PARP-1 and pEGFP-C3. The final lane represents those cells that were co-transfected with FLAG-tagged pCMV7-PARP-1 and FLAG-tagged pCMV6-Hsf1. There appeared to be no increase in Hsp70, Hsp90, or HspB1 protein expression following exogenous expression of PARP-1 or PARP-1/Hsf1 in cells when compared to the GFP control.

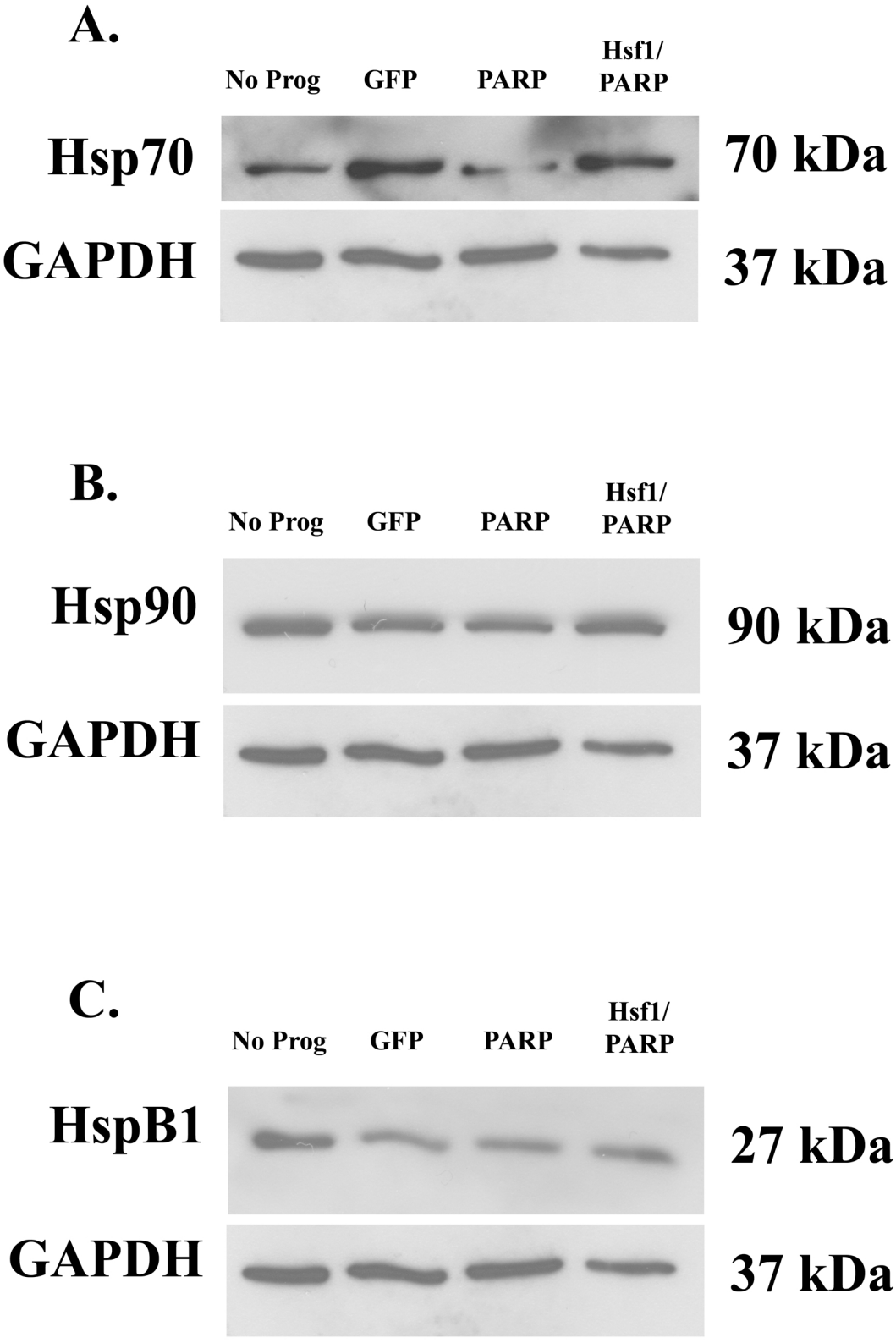
A.
No Prog
GFP
PARP
Hsf1/
PARP
Hsp70
70 kDa
GAPDH
37 kDa
B.
No Prog
GFP
PARP
Hsf1/
PARP
Hsp90
90 kDa
GAPDH
37 kDa
C.
No Prog
GFP
PARP
Hsf1/
PARP
HspB1
27 kDa
GAPDH
37 kDa

pCMV7-PARP-1 or following co-transfection of pCMV6-Hsf1 and pCMV7-PARP-1 (Figure 3.33). The results indicate a role for PARP-1 in regulating cell proliferation, but not Hsf1.

Figure 3.33 Assessment of proliferation following transfection with pcMV6-Hsf1 and pCMV7-PARP-1 expression vectors. hTERT-HM cells were transfected with pEGFP-C3 alone, pCMV6-Hsf1 alone, pcMV7PARP-1 alone or co-transfected with both pCMV6-Hsf1 and pcMV7PARP-1 expression vectors. Following an MTS proliferation assay, it was shown that cell proliferation (shown as percent cell survival) did significantly increase post transfection with pcMV7-PARP-1 and following co-transfection when compared to the GFP control ($p<0.05$).

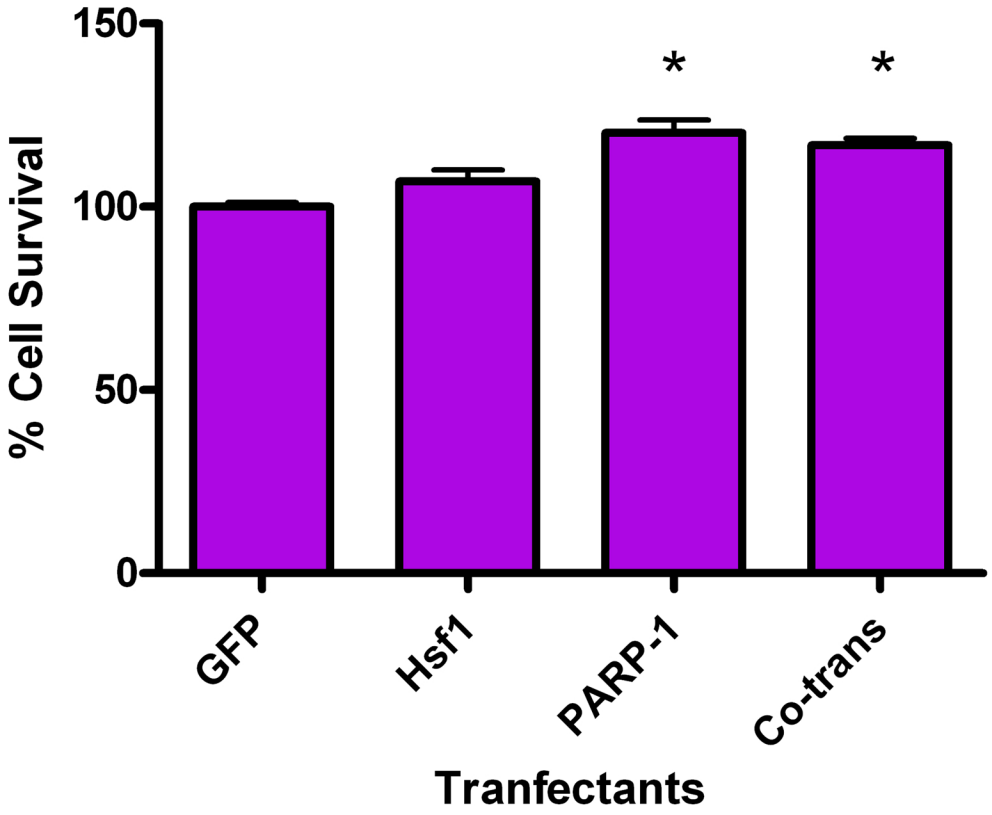
150
100
50
0
% Cell Survival
*
*
GFP
Hsf1
PARP-1
Co-trans
Tranfectants

Chapter 4

Discussion

4.1 Expression of Hsf1 during Normal Pregnancy and Labour

Little information is known about Hsf1 in the myometrium, as only one other paper has studied Hsf1 expression in the uterus. Stephens et al. (2010) conducted a proteomic study examining altered Hsf1 abundance in human eutopic endometrium of endometriosis patients in the mid-secretory phase of the menstrual cycle; however, this paper only stated that it was found in the uterus and nothing about Hsf1 expression or potential function. This research was also conducted in the endometrium, and in human subjects; therefore, the results presented in this thesis provide novel data on the expression of Hsf1 in uterus smooth muscle or myometrium. It was hypothesized that Hsf1 would be expressed in the myometrium during pregnancy and that it could be important during the proliferative phase of myometrial differentiation to activate expression of key genes necessary for this process.

Expression of total Hsf1 protein was most elevated before pregnancy (NP) and up until d12 of gestation. The expression was highest at d6 and then showed a significant decrease ($p<0.05$) in expression at d15, d17 and d22. This pattern supports our initial hypothesis that Hsf1 could contribute to the proliferation of myocytes, which occurs early in gestation. In contrast, immunofluorescence studies showed that Hsf1 was robustly detected throughout gestation, primarily in the cytoplasm of myometrial cells, with detection also in speckles within nuclei. Although the pattern of expression seen in immunoblot analysis did not correlate with immunofluorescence detection, this may be

attributed to the fact that immunofluorescence is a less sensitive technique for quantification than immunoblot analysis and may not have been able to detect the fluctuations in expression. The presence of Hsf1 in the nucleus was confirmed by confocal analysis that showed there was a speckled appearance of Hsf1 detection in the nucleus. Hsf1 normally shuttles between the nucleus and cytoplasm (Yang et al., 2008), and our immunofluorescence detection of Hsf1 primarily in the cytoplasm of myometrial cells, and a lesser extent in cell nuclei agrees with the published literature (Anckar & Sistonen, 2007). The data also indicate that Hsf1 is available in myometrial cells to drive expression of key genes such as stress proteins.

Detection of the active, phosphorylated (pSer-230) form of Hsf1 was also elevated early in pregnancy and subsequently decreased until PP. In comparison to the immunoblot analysis of total Hsf1, active Hsf1 expression decreased more gradually. A pHsf1 to total Hsf1 ratiometric analysis was not completed as it is an insensitive and inappropriate comparison (Janes, 2015). According to Janes (2015), comparing two different antibodies with different affinities for total and phosphorylated Hsf1 is not an accurate evaluation of the amount of total protein to phosphorylated protein. The expression of pSer-230 was highest at d12 and was found to be significantly lower at d22 when compared to d12 ($p<0.05$). Of note, the pSer230 Hsf1 band of interest was detected at a lower molecular weight than the total Hsf1 form. This may be attributed to the fact that in the literature, Hsf1 has been found to have a molecular weight range of about 60-75kDa, and can appear on immunoblots as a large smear (Chou et al., 2012). This was also shown in figure 3.8 A. Hsf1 can undergo other post-translational modifications such as sumoylation and acetylation altering the observed molecular weight (Knauf et al.,

1996; Chou et al., 2012). Therefore, it is possible that pHsf1 could be detected at a lower molecular weight than the total form of Hsf1.

The expression of Hsf1 and pHsf1 protein in the uterus by immunoblot analysis supported our initial hypothesis that Hsf1 could be involved in myocyte proliferation. It has already been well established by Shynlova and colleagues (2006) that myocyte proliferation peaks in this time frame when they detected an increased incorporation of 5-bromo-2′-deoxyuridine incorporation, a well-known indicator of proliferation, in uterine myocytes during the early phase of pregnancy. Furthermore, several cancer studies have shown a relationship between Hsf1 and tumour cell proliferation (Dai et al., 2007; Santagata et al., 2011). In breast cancer and skin cancer models, Hsf1 is able permit cancer cells to cope with various stressors, allowing tumour cells to reconfigure their metabolism, physiology, and protein homeostasis. If this adaptation to stress allows tumour cells to proliferate, then perhaps a similar mechanism occurs in the myometrium during early gestation. During this phase, several endocrine signals, such as 17β-Estradiol and the IGF, become abundantly present in the uterus to promote proliferation (Le Roith, 2003; Yin et al., 2007). This, coupled with embryonic implantation and other hormonal cues could create a stressful environment for developing myocytes. Therefore, it is possible that Hsf1 could be present to initiate the HSR, allow the uterine cells to proliferate, and to cope with these new stressors.

4.2 The Effect of Distension on Hsf1 Expression

Uterine stretch in the rat, as a result of growing fetuses, is known to contribute to induction of labour at the end of gestation, and therefore places the uterus under a huge

amount of stress (Shynlova et al., 2010). Since Hsf1 is known to regulate the HSR under different physiological stresses, it was hypothesized that perhaps Hsf1 protein expression may be influenced by distension, mechanical stress, in the uterus during pregnancy. A unilateral tubal ligation was performed on virgin female rats, so that they were only able to become pregnant in one horn. This model is useful for researchers to observe the effect of distension on gene expression, while both horns (gravid and non-gravid) are still exposed to the relatively same endocrinological environment; however, it is important to note that the gravid horn will be exposed to paracrine factors produced by the surrounding fetal membranes and tissues during conception unlike the non-gravid horn (Ou et al., 2007).

The levels of Hsf1 and pSer-230 Hsf1 protein expression were analyzed between the two horns to see if Hsf1 expression was influenced by stretch-induced stress at d15, d19 and d23 at which point mechanical stretch on the uterus should be maximal. There was no significant change in Hsf1 or pSer-230 Hsf1 protein expression between the stretched (gravid) and the non-stretched (non-gravid) horn, indicating Hsf1 may not be involved in stretch-induced gene expression in the myometrium. Only one other study has looked at the relationship between stretch and Hsf1 protein expression. Li et al. (2013) looked at the protein expression of Hsf1 in both stretched and non-stretched coronary artery fibroblasts in a mechanical stretch model. Through polymerase chain reaction (PCR) and Western Blot analysis, they did find a positive correlation between mechanical stretch and Hsf1 mRNA and protein expression. Although this relationship between Hsf1 protein expression and stretch was not supported by our data, it should be noted that this was an *in vitro* model of coronary artery perforation where our stretch

studies were completed *in vivo.* Also, Hsf1 is ubiquitously expressed in tissues, and therefore it is possible that it behaves differently in different cell types. It should also be noted that this study was only tested at three time points, d15, d19 and d23. It is possible that the correlation between stretch and Hsf1 may have occurred earlier in gestation, such as d6 when we know Hsf1 protein expression is high. Although stretch would not be as prominent at this time point, it is still present as the fetuses are growing rapidly at this time point as well. Our data is a novel study reflecting Hsf1 expression in both gravid and non-gravid myometrial tissue, and therefore further research is needed in this area.

4.3 Expression of Hsf1 Associated Proteins in the Myometrium During Gestation

Several proteins have been shown to associate with Hsf1 in order to promote its transcriptional activity such as PARP-1 and Hsf2 (Anckar & Sistonen, 2007; Petesch et al., 2008). The expression of these two proteins, in particular, has yet to be shown in the myometrium, and therefore protein expression analysis was performed in order to begin investigating their potential role during pregnancy.

Although PARP-1 has been historically known for its role in cell death, in more recent years its role in transcriptional activation has been well documented (Ziegler & Oei, 2001; Chiarugi, 2002; Kraus & Lis, 2003). The association between Hsf1 and PARP-1 (described in further detail in section 1.9) leads to the initial round of nucleosome displacement so that transcription of the target gene can occur. PARP-1 was detected in the rat myometrium with a pattern of expression similar to Hsf1. It was robustly expressed early in gestation, decreased in mid gestation (during the synthetic

phase) followed again by increased expression until labour. Specifically, PARP-1 expression was significantly expressed at NP, d6, d21, d22, d23 and PP when compared to all other time points examined.

When DNA damage occurs, PARP-1 can positively contribute to the survival or proliferating cells. It uses NAD^+ to synthesize a linear or multi-branched polymer of ADP- ribose on various nuclear protein acceptors usually associated with chromatin, or, itself in an auto-modification reaction. This modification of acceptors is what also helps with cell survival during times of stress (Amé et al., 2004). Up until approximately d14, myocytes are rapidly proliferating. This phase of hyperplasia is likely to cause some level of stress on myometrial cells, and with rapid cell proliferation, damage may occur. Therefore, PARP-1 expression early in gestation may be attributed to a potential role in repairing damaged myometrial cells.

The observed pattern of PARP-1 protein expression in the myometrium may also be related to its known role in apoptosis (Elkholi & Chuphuk, 2014). During the synthetic phase (~d14) there is significant up-regulation of specific caspases, such as initiator caspase-9 and effector caspases 3, 6 and 7, which are essential for apoptosis (Shynlova et al., 2006). These caspases have been shown to cleave PARP-1 in order to initiate the apoptotic pathway (Kaufmann et al., 1993). The antibody used in the experiments described in this thesis detected the non-cleaved form of PARP-1 and during the synthetic phase, when several apoptotic machinery proteins become activated, non-cleaved PARP-1 expression was much lower. These findings also support the possibility that PARP-1 could be involved in apoptosis during the synthetic phase of rat gestation.

It has been previously demonstrated that although Hsf2 does not respond to acute stress stimuli, like heat shock, it is constitutively active in mouse embryonic carcinoma cells, the blastocyst stage during mouse embryogenesis and during spermatogenesis (Mezger et al., 1994; Murphy et al., 1994; Sarge et al., 1994). This suggests that Hsf2 is a heat shock protein regulator during both differentiation and developmental processes by binding to HSEs of developmentally critical target genes (Yamamoto et al., 2009). Throughout pregnancy, the uterus undergoes several phases of differentiation (Shynlova et al., 2009). Therefore, it is possible, based on the constitutive Hsf2 protein expression pattern observed by both immunofluorescence and immunoblot analysis, that Hsf2 has a more developmental role in the uterus instead of a stress-mediated response (Leppa et al., 1997).

4.4 Expression of Hsf1 and Target Proteins *in vitro.*

Hsf1 will bind to HSEs in the promoter region of a variety of stress and developmentally related genes. Some examples of these HSE containing genes are Hsp70, Hsp90 and HspB1 (Holbrook & Udelsman, 1994; Heldens et al., 2012; Neckers & Workman, 2012). Previous research in our lab has demonstrated that some target genes of Hsf1 are in fact induced in the myometrium late in pregnancy and therefore could be regulated by Hsf1. White et al. (2005) showed that HspB1 mRNA and protein expression were upregulated from d15 of gestation and onwards, a time period directly following the observed increased expression of pSer-230 Hsf1. Evidence from our laboratory has also indicated that Hsp70 protein expression is upregulated late in gestation (Marsh et al., in preparation). Since these proteins are highly expressed during the synthetic and contractile phases of differentiation, when the uterus experiences

considerable stress from hypertrophic growth, changes in the cytoskeletal organization and cell-ECM contacts, it is possible that Hsf1 induces the expression of these target genes early in gestation to act as a coping mechanism to aid with changes in the uterus at later periods.

Through *in vitro* experiments using a human myometrial cell line, exogenous Hsf1 was transiently expressed in hTERT-HM cells to see if this could influence the expression of target genes such as HspB1 and Hsp70. After collection of cell lysates 24 and 72 hours post transfection, immunoblot analysis showed that none of the target genes were affected by expressing exogenous Hsf1. Co- expression of Hsf1 and PARP-1 was also performed, in the event that both proteins were required for gene upregulation; however, similar results were observed.

Hsf1 or Hsf1 and PARP-1 co-expression did not induce target gene expression, but this could be due to potential limitations of using transient transfections to induce gene/protein expression. One major difficulty with transiently expressing proteins is that it produces a large population of heterogeneous cells. These cells not only contain highly variable amounts of the target proteins, but frequently manifest disruptions in cycling and growth properties (Walker et al., 1999). Furthermore, Hsf1 binds to genes in order to upregulate mRNA expression followed by expression of proteins. Therefore, it may have been more appropriate to look at the resulting mRNA levels of target genes rather than protein expression alone. Finally, the HSR is often a quick response in most cases. In fact, rapid induction of Hsp70 gene expression in response to cellular stresses, including heat shock, can occur in just minutes (Boehm et al., 2003; Yao et al., 2006). It is possible that the 24 and 72 hour time points examined for Hsf1 induced gene expression were

inappropriate. Perhaps a more effective time point would have been only minutes post-transfection. Based on the current finding and the available data in the literature it is unclear whether or not Hsf1 or Hsf1 and PARP-1 can influence Hsp70 and HspB1 expression in a myometrial cell line.

4.5 The role of Hsf1 in Myocyte Proliferation

Since Hsf1 is upregulated early in gestation, it may be important in inducing Hsp mRNA levels early in gestation to create a pool of stress proteins. This abundance of stress proteins would then be readily available later in pregnancy. Hsf1 also upregulates proteins not involved in stress, such as those involved in development and differentiation (Jedlicka et al., 1997). Therefore, it is possible that Hsf1 also upregulates proteins involved in myometrial proliferation and differentiation early in pregnancy which decreases afterwards once they are no longer needed. Jedlicka et al., (1997) demonstrated that Hsf1 is involved in *Drosophila* larval development and oogenesis, mediating processes like cell growth, chromosomal endoreplication and cell proliferation and differentiation. Therefore, perhaps in utero, Hsf1 could increase myocyte proliferation.

To test this hypothesis, hTERT-HM cells were transiently transfected with Hsf1 or PARP-1 or co-transfected with both Hsf1 and PARP-1 and then any changes in myometrial cell proliferation assayed as a result of increased exogenous levels of these proteins. Cells transfected with PARP-1 and Hsf1/PARP-1 exhibited significantly higher proliferation than the control cells. This result indicated that it is most likely PARP-1 and not Hsf1 that can induce proliferation in myometrial cells grown in vitro.

4.6 Future Directions

This current work provides much needed insight into the expression and potential role of Hsf1 and associated proteins in the myometrium throughout gestation. As little information was known about Hsf1 in the uterus at all, this novel study will help provide a better knowledge of the potential factors affecting myometrial development. The pattern of expression of Hsf1, pSer-230 Hsf1, Hsf2, and PARP-1 indicate that these factors could play a role in regulating myometrial differentiation during early pregnancy, but only PARP-1 appears to regulate myometrial proliferation in myometrial cells in vitro. Despite all of this new knowledge, there are several more avenues that should be explored to study Hsf1 and the myometrium.

First of all, additional studies should be performed to determine the targets for Hsf1-induced transcription. Using the tissue samples collected throughout rat gestation and the hTERT-HM cell lysates, a chromatin immunoprecipitation (ChIP) assay could be performed with Hsf1-specific antisera to see exactly what genes it interacts with. Specifically, a cross-linked ChIP (XChIP) could be performed. Once the DNA is sheared in the initial steps of the XChIP, an antibody specific to Hsf1 could be used, since Hsf1 binds directly to the DNA. Then the DNA associated with Hsf1 could be purified and identified using a PCR or direct high-throughput sequencing. Through this assay, it could be determined if in fact Hsf1 interacts with specific Hsp genes, including those studied in our lab, or if it interacts with other factors that could be involved in proliferation and subsequently studied.

Although it was shown through confocal microscopy that Hsf1 was detectable as speckles in the nuclei of uterine myometrial cells throughout gestation, further investigations that show Hsf1 is truly a nuclear protein should be performed. To do this cellular fractionation studies could be performed. At each gestational time point, myometrial samples would be fractionated into both the nuclear and cytoplasmic fractions. The nuclear cell lysate would then be analyzed by SDS-PAGE and Western blots for the presence of Hsf1 using a Hsf1 specific antibody. This would help confirm the presence of Hsf1 in the nucleus of uterine myocytes.

Hsf1 is also known to form complexes with several proteins, such as PARP-1 and Hsf2 which were studied in this thesis. However, a direct interaction between these proteins was not investigated. Therefore, co-immunoprecipitation experiments should be performed. Following pull-downs with Hsf1 specific antisera, gel electrophoresis and immunoblotting, the blots would be probed with antibodies specific to Hsf2 and PARP-1 to confirm whether there is a direct interaction between these proteins and Hsf1. This could be performed in both the rat tissue samples and the hTERT-HM cell lysates to show if this potential interaction occurs in both rat and human tissues. Confirming or disproving these interactions would lead to a better understanding of the exact mechanisms underlying Hsf1 upregulation of target genes.

Since Hsf1 was shown to be upregulated during the proliferation phase of myometrial differentiation, more studies involving this mechanism should be performed. Although the literature suggests that Hsf1 is most likely what induces proliferation (Dai et al., 2007; Santagata et al., 2011), this current study showed that Hsf1 does not appear to induce proliferation. However, the reverse possibility that proliferation induces Hsf1

expression also needs to be studied. If proliferation was induced in myometrial cells, we may then see a subsequent upregulation in Hsf1 expression. Perhaps certain growth factors could be added to hTERT-HM cells to induce proliferation. Proliferation could then be confirmed using an MTS assay, and if cells are experiencing increased levels of proliferation, then lysates could be collected for protein analysis. The lysates could then be subjected to immunoblot analysis using an antibody specific to Hsf1. PARP-1 could also be studied since it was shown to be involved in proliferation in our previous studies.

These future experiments should help expand our knowledge of Hsf1 and its associated factors in the uterus, and therefore lead to a better understanding of how Hsf1 may influence the development of the myometrium throughout pregnancy.

References

Adams JM, Cory S. (1998). The Bcl-2 protein family: arbiters of cell survival. *Science.* 281(5381):1322-6.

Aguilar H, Mitchell B. (2010). Physiological pathways and molecular mechanism regulating uterine contractility. *Human Reproduction Update.* 16(6): 724-44.

Aguilera G. (2011). HPA axis responsiveness to stress: implications for healthy aging. *Exp Gerontol.* 46(2-3):90-5.

Akerfelt M, Trouillet D, Mezger V, Sistonen L. (2007). Heat shock factors at a crossroad between stress and development. *Ann N Y Acad Sci.* 1113:15-27.

Akerfelt M, Morimoto RI, Sistonen L. (2010). Heat shock factors: integrators of cell stress, development and lifespan. *Nat Rev Mol Cell Biol*. 11(8):545-55.

Amé JC, Spenlehauer C, de Murcia G. (2004). The PARP superfamily. *Bioessays*. 26(8):882-93.

Amin J, Ananthan J, Voellmy R. (1988). Key features of heat shock regulatory elements. *Mol. Cell Biol.* 8(9): 3761-3769.

Anckar J, Sistonen L. (2007). Heat shock factor 1 as a coordinator of stress and developmental pathways. *Adv Exp Med Biol*. 594:78-88.

Ardehali MB, Yao J, Adelman K, Fuda NJ, Petesch SJ, Webb WW, Lis JT. (2009). Spt6 enhances the elongation rate of RNA polymerase II in vivo. *EMBO J.* 28(8):1067-77.

Arrigo AP, Simon S, Gibert B, Kretz-Remy C, Nivon M, Czekalla A, Guillet D, Moulin M, Diaz-Latoud C, Vicart P. (2007). Hsp27 (HspB1) and alphaB-crystallin (HspB5) as therapeutic targets. *FEBS Lett.* 581(19):3665-74.

Beck S, Wojdyla D, Say L, Betran AP, Merialdi M, Requejo JH, Rubens C, MenonR, Van Look PF. (2010). The worldwide incidence of preterm birth: a systematic review of maternal mortality and morbidity. *Bull World Health Organ*. 88(1):31-8.

Blanks AM, Thornton S. (2003). The role of oxytocin in parturition. *BJOG.* 110 Suppl 20:46-51.

Boellmann F, Guettouche T, Guo Y, Fenna M, Mnayer L, Voellmy R. (2004). DAXX interacts with heat shock factor 1 during stress activation and enhances its transcriptional activity. *Proc Natl Acad Sci U S A.* 101(12):4100-5.

Boehm AK, Saunders A, Werner J, Lis JT. (2003). Transcription factor and polymerase recruitment, modification, and movement on *dhsp70 in vivo* in the minutes following heat shock. *Mol Cell Biol.* 23:7628–7637.

Bond M, Somylo AV. (1982). Dense bodies and actin polarity in vertebrate smooth muscle. *J. Cell Biol.* 95; 403-413.

Bradford MM. (1976). A rapid and sensitive method for the quantitation of microgram quantities of protein utilizing the principle of protein-dye binding. *Anal Biochem.* 72:248-54.

Brès V, Yoh SM, Jones KA. (2008). The multi-tasking P-TEFb complex. *Curr. Opin. Cell Biol.* 20:334-40.

Bruey JM, Paul C, Fromentin A, Hilpert S, Arrigo AP, Solary E, Garrido C. (2000). Differential regulation of HSP27 oligomerization in tumor cells grown in vitro and in vivo. *Oncogene*. 19(42):4855-63.

Calderwood SK, Gong J. (2011). Molecular chaperones in mammary cancer growth and breast tumor therapy. *J Cell Biochem*. doi: 10.1002/jcb.23461. [Epub ahead of print]

Carson DS, Guastella AJ, Taylor ER, McGregor IS. (2013). A brief history of oxytocin and its role in modulating psychostimulant effects. *J Psychopharmacol*. 27(3):231-47.

Challis JRG, Matthews SG, Gibb W, Lye SJ. (2000). Endocrine and paracrine regulation of birth at term and preterm. *Endocr Rev*. 21(5):514-50.

Challis J. (2001). Understanding pre-term birth. *Clinical and Investigative Medicine.* 24(1):60-7.

Challis JRG, Lye SJ. (2004). Characteristics of parturition. *Maternal-Fetal Medicine: Principles and Practice.* Edited by Resnik R, Creasy RK,. Philadelphia PA.

Chiarugi, A. (2002). PARP-1: killer or conspirator? The suicide hy- pothesis revisited. *Trends Pharmacol. Sci.* 23: 122–129.

Chou S, Prince T, Gong S, Calderwood SK. (2012). mTOR Is Essential for the Proteotoxic Stress Response, HSF1 Activation and Heat Shock Protein Synthesis. *PLoS One.* 7(6): e39679.

Christians E, Davis AA, Thomas SD, Benjamin IJ. (2000). Maternal effect of Hsf1 on reproductive success. *Nature.* 407(6805):693-4.

Communal C, Sumandea M, de Tombe P, Narula J, Solaro RJ, Hajjar RJ. (2002). Functional consequences of caspase activation in cardiac myocytes. *Proc Natl Acad Sci U S A*. 99: 6252 6256.

Condon J, Yin S, Mayhew B, Word RA, Wright WE, Shay JW, Rainey WE. (2002). Telomerase immortalization of human myometrial cells. *Biol Reprod*. 67(2):506-14.

Cornu M, Albert V, Hall MN. (2013). mTOR in aging, metabolism, and cancer. *Curr Opin Genet Dev.* 23(1):53-62.

Cotto JJ, Kline M, Morimoto RI. (1996). Activation of heat shock factor 1 DNA binding precedes stress-induced serine phosphorylation. Evidence for a multistep pathway of regulation. *J Biol Chem.* 271(7):3355-8.

Creasy RK, Gummer BA, Liggins GC. (1980). System for predicting spontaneous preterm birth. *Obs Gyn,* 55(6): 692-5.

Dai C, Whitesell L, Rogers AB, Lindquist S. (2007). Heat shock factor 1 is a powerful multifaceted modifier of carcinogenesis. *Cell*. 130(6):1005-18.

Damberger FF, Pelton JG, Harrison CJ, Nelson HC, Wemmer DE. (1994). Solution structure of the DNA-binding domain of the heat shock transcription factor determined by multidimensional heteronuclear magnetic resonance spectroscopy. *Protein Sci*. 3(10):1806-21.

Ehrnsperger M, Gräber S, Gaestel M, Buchner J. (1997). Binding of non-native protein to Hsp25 during heat shock creates a reservoir of folding intermediates for reactivation. *EMBO J*. 16(2):221-9.

Elkholi R, Chipuk JE. (2014). How do I kill thee? Let me count the ways: p53 regulates PARP-1 dependent necrosis. *Bioessays.* 36(1):46-51.

Fossati S, Formentini L, Wang ZQ, Moroni F, Chiarugi A. (2006). Poly(ADP-ribosyl)ation regulates heat shock factor-1 activity and the heat shock response in murine fibroblasts. *Biochem Cell Biol*. 84(5):703-12.

Gabella G. (1990). Hypertrophy of visceral smooth muscle. *Anat Embryol (Berl)*. 182(5):409-24.

Gaestel M. (2002). sHsp-phosphorylation: enzymes, signaling pathways and functional implications. *Prog Mol Subcell Biol*. 2002;28:151-69.

Garfield R, Maner W. (2007). Physiology and electrical activity of uterine contractions. *Sem Cell Develop Biol.* 18(3): 289-95.

Gielen SC, Hanekamp EE, Blok LJ, Huikeshoven FJ, Burger CW. (2005). Steroid-modulated proliferation of human endometrial carcinoma cell lines: any role for insulin-like growth factor signaling? *J Soc Gynecol Investig*. 12(1):58-64

Gober, M. D., Smith, C. C., Ueda, K., Toretsky, J. A., and Aurelian, L. (2003). Forced expression of the H11 heat shock protein can be regulated by DNA methylation and trigger apoptosis in human cells. *J Biol Chem*. 278:37600–9.

Goldenberg RL, Mercer BM, Meis PJ, Cooper RL, Das A, McNeillis D. (1996). The preterm birth prediction study; fetal fibronectin testing and spontaneous preterm birth. *Obs Gyn,* 87(5 pt 1): 643-8.

Goldenberg RL, Culhane JF, Iams JD, Romero R. (2008). Epidemiology and causes of preterm birth. *Lancet*. 371(9606):75-84.

Golenhofen N, Der Perng M, Quinlan RA & Drenckhahn D (2004). Comparison of the small heat shock proteins αB crystalline, MKBP, HSP25, HSP20, and cvHSP in heart and skeletal muscle. *Histochem Cell Biol, 122,* 415-425.

Groenen PJ, Merck KB, de Jong WW, Bloemendal H. (1994). Structure and modifications of the junior chaperone alpha-crystallin. From lens transparency to molecular pathology. *Eur J Biochem*.1;225(1):1-19.

Guettouche T, Boellmann F, Lane WS, Voellmy R. (2005). Analysis of phosphorylation of human heat shock factor 1 in cells experiencing a stress. *BMC Biochem.* 6:4.

Guilford WH, Warshaw DM. (1998). The molecular mechanics of smooth muscle myosin. *Comp Biochem Physiol B Biochem Mol Biol*. 119(3):451-8.

Gusev NB, Bukach OV & Marston SB (2005). Structure, properties, and probably physiological role of small heat shock protein with molecular mass 20 kD (Hsp20, HspB6). *Biochem (Moscow), 70,* 629-637.

Hack M, Fanaroff AA. **(1999).** Outcomes of children of extremely low birthweight and gestational age in the 1990s. *Early Hum Dev*. 53:193–218

Harkness ML, Harkness RD. (1954). The collagen content of the reproductive tract of the rat during pregnancy and lactation. *J Physiol.* 23(3):492-500.

Heldens L, van Genesen ST, Hanssen LL, Hageman J, Kampinga HH, Lubsen NH. (2012). Protein refolding in peroxisomes is dependent upon an HSF1-regulated function. *Cell Stress Chaperones*. 2012 Sep;17(5):603-13.

Herrera AM, McParland BE, Bienkowska A, Tait R, Paré PD, Seow CY. (2005). 'Sarcomeres' of smooth muscle: functional characteristics and ultrastructural evidence. *J Cell Sci.* 118(Pt 11):2381-92.

Hertelendy F, Zakar T. (2004). Regulation of myometrial smooth muscle functions. *Curr Pharm Des.* 10(20):2499-517.

Hietakangas, V. Anckar, J. Blomster, H. A. Fujimoto, M. Palvimo, J. J. Nakai, A. Sistonen, L. (2006). PDSM, a motif for phosphorylation-dependent SUMO modification. *Proc. Natl. Acad. Sci.* 103 (1), 45–50.

Holbrook NJ, Udelsman R. (1994). Heat shock protein expression in response to physiological stress and aging. *Biol. Of Heat Shock Proteins and Mol. Chap.* Pp 573-593, Cold Spring Harbor Laboratory Press, Cold Spring Harbor, NY.

Holmberg CI, Hietakangas V, Mikhailov A, Rantanen JO, Kallio M, Meinander A, Hellman J, Morrice N, MacKintosh C, Morimoto RI, Eriksson JE, Sistonen L. (2001). Phosphorylation of serine 230 promotes inducible transcriptional activity of heat shock factor 1. *EMBO.* 20(14): 3800-10.

Hong SK, Son H, Kim SW, Oh SJ, Choi H. (2005). Effect of glycine on recovery of bladder smooth muscle contractility after acute urinary retention in rats. *BJU Int.* 96: 1403-1408.

Horwitz J. (2009). Alpha crystallin: the quest for a homogeneous quaternary structure. *Exp Eye Res.* 88(2):190-4.

Huszar G, Naftolin F. (1984). The myometrium and uterine cervix in normal and preterm labor. *N Engl J Med*. (9):571-81.

Ilić D, Furuta Y, Kanazawa S, Takeda N, Sobue K, Nakatsuji N, Nomura S, Fujimoto J, Okada M, Yamamoto T. (1995). Reduced cell motility and enhanced focal adhesion contact formation in cells from FAK-deficient mice. *Nature.* 377(6549):539-44.

Jaffer S, Shynlova O, Lye S. (2009). Mammalian target of rapamycin is activated in association with myometrial proliferation during pregnancy. *Endocrinology.* 150(10):4672-80.

Janes K. (2015). An analysis of critical factors for quantitative immunoblotting. *Sci Signal.* 8(371).

Jedlicka P, Mortin MA, Wu C. (1997). Multiple functions of Drosophila heat shock transcription factor in vivo. *EMBO J.* 1;16(9):2452-62.

Jurivich DA, Pachetti C, Qiu L, Welk JF. (1995). Salicylate triggers heat shock factor differently than heat. *J Biol Chem*. 270(41):24489-95.

Katzenellenborgen BS (2000). Mechanisms of Action and Cross-Talk Between Estrogen Receptor and Progesterone Receptor Pathways. *Journ Soc Gyn Invest, 7,* S33-S37.

Kaufmann SH, Desnoyers S, OttavianoY, Davidson NE, Poirier GG. (1993). Specific proteolytic cleavage of poly(ADP-ribose) poly- merase: An early marker of chemotherapy-induced apoptosis. *Cancer Res.* 53: 3976–3985.

Kelly RE, Rice RV. (1969). Ultrastructural studies on the contractile mechanism of smooth muscle. *J Cell Biol.* 42(3):683-94.

Kline MP, Morimoto RI. (1997). Repression of the heat shock factor 1 transcriptional activation domain is modulated by constitutive phosphorylation. *Mol Cell Biol.* 17(4):2107-15.

Knauf U, Newton EM, Kyriakis J, Kingston RE. (1996). Repression of human heat shock factor 1 activity at control temperature by phosphorylation. *Genes Dev.* 10(21):2782-93.

Kraus, W.L., and Lis, J.T. (2003). PARP goes transcription. *Cell.* **113**: 677–683.

Kumar V, Chambon P. (1988). The estrogen receptor binds tightly to its responsive element as a ligand-induced homodimer. *Cell.* 55(1):145-56.

Laemmli UK. (1970). Cleavage of structural proteins during the assembly of the head of the bacteriophage T4. *Nature.* 227: 680-685.

Landry, J., Lambert, H., Zhou, M., Lavoie, J. N., Hickey, E., Weber, L. A., & Anderson, C. W. (1992). Human HSP27 is phosphorylated at serines 78 and 82 by heat shock and mitogen-activated protein kinases that recognize the same amino acid motif as S6 kinase II. *Journ Biol Chem.* 267, 794-803.

Lasiuk GC, Comeau T, Newburn-Cook C. (2013). Unexpected: an interpretive description of parental traumas' associated with preterm birth. *BMC Preg Childbirth.* 13 Suppl 1:S13.

Laskowska E, Matuszewska E, Kuczyńska-Wiśnik D. (2010). Small heat shock proteins and protein-misfolding diseases. *Curr Pharm Biotechnol*. 11(2):146-57.

Lee CH, Inoki K, Guan KL. (2007). mTOR pathway as a target in tissue hypertrophy. *Annu Rev Pharmacol Toxicol.* 47:443-67.

Leppä S, Pirkkala L, Saarento H, Sarge KD, Sistonen L. (1997). Overexpression of HSF2-beta inhibits hemin-induced heat shock gene expression and erythroid differentiation in K562 cells. *J Biol Chem.* 272(24):15293-8.

Leppert PC. (1998). Proliferation and apoptosis of fibroblasts and smooth muscle cells in rat uterine cervix throughout gestation and the effect of the antiprogesterone onapristone. *Am J Obstet Gynecol*. 178(4):713-25.

Le Roith D. (2003). The insulin-like growth factor system. *Exp Diabesity Res.* 4(4):205-12.

Leroux, M. R., Melki, R., Gordon, B., Batelier, G., & Candido, E. P. (1997). Structure-function studies on small heat shock protein oligomeric assembly and interaction with unfolded polypeptides. *Journ Biol Chem*. 272, 24646-24656.

Li J, Zhang Y, Cui L, Wang J, Pang X, Lai Y, Yao Y, Liu X, Li Y. (2013). Mechanical stretch changes coronary artery fibroblasts function by upregulating HSF1 protein expression. *Int J Biol Macromol*. 59:105-10.

López Bernal A. (2007). Overview. Preterm labour: mechanisms and management. *BMC Preg Childbirth*. 7 Suppl 1:S2.

Lumley J. (1993). The epidemiology of preterm birth. *Baillieres Clin Obstet Gynaecol.* (3):477-98.

Lye SJ, Mitchell J, Nashman N, Oldenhof A, Ou R, Shynlova O, Langille L. (2001). Role of mechanical signals in the onset of term and preterm labor. *Front Horm Res*. 27:165-78.

Ma X, Wang Y, Stephens NL. (1998). Serum deprivation induces a unique hypercontractile phenotype of cultured smooth muscle cells. *Am J Physiol.* 274(5 Pt 1):C1206-14.

Macphee DJ, Lye SJ. (2000). Focal adhesion signaling in the rat myometrium is abruptly terminated with the onset of labor. *Endocrinology*. (1):274-83.

Marshall NF, Peng J, Xie Z, Price DH. (1996). Control of RNA polymerase II elongation potential by a novel carboxyl-terminal domain kinase. *J. Biol. Chem.* 271:27176–83.

McMillan DR, Xiao X, Shao L, Graves K, Benjamin IJ. (1998). Targeted disruption of heat shock transcription factor 1 abolishes thermotolerance and protection against heat-inducible apoptosis. *J Biol Chem*. 273(13):7523-8. P

Mesiano S, Welsh TN. **(2007).** Steroid hormone control of myometrial contractility and parturition. *Semin Cell Dev Biol.* 18(3):321-31.

Mesiano S, Wang Y, Norwitz ER. (2011). Progesterone receptors in the human pregnancy uterus: do they hold the key to birth timing? *Reprod Sci.* 18(1):6-19.

Mezger V, Rallu M, Morimoto RI, Morange M, Renard JP. (1994). Heat shock factor 2-like activity in mouse blastocysts. *Dev Biol.* 166(2):819-22.

Monga M, Sanborn BM. (1995). Uterine Contractile Activity. Introduction. *Semin Perinat.* (1): 1-2.

Morimoto RI. (2012). The Heat Shock Response: Systems Biology of Proteotoxic Stress in Aging and Disease. *Cold Spring Harb Symp Quant Biol.* [Epub ahead of print].

Mounier N, Arrigo AP. (2002). Actin Cytoskeleton and small heat shock proteins: how do they interact? *Cell Stress and Chaperones.* 7(2): 167-76.

Mu J, Kanzaki T, Tomimatsu T, Fukuda H, Wasada K, Fujii E, Endoh M, Kozuki M, Murata Y, Sugimoto Y, Ichikawa A. (2002). Expression of apoptosis in placentae from mice lacking the prostaglandin F receptor. *Placenta.* 23(2-3):215-23.

Murphy SP, Gorzowski JJ, Sarge KD, Phillips B. (1994). Characterization of constitutive HSF2 DNA-binding activity in mouse embryonal carcinoma cells. *Mol Cell Biol.*14(8):5309-17.

Murshid A, Chou SD, Prince T, Zhang Y, Bharti A, Calderwood SK. (2010). Protein kinase A binds and activates heat shock factor 1. *PLoS One.* 5(11):e13830.

Nadeau K, Das A, Walsh CT. (1993). Hsp90 chaperonins possess ATPase activity and bind heat shock transcription factors and peptidyl prolyl isomerases. *J Biol Chem.* 268(2):1479-87.

Neckers L, Workman P. (2012). Hsp90 molecular chaperone inhibitors: are we there yet? *Clin Cancer Res.* 1;18(1):64-76.

Neumann I, Douglas AJ, Pittman QJ, Russell JA, Landgraf R. (1996). Oxytocin released within the supraoptic nucleus of the rat brain by positive feedback action is involved in parturition-related events. *J Neuroendocrinol.* 8(3):227-33.

Newton EM, Knauf U, Green M, Kingston RE. (1996). The regulatory domain of human heat shock factor 1 is sufficient to sense heat stress. *Mol Cell Biol.* 16(3):839-46.

Orejuela D, Bergeron A, Morrow G, Tanguay R. (2007). Small heat shock proteins in physiological and stress-related processes. *Biomed and Life Sci.* 7(3): 143-177.

Ou CW, Orsino A, Lye SJ. (1997). Expression of connexin-43 and connexin-26 in the rat myometrium during pregnancy and labor is differentially regulated by mechanical and hormonal signals. *Endocrinology.* 138(12):5398-407.

Ou CW, Chen ZQ, Qi S, Lye SJ. (1998). Increased expression of the rat myometrial oxytocin receptor messenger ribonucleic acid during labor requires both mechanical and hormonal signals. *Biol Reprod*. 59(5):1055-61.

Pedersen W. A., Wan R., Mattson M. P. (2001). Impact of aging on stress-responsive neuroendocrine systems. *Mech. Ageing Dev*. 122, 963–983.

Petesch SJ, Lis JT. (2008). Rapid, transcription-independent loss of nucleosomes over a large chromatin domain at Hsp70 loci. *Cell*. 134(1):74-84.

Pirkkala L, Nykänen P, Sistonen L. (2001). Roles of the heat shock transcription factors in regulation of the heat shock response and beyond. *FASEB* J. 15(7):1118-31.

Rabindran SK, Haroun RI, Clos J, Wisniewski J, Wu C. (1993). Regulation of heat shock factor trimer formation: role of a conserved leucine zipper. *Science.* 259(5092):230-4.

Rasmussen EB, Lis JT. (1993). In vivo transcriptional pausing and cap formation on three Drosophila heat shock genes. *Proc Natl Acad Sci U S A.* 90(17):7923-7.

Robinson EE, Foty RA, Corbett SA. (2004). Fibronectin matrix assembly regulates alpha5beta1-mediated cell cohesion. *Mol Biol Cell.* 15(3):973-81.

Russell RB, Green NS, Steiner CA, Meikle S, Howse JL, Poschman K, Dias T, Potetz L, Davidoff MJ, Damus K, Petrini JR. (2007). Cost of hospitalization for preterm and low birth weight infants in the United States. *Pediatrics.* 120(1):e1-9.

Ruvinsky I, Sharon N, Lerer T, Cohen H, Stolovich-Rain M, Nir T, Dor Y, Zisman P, Meyuhas O. (2005). Ribosomal protein S6 phosphorylation is a determinant of cell size and glucose homeostasis. *Genes Dev*. 15;19(18):2199-211.

Salinthone S, Tyagi M, Gerthoffer WT. (2008). Small heat shock proteins in smooth muscle. *Pharmacol Ther*. 119(1):44-54.

Santagata S, Hu R, Lin NU, Mendillo ML, Collins LC, Hankinson SE, Schnitt SJ. (2011). High levels of nuclear heat-shock factor 1 (HSF1) are associated with poor prognosis in breast cancer. *Eur J Obstet Gynecol Reprod Biol.* Suppl 144:S2-10.

Sarge KD, Park-Sarge OK, Kirby JD, Mayo KE, Morimoto RI. (1994). Expression of heat shock factor 2 in mouse testis: potential role as a regulator of heat-shock protein gene expression during spermatogenesis. *Biol Reprod.* 50(6):1334-43.

Saunders A, Werner J, Andrulis ED, Nakayama T, Hirose S, Reinberg D, Lis JT. (2003). Tracking FACT and the RNA polymerase II elongation complex through chromatin in vivo. *Science*. 301(5636):1094-6.

Shynlova O, Mitchell JA, Tsampalieros A, Langille BL & Lye SJ (2004). Progesterone and gravidity differentially regulate expression of extracellular matrix components in the pregnant rat myometrium. *Biol Reprod.* 70, 986-992.

Shynlova O, Tsui P, Dorogin A, Chow M, Lye SJ. (2005). Expression and localization of alpha-smooth muscle and gamma-actins in the pregnant rat myometrium. *Biol Reprod.* 73(4):773-80.

Shynlova O, Oldenhof A, Dorogin A, Xu Q, Mu J, Nashman N, Lye SJ. (2006). Myometrial apoptosis: activation of the caspase cascade in the pregnant rat myometrium at midgestation. *Biol Reprod.* 74: 839-849.

Shynlova O, Tsui P, Dorogin A, Xu Q, Mu J, Nashman N, Lye SJ. (2007). Insulin-like growth factors and their binding proteins define specific phases of myometrial differentiation during pregnancy in the rat. *Biol Reprod.* 76: 571-578.

Shynlova O, Tsui P, Jaffer S, Lye SJ. (2009). Integration of endocrine and mechanical signals in the regulation of myometrial functions during pregnancy and labour. *Eur J Obstet Gynecol Reprod Biol*. 144 Suppl 1:S2-10.

Shynlova O, Dorogin A, Lye SJ. (2010). Stretch-induced uterine myocyte differentiation during rat pregnancy: involvement of caspase activation. *Biol Reprod.* 82(6):1248-55.

Silverthorn DU. (2010). *Human Physiology: An integrated approach (5th edition).* San Francisco, CA: Pearson Education Inc.

Sistonen L, Sarge Kd, Morimoto RI. (1994). Human heat shock factors 1 and 2 are differentially activated and can synergistically induce hsp70 gene transcription. *Mol. Cell. Biol.* 14:2087-2099.

Smith R, Mesiano S, Chan EC, Brown S, Jaffe RB. (1998). Corticotropin-releasing hormone directly and preferentially stimulates dehydroepiandrosterone sulfate secretion by human fetal adrenal cortical cells. *J Clin Endocrinol Metab*. 83(8):2916-20.

Sorger PK, Nelson HC. (1989). Trimerization of a yeast transcriptional activator via a coiled-coil motif. *Cell.* 59(5):807-13.

Strauss JF, Barbieri RL. (2009). *Yen and Jaffe's Reproductive Endocrinology (6th edition).* Philidelphia PN: Elsevier.

Stephens AN, Hannan NJ, Rainczuk A, Meehan KL, Chen J, Nicholls PK, Rombauts LJ, Stanton PG, Robertson DM, Salamonsen LA. (2010). Post-translational modifications and protein-specific isoforms in endometriosis revealed by 2D DIGE. *J Proteome Res.*7;9(5):2438-49.

Sun J, Meyers MJ, Fink BE, Rajendran R, Katzenellenbogen JA & Katzenellenbogen BS (1999). Novel Ligands that Function as Selective Estrogens or Antiestrogens for Estrogen Receptor-α or Estrogen Receptor-β. *Endocrinology, 140,* 800-804.

Sun Y, MacRae TH. (2005). Small heat shock proteins: molecular structure and chaperone function. *Cell Mol Life Sci*. 62(21):2460-76.

Supinski GS, Callahan LA. (2006). Caspase activation contributes to endotoxin-induced diaphragm weakness. *J Appl Physiol*.100: 1770 1777

Taggart M, Morgan K. (2007). Regulation of uterine contractile apparatus and cytoskeleton. *Semin Cell Developl Biol.* 18(3):296-304.

Tollenaar MS, Beijers R, Jansen J, Riksen-Walraven JM, de Weerth C. (2011). Maternal prenatal stress and cortisol reactivity to stressors in human infants. *Stress.* 14(1):53-65.

Trinklein ND, Murray JI, Hartman SJ, Botstein D, Myers RM. (2004). The role of heat shock transcription factor 1 in the genome-wide regulation of the mammalian heat shock response. *Mol Biol Cell.* 15(3):1254-61.

Tsigos C, Chrousos GP. (2002). Hypothalamic-pituitary-adrenal axis, neuroendocrine factors and stress. *J Psychosom Res*. 53(4):865-71.

Vandaele L, Van Soom A. (2011). Intrinsic factors affecting apoptosis in bovine in vitro produced embryos. *Verh K Acad Geneeskd Belg*. 73(1-2):79-104.

Van Montfort RL, Basha E, Friedrich KL, Slingsby C & Vierling E (2001). Crystal structure and assembly of a eukaryotic small heat shock protein. *Nat Struct Biol, 8,* 1025-1030.

Virgo BB, Bellward GD. (1974). Serum progesterone levels in the pregnant rat and post-partum laboratory mouse. *Endocrinology.* 95:1486-1490.

Vrekoussis T, Kalantaridou SN, Mastorakos G, Zoumakis E, Makrigiannakis A, Syrrou M, Lavasidis LG, Relakis K, Chrousos GP. (2010). The role of stress in female reproduction and pregnancy: an update. *Ann N Y Acad Sci.* 1205:69-75.

Walker D, Htun H, Hager GL. (1999). Using inducible vectors to study intracellular trafficking of GFP-tagged steroid/nuclear receptors in living cells. *Methods*.19(3):386-93.

Ward RM, Beachy JC. (2003). Neonatal complications following preterm birth. *BJOG.* 110(Suppl. 20):8–16.

Westerheide SD, Anckar J, Stevens SM Jr, Sistonen L, Morimoto RI. (2009). Stress-inducible regulation of heat shock factor 1 by the deacetylase SIRT1. *Science.* 323(5917):1063-6.

White BG, Williams SJ, Highmore K, Macphee DJ. (2005). Small heat shock protein 27 (Hsp27) expression is highly induced in rat myometrium during late pregnancy and labour. *Reproduction.* 129(1):115-26.

White BG, MacPhee DJ. (2011). Distension in the uterus induces HspB1 expression in rat uterine smooth muscle. *Am J Physiol Regul Integr Comp Physiol.* 301; R1418-R1426.

Whitesell L, Tamimi RM, Lindquist S, Ince TA. (2011). High levels of nuclear heat-shock factor 1 (HSF1) are associated with poor prognosis in breast cancer. *Proc Natl Acad Sci* USA. 108(45):18378-83.

Williams KC, Renthal NE, Condon JC, Gerard RD, Mendelson CR. (2012). Micro-RNA-200a serves a key role in the decline of progesterone receptor function leading to term and preterm labor. *Proc Natl Sci USA.* [Epub ahead of print].

Williams SJ, White BG, MacPhee DJ (2005). Expression of alpha5 integrin (Itga5) is elevated in the rat myometrium during late pregnancy and labor: implications for development of a mechanical syncytium. *Biol Reprod*. 72;1114-1124.

Williams SJ, Shynlova O, Lye SJ, MacPhee DJ. (2010). Spatiotemporal expression of α_1, α_3 and β-integrin subunits is altered in rat myometrium during pregnancy and labour. *Reprod Fertil Dev.* 22: 718-732.

Wray, S. (1993). Uterine contraction and physiological mechanisms of modulation. *Am J Physiol.* 264(1 Pt 1): p. C1-18.

Wu C. (1984). Activating protein factor binds in vitro to upstream control sequences in heat shock gene chromatin. *Nature.* 311(5981):81-4.

Wullschleger S, Loewith R, Hall MN. (2006). TOR signaling in growth and metabolism. *Cell*. 124(3):471-84.

Xiao X, Zuo X, Davis AA, McMillan DR, Curry BB, Richardson JA, Benjamin IJ. (1999). HSF1 is required for extra-embryonic development, postnatal growth and protection during inflammatory responses in mice. *EMBO J*. 18(21):5943-52.

Yamamoto N, Takemori Y, Sakurai M, Sugiyama K, Sakurai H. (2009). Differential recognition of heat shock elements by members of the heat shock transcription factor family. *FEBS J.* 276(7):1962-74.

Yang J, Bridges K, Chen KY, Liu AY. (2008). Riluzole increases the amount of latent HSF1 for an amplified heat shock response and cytoprotection. *PLoS One*. 3(8):e2864.

Yang X, Dale EC, Diaz J, Shyamala G. (1995). Estrogen dependent expression of heat shock transcription factor: implications for uterine synthesis of heat shock proteins. *J Steroid Biochem Mol Biol*. 52(5):415-9.

Yao J, Munson KM, Webb WW, Lis JT (2006). Dynamics of heat shock factor association with native gene loci in living cells. *Nature*. 442(7106):1050-3.

Yin XJ, Wang G, Khan-Dawood FS. (2007). Requirements of phosphatidylinositol-3 kinase and mammalian target of rapamycin for estrogen-induced proliferation in uterine leiomyoma- and myometrium-derived cell lines. *Am J Obstet Gynecol*.196(2)

Ziegler, M., and Oei, S.L. (2001). A cellular survival switch: poly(ADP-ribosyl)ation stimulates DNA repair and silences transcription. *Bioessays*, **23**: 543–548.

Appendix A: Permission for Figure

Primary Healthcare Research Unit
Room 1774, Health Science Centres
300 Prince Philip Drive, St. John's, NL A1B 3V6
Tel: 709 777 6645 Fax: 709 777 6118
Email: Phru@med.mun.ca
Website: www.med.mun.ca/PHRU/Home.apsx

April 2, 2012

To Whom It May Concern:

I give permission for Masters' student Sarah Dinn to use and adapt my diagrams 'Phases of Myometrial Differentiation' and 'Layers of the Myometrium' in her thesis.

Yours sincerely,

M. Peach

Mandy Peach, MSc
Research Assistant
Primary Healthcare Research Unit
Faculty of Medicine
Memorial University

Appendix B: Permission for Figure

OXFORD UNIVERSITY PRESS LICENSE
TERMS AND CONDITIONS

Dec 30, 2014

This is a License Agreement between Sarah Dinn ("You") and Oxford University Press ("Oxford University Press") provided by Copyright Clearance Center ("CCC"). The license consists of your order details, the terms and conditions provided by Oxford University Press, and the payment terms and conditions.

All payments must be made in full to CCC. For payment instructions, please see information listed at the bottom of this form.

License Number	3157181364353
License date	May 27, 2013
Licensed content publisher	Oxford University Press
Licensed content publication	Human Reproduction Update
Licensed content title	Physiological pathways and molecular mechanisms regulating uterine contractility:
Licensed content author	Hector N. Aguilar, B.F. Mitchell
Licensed content date	11/01/2010
Type of Use	Thesis/Dissertation
Institution name	None
Title of your work	Characterization of Hsf1 Expression in the Rat Myometrium
Publisher of your work	n/a
Expected publication date	Oct 2013
Permissions cost	0.00 USD
Value added tax	0.00 USD
Total	0.00 USD
Total	0.00 USD